



NTNU – Trondheim
Norwegian University of
Science and Technology

Effects of cPLA₂α inhibition in the MDA-MB-468 cell model system for basal-like breast cancer and/or triple negative breast cancer

Master Thesis in Pharmacy (2 years)

Submission date: September, 2016

Supervisor: Berit Johansen, IBI

Co-supervisor: Astrid J Feuerherm, IBI

Norwegian University of Science and Technology

The medical faculty

Department of Biology

Anfal Hussin, 2016

Abstract

Basal-like breast cancer (BLBC) is a highly aggressive breast cancer sub-type and represents ~15% of all breast cancers. BLBC are often associated with early age of onset, early relapse and poor overall survival in contrast to other types of breast cancers. Moreover, patients diagnosed with BLBC do not benefit from currently available targeting treatments on the market, such as anti-oestrogen, anti-progesterone and antibody against the HER2-receptor, and therefore, BLBC are also referred to as triple negative breast cancer (TNBC). In the last years, many researches have focused on studying the molecular characteristic of BLBC/TNBC to develop molecular targets against BLBC/TNBC and several molecular targets are currently being investigated and some are already proposed. BLBC/TNBC has shown overexpression and/or amplification of various receptors and proteins involved in cell survival, proliferation and apoptosis. Thus, targeting these pathways have shown increasing interests for researchers who want to develop such inhibitors for the treatment of BLBC/TNBC.

It has previously been shown that BLBC/TNBC overexpress the gene PLA2G4A that encode the cPLA₂ α -enzyme, which is responsible for regulating the production of eicosanoids by liberating arachidonic acid (AA). The eicosanoids are biologically active lipid mediators, which are involved in regulating many responses in the cells, such as inflammation, proliferation, apoptosis, metastasis and angiogenesis. To our knowledge, the exact role of cPLA₂ α in cell proliferation in BLBC/TNBC is not fully identified. In this master thesis, we investigate the cellular effects of cPLA₂ α inhibition by using the MDA-MB-468 cell line as a model for BLBC/TNBC. More specifically, cell proliferation and/or viability, apoptosis and cell cycle distribution of these cells was investigated. Another goal of this master project was to evaluate the possible synergistic/additive effects of combining cPLA₂ α -inhibitors with selective mTOR/PI3K inhibitors, which represent a promising treatment strategy for BLBC/TNBC.

By using the resazurin viability assay, the effects of different compounds/inhibitors/-comparative drugs on the viability of the MDA-MB-468 cells were investigated. A dose-response experiment was conducted for each compound/inhibitor/comparative drug in order to select a sub-optimal concentration to further experiments. Caspase activity of cells treated with selective cPLA₂ α inhibitors alone and in combination with pan-PI3K inhibitor

buparlisib/BKM120 were measured by caspase GLO®. Flow cytometry was utilized to measure cell cycle phase distribution of the MDA-MB-468 cells treated with AVX002 separately, buparlisib/BKM120 separately and when combined with AVX002. Doxorubicin was used as apoptosis control.

Rezasurin viability assay, revealed positive results and reduced the viability of the MDA-MB468 cells in a dose-dependent manner for all the tested compounds. Combination treatment of selective cPLA₂α-inhibitors with buparlisib/BKM120 revealed additive effects in the MDA-MB-468 cells. Caspase assay showed increased caspase activity of cells treated with different cPLA₂α-inhibitors and combining these inhibitors with buparlisib/BKM120 increased these effects considerably. Flow cytometry analyses showed cell cycle arrest at G1 phase in cells treated with AVX002. Cells treated with buparlisib/BKM120 showed increased number of cells at the G2+M phase of the cell cycle.

The use of selective cPLA₂α inhibitors could offer a novel targeted therapy for BLBC/TNBC which otherwise have low survival prognosis. Also, combining selective cPLA₂α inhibitors with selective PI3K inhibitors could potentially balance the side effect profile of each inhibitor and reduce resistance problems. Further studies need to be conducted in order to confirm or reject these observations.

Sammendrag

Basal-like brystkreft (BLBC) er en aggressiv type brystkreft og utgjør ~15% av alle brystkreft former. BLBC er ofte assosiert med tidlig debut, tidlig tilbakefall og lavt total overlevelse i motsetning til andre kreftformer. I tillegg kan pasienter som er diagnostisert med BLBC ikke ta nytte av dagens målrettede behandling som inkluderer bruk av anti-østrogen, anti-progesteron og antistoff mot HER2- reseptor. Dermed er BLBC også referert til som trippel negative bryst kreft (TNBC). I de siste årene har forskning fokusert på å studere molekylære karakteristiske kjennetegn av BLBC for å utvikle molekylær målrettet behandling mot BLBC/TNBC og flere ulike behandlinger er blitt foreslått og en del er under utvikling. BLBC/TNBC har vist overuttrykk og/eller amplifikasjon av en rekke ulike reseptorer og proteiner som er involvert i celle overlevelse, proliferasjon og apoptose. Å utforme en behandling som retter seg mot disse prosessene i cellene har vist økt interesse for forskere som ønsker å utvikle slike hemmere for å kunne tilby bedre behandling for BLBC/TNBC.

Det har tidligere blitt vist at BLBC/TNBC har overuttrykk av genet PLA2G4A som koder for cPLA₂α-enzymet som er ansvarlig for å regulere produksjon av eikosanoider gjennom frigjøring av arakidonsyre (AA). Eikosanoider er biologisk aktive lipid mediatorer som er involvert i regulering av mange ulike responser i cellen som inkluderer inflammasjon, proliferasjon, apoptose, metastase og angiogenese. Til vår kjennskap, er den eksakte rollen av cPLA₂α i celle proliferasjon ikke fullstendig klarlagt. I denne master oppgaven, undersøker vi cellulære effekter av cPLA₂α ved å bruke MDA-MB-468 celler som en modell for BLBC/TNBC. Mer spesifikt, celle proliferasjon og/eller viabilitet, apoptose og cellesyklusen av disse cellene ble undersøkt. Et annet mål med denne oppgaven var å evaluere mulige synergistiske/additive effekter av å kombinere cPLA₂α hemmere med selektive mTOR/PI3K hemmere som representerer en lovende behandlingsstrategi for BLBC/TNBC.

Ved bruk av resazurin viabilitets assay, ble effekten av ulike kjemiske forbindelser/hemmere/-komparative legemidler undersøkt på MDA-MB-468 cellers viabilitet. Et dose-respons forsøk ble utført for hver kjemiske forbindelse/hemmer/-komparativ legemiddel for å velge en sub-optimal dose til fremtidige eksperimenter. Caspase aktivitet av celler behandlet med selektive cPLA₂α hemmere aleine og i kombinasjon med pan-PI3K hemmer buparlisib/BKM120 ble målt ved bruk av caspase GLO®. Flow cytometri ble benyttet til å analysere cellesyklusen av

MDA-MB-468 celler behandlet med AVX002 aleine, buparlisib/BKM120 aleine og kombinasjonen av disse. Doxorubicin ble valgt som apoptose control.

Resazurin viabilitets assay viste positive resultater og redusert viabilitet av MDA-MB-468 celler på en doseavhengig måte for alle uttestede forbindelser. Kombinasjonsbehandling av selektive cPLA₂α hemmere med buparlisib/BKM120 viste additive effekter på MDA-MB-468 celler. Caspase assay viste økt caspase aktivitet av celler behandlet med ulike cPLA₂α-hemmere og kombinasjon med buparlisib/BKM120 førte til en betydelig effekt økning.

Flow cytometri analyse viste positive resultater hvor cellesyklus arrest ved G1 fasen ble observert i celler behandlet med AVX002. Celler behandlet med buparlisib/BKM120 viste økt antall celler i G2+M fasen av cellesyklusen.

Konkludert, kan bruken av selektive cPLA₂α hemmere tilby ny målrettet behandling for BLBC/TNBC som ellers har lav prognose. I tillegg, kan kombinerings av selektive cPLA₂α hemmere med selektive PI3K hemmere potensielt balansere bivirkningsprofilen av hver hemmer og eventuelt redusere resistens problematikk. Flere studier er nødvendige for å kunne bekrefte eller avvise disse observasjonene.

List of abbreviations

AA	Arachidonic Acid
$\alpha\beta$ -Crystallin	A heat shock protein that prevents apoptosis by inhibiting caspase 3, a pro-apoptotic protein
ad-PLA ₂	Adipose phospholipase A2
ATCC	American Type Culture Collection
AVX002	cPLA ₂ α inhibitor, (1-octadeca-3,6,9,12,15-pentaenylsulfanyl-propan- 2-one)
AVX420	cPLA ₂ α inhibitor
AVX235	cPLA ₂ α inhibitor (methyl 2-(2- (4-octylphenoxy)acetyl)thiazole-4-carboxylate)
ATK	AACOCF3- arachidonyl-trifluoromethyl ketone, cPLA ₂ α inhibitor
BCS	Breast conservative surgery
BLBC	Basal-like breast cancer
BRC	Biological resource centre
BRCA1	Breast cancer 1, a tumour suppressor gene
CamKII	Calmodulin kinase II
Caspase 3	Cysteine-aspartic acid-specific proteases
CDK	Cyclic dependent kinases
C _f	Final concentration
CKI	Cyclic dependent kinase-inhibitors
COX	Cyclooxygenase
cPLA ₂ α	Cytosolic phospholipase A2 –alpha
CYP450	Cytochrome p-450
DSB	Double-strand DNA break
DEVD	Tetra peptide sequence containing the amino acids in the following order: (Aspartic acid- Glutamine- Valine - Aspartic acid)
DHA	Docosahexaenoic acid
DMEM	Dulbecco's modified eagle medium
DMSO	Dimethyl sulfoxide
DNA	Deoxyribonucleic acid
EGF	Epidermal growth factor
EGFR	Epidermal growth factor receptor
ER	Estrogen receptor

ET	Endocrine therapy
FBS	Fetale bovine serum
FOXO1	Forkhead box O1
IC50	Half maximum inhibitory concentration
iPLA ₂	Calcium-independent phospholipase A2
JAK	Janus family of tyrosine kinase
JNK	c-Jun N-terminal kinase
LOX	Lipooxygenase
LPC	Lyso-phosphatidylcholine
LPLA ₂	Lysosomal phospholipase A2
LTs	Leukotrienes
LXs	Lipoxins
LYN	Lck/Yes novel tyrosine kinase (belong to SRC family of kinases, and are involved in cancer signaling pathways, such as survival, metastasis, proliferation and apoptose regulation)
MAPKs	Mitogen activated protein kinases
MKK1	MAPK-interacting kinase
NSAIDS	Non-steroidal anti-inflammatory drugs
PAF-AH	Platelet-activating factor acetyl-hydrolase
PARP	Poly (ADP) ribose polymerase
PBS	Phosphate buffered saline
PC	Phosphatidylcholine
PE	Phosphatidylethanoamine
PDT	Population doubling time
PGs	Prostaglandins
PGE ₂	Prostaglandin E2
PGIs	Prostacyclines
PI	Phosphatidylinositol
PI3K	Phosphatidylinositol-3- kinases
PLA ₂	Phospholipase A2 enzyme
PR	Progesterone receptor
PTEN	Phosphatase and tensin homolog
PUFA	Poly unsaturated acid
RA	Rheumatoid arthritis
RPMI-1640	Roswell Park memorial institute -1640 medium

sPLA ₂	Secretory phospholipase A2
SD	Standard deviation
SF-RPMI	Serum free RPMI-1640 (growth medium contains only L-glutamin and Gentamycin)
SIRT2	Sirtuin2
SSB	Single-strand DNA-break
STAT	Signal transducer and activator of transcription
TF	Transcription factor
TGF α	Transforming growth factor alpha
TNBC	Triple negative breast cancer
TNF	Tumour necrosis factor
TNM	Tumour-node-metastases
TP53	Tumour protein 53
TXs	Thromboxanes
UDPGA	Uridine diphosphoglucuronic acid
UGT1A6	UDP-glucuronosyltransferase 1A6
VEGFR	Vascular endothelial growth factor receptor

Preface

This master thesis was performed as a final task of the 2 years' pharmacy masters programme (MFARMASI). The study was completed in the Lipid signalling group/PLA2 group, Department of Biology at the Norwegian University of Science and Technology (NTNU), from August, 2015 until September, 2016. Professor Berit Johansen was the main supervisor and my co-supervisors were Senior researcher Astrid Jullumstrø Feuerherm and Postdoc. Randi Magnus Sommerfelt.

A sincere gratitude goes to Senior researcher Astrid for helping and guiding me along this challenging path. You have been there for me when I needed assistance in the laboratory, gave me advices and assisted me with so much more. I will always remember your beautiful smile and your positive energy; you are truly an inspiration to me. I would also like to thank my main supervisor prof. Berit Johansen. Thank you for your time and help, for motivating me to be a hard worker, and pushing me to be a better scientist. Also, I would like to thank all the researchers & the co-workers in the PLA2 group for their time and help, and for providing me a good working environment.

Last but not least, I would like to mention my dear family & friends. A sincere gratitude to my great parents, mom & dad for always being there for me, supporting me and believing in me. My beautiful sister, Abrar, what would I do without your beautiful smile and endless support, you are one of a kind sister. Thanks to all my friends who cheered me up when I was stuck with my project. You are all diamonds for me and I love you so much.

Trondheim, September 2016

Anfal Hussin

1	INTRODUCTION	2
1.1	Breast cancer epidemiology; a global health problem.....	2
1.1.1	Breast cancer treatment	2
1.1.2	Basal-like breast cancer	4
1.1.3	Targeted therapy of BLBC.....	5
1.2	Phospholipase A2 (PLA ₂) enzymes.....	7
1.2.1	Cytosolic phospholipase A2 α and role of lipid mediators in cancer	8
1.2.2	Role of cPLA ₂ α in cell-cycle arrest and apoptosis.....	11
1.3	A new targeted treatment: specific cPLA ₂ α inhibitors	13
1.4	The MDA-MB-468 cell line as an <i>in vitro</i> model for BLBC.....	15
1.5	The aims of this thesis	16
2	MATERIALS AND METHODS	18
2.1	Reagents solution and materials	18
2.2	Cell culture and cell experiments:.....	19
2.3	Establishing the growth curve of MDA-MB-468 cell:.....	20
2.4	Dose-Response:.....	21
2.4.1	Combination treatment of cPLA ₂ α and selective PI3K inhibitors	24
2.4.2	Caspase-3 and -7 assay	25
2.5	Cell-cycle assay.....	27
2.5.1	Fixing and permeabilizing cells	28
2.5.2	Removal of RNA.....	28
2.5.3	Staining the cells and analysis by using flow cytometer	28
2.6	Statistical analysis	28
3	RESULTS	29
3.1	MDA-MB-468 cells do not enter stationary and decline phase.....	29
3.2	Methotrexate, doxorubicin, etoposide and EGF as apoptosis-inducing agents	33
3.3	Selective cPLA ₂ α inhibitors affect the viability of the MDA-MB-468 cells	37
3.4	PI3K/mTOR-inhibitors reduce viability of MDA-MB-468 cells in a dose-dependent manner.....	41
3.5	Combination of buparlisib/BKM120 with cPLA ₂ α inhibitors demonstrated additive effects	44
3.6	Buparlisib/BKM120 and cPLA ₂ α inhibitors increase the caspase activity of the MDA-MB-468 cells.....	46
3.7	AVX002 and buparlisib/BKM120 induce cell cycle arrest in the MDA-MB-468 cells.....	48
4	DISCUSSION	51
4.1	Different seeding numbers affects the growth of the MDA-MB468 cells	52
4.2	Cells keep growing even though the total surface of the flask are occupied	53
4.3	Comparison of EGF, methotrexate, etoposide and doxorubicin.....	54
4.4	Comparison of different cPLA ₂ α inhibitors.....	55
4.5	Comparison of selective PI3K/(mTOR) inhibitors	58
4.6	Comparison of combo-treatment with selective PI3K inhibitors and cPLA ₂ α inhibitors	59
4.7	Selective cPLA ₂ α inhibitors increase caspase activity.....	60
4.8	Cells arrested at different cell cycle phases in response to AVX002 and buparlisib/BKM120	61
4.9	cPLA ₂ α may regulate pathways such as PI3K and RAF/MEK/ERK in BLBC/TNBC.....	62

4.10 Technical variations in cell experiments	64
4.11 Future research.....	65
5 Conclusion.....	66
6 REFERENCES.....	67
APPENDIX.....	73
A. All biological replicas (n=3) for the representative experiment in figure 8:.....	73
B. All biological replicas (n=3) for the representative experiment in figure 9:.....	75
C. All biological replicas (n=3) for the representative experiment in figure 10:	77
D. All biological replicas (n=3) for the representative experiment in figure 11:.....	79
E. All biological replicas (n=3) for the representative experiment in figure 12:	82

1 INTRODUCTION

1.1 Breast cancer epidemiology; a global health problem

Breast cancer is one of the most common cancers that affect mainly women in both more and less developed countries. Accounting for 23% of the total cancer cases and 14% of the total cancer deaths in 2008, breast cancer is the leading cause of cancer deaths in females worldwide (1). In 2012, approximately 1.67 million new breast cancer cases were registered globally (2).

The current data in incidence rates indicates a higher number of breast cancer cases in developed countries compared to less developed countries, possibly due to better diagnostic tools such as mammography and screening programs that detect cancer more effectively (3, 4). Furthermore, the changing patterns in childbearing and breastfeeding, exogenous hormonal intake, lifestyle factors such as reduced physical activity, increased alcohol consumption and obesity may also contribute to the high incidence rates in developed countries (5). Despite a high number of new cancer cases, breast cancer survival has also improved remarkably the last decades, probably due to the improved therapeutic advances arising from better knowledge of the molecular characteristics of this disease and early detection of breast cancer (6).

1.1.1 Breast cancer treatment

In recent years, better knowledge of tumour phenotypes, based on biomarker expression and classification of breast cancer into molecular subtypes has been used for individualized targeted treatment. The concept of targeted therapy is based on targeting specific molecules, such as proteins and/or enzymes that are involved in cancer cell invasion, metastasis, apoptosis, cell-cycle control, and tumour related angiogenesis (7). A more detailed description of targeted therapy and different therapeutics within this field is found in section 1.1.3.

Today's breast cancer treatment takes into account the patient's complete medical history, family history relating to breast/ovarian and other cancers, menopausal status, hormone status, age and the stage of the tumour (8). Prior to treatment, the stage of the cancer must be evaluated. Hence, an international classification system has been developed to categorize the stage of cancer before initiation of any treatment. The tumour-nodule-metastases (TNM) staging system is one of the most widely used cancer-staging systems. It is based on

characterizing the size and/or the extent of the primary tumour (T), the amount of spread to lymph nodes (N), and the presence of metastasis (M) or by secondary tumours produced by the spread of cancer cells to other parts of the body. A number is added to each letter that indicates the size and/or the extent of primary tumour and the degree of cancer spread (9). Classification of breast cancer in stages is a method used to differentiate between localized disease and metastatic disease. In localized disease the cancer is restricted to the breast and the main treatment options are surgical removal of the breast (mastectomy) or breast conservative-surgery (BCS), depending on the tumour size and grade of invasiveness (8).

In addition to surgery, most patients receive endocrine therapy (ET) such as chemotherapy and/or hormone therapy if the cancer cells are hormone receptor positive. The most common chemotherapies used in breast cancer treatment alone or in combination with other drugs, are taxanes such as paclitaxel and docetaxel, and anthracyclines such as doxorubicin and epirubicin (10). A common feature of these compounds is their mechanism of action. Most chemotherapies act directly or indirectly on the DNA or on the cell proliferation machinery and affects both healthy and malignant cells, producing many side effects due to their low specificity (11). Targeted treatments on the other hand, are highly specific and block the action of specific receptors and/or enzymes, which are involved in the cancer cells mitosis mechanism (12). Such treatments have less harmful effects on healthy non-malignant cells and are considered as effective treatments against breast cancer (13). Targeted therapies used for treating hormone sensitive breast cancers include aromatase inhibitors (letrozol, anastrozol) and the anti-oestrogen tamoxifen (14). Patients that have overexpression of human epidermal growth factor receptor 2 (HER2) can be offered trastuzumab, which is a monoclonal antibody against HER2-receptor (15).

Radiotherapy is also used for treating breast cancer in some cases and is specially indicated for patients that have removed their tumour by BCS. In certain cases, when the patient is not able to undergo surgery due to various reasons (big tumour size, medical reasons, etc.), radiotherapy can be the only option. When treating localized disease, the goal is always to cure the patient. However, in tumour metastasis, when the cancer has spread to distant organs, curative treatment is no longer possible. The main goal is then to reduce symptoms and relief pain. In such cases, the treatments are less aggressive and the tolerance for unwanted side effects is much lower. Some patients can be offered hormonal therapy and/or chemotherapy in lower doses (16).

1.1.2 Basal-like breast cancer

Breast cancer is normally classified into different molecular subtypes based on histological type and grade, expression of oestrogen receptor (ER), progesterone receptor (PR) and overexpression and/or amplification of HER2. There are four main intrinsic molecular subtypes of breast cancers, namely; luminal-A, luminal-B, basal-like and HER2-positive enriched (17). The different subtypes of breast cancer are extensively reviewed (18, 19) and will not be further described. Based on what is considered relevant for this master project, the focus in this thesis will hereafter be on basal-like breast cancer (BLBC).

Classification of breast cancer into different molecular subtypes has been an important tool for determining prognosis and the potential response to ET and other targeted therapies (18). Basal-like tumour represent ~15% of all breast cancer subtypes and are often associated with a high proliferation rate, early age of onset, early relapse, and poor overall survival in contrast to other breast cancer subtypes (20). Such tumours are usually characterised by the expression of epidermal growth factor–receptor (EGFR), high molecular weight cytokeratins (CK5/6, CK14 and CK17), c-KIT receptor (also referred to as stem cell factor receptor or CD117, a receptor tyrosine kinase involved in cell survival and proliferation), by frequent mutation of the gene tumour protein 53 (TP53) encoding the p53 protein and by breast cancer 1 (BRCA1) mutations (21, 22).

EGFR is a receptor that stimulates proliferation by activating the Ras-/ MAPK/MAPK kinase (MEK) pathway (23). EGFR can also activate the phosphatidylinositol-3-kinases (PI3K)/Akt/mTOR pathway, resulting in cell survival and resistance to apoptosis. Both p53 and BRCA1 function as tumor-suppressing proteins, which activates DNA repair, initiate cell cycle arrest and/or apoptosis in the presence of DNA damage. Therefore, loss of function in these proteins can lead to genomic instability and promote tumor growth (23).

BLBC also express the heat shock protein $\alpha\beta$ -crystallin, which prevent apoptosis by preventing the proteolytic activation of a pro-apoptotic protease called caspase 3. Low levels of the tumor suppressor gene phosphatase and tensin homolog (PTEN) are also observed in BLBC, resulting in abnormal activation of the PI3K/Akt/mTOR pathway (23).

BLBC usually lack the expression of molecular targets such as ER, PR and HER2 that is used to define the responsiveness to highly effective targeted therapies such as tamoxifen, aromatase inhibitors and trastuzumab (22). Therefore, this breast cancer subtype is often

referred to as triple negative breast cancer (TNBC). To date, there are no specific targeted therapies against BLBC/TNBC, and the only optional ET for these patients is traditional use of chemotherapy with high risk of therapeutic failure and early relapse (22). There is however on-going research to develop targeted therapies against BLBC/TNBC, and several molecular therapeutic targets for this highly deadly breast cancer subtype are already suggested (22-24).

1.1.3 Targeted therapy of BLBC

As mentioned above, BLBC has overexpression and/or amplification of several receptors and proteins involved in cell survival, proliferation and apoptosis. Imbalance of the cell mitosis machinery plays a central role in the pathogenesis of many cancers, including BLBC. Hence, in the last years, researchers have developed several molecular agents that specifically target BLBC/TNBC through different cellular pathways (23).

An interesting targeted approach that has been proposed is use of poly (ADP) ribose polymerase (PARP)-inhibitors, an enzyme involved in DNA base-excision repair. Inhibiting this enzyme prevents the repair of single stranded DNA breaks, which results in multiple double-strand DNA breaks. BRCA1's function is to repair double strand DNA breaks, but in the presence of BRCA1 mutations this repair mechanism is defective, leading the cell to apoptosis. Normal cells, on the other hand, is capable of repairing its DNA and survives the inhibition of PARP. The PARP-inhibitors are also suggested for use as combination therapy with chemotherapy. Other targeted approaches, which are under investigation aim to target angiogenesis (the process of formation of new blood vessel to the tumour) and proliferation signalling pathways. Targeting angiogenesis includes the use of antibodies against vascular endothelial growth factor receptor (VEGFR), such as bevacizumab and small-molecule multikinase inhibitors, like surafenib and sunitinib. To target cell proliferation signalling, antibodies against EGFR such as cetuximab and small-molecule protein-kinase inhibitors like erlotinib, gefitinib and lapatinib are available (22, 23).

A simplified schematic overview of signal transduction pathways involved in the pathogenesis of BLBC/TNBC and possible molecular targets is shown in figure 1. Not all of the processes and potential targets of BLBC/TNBC are explained in this subchapter. Only the most relevant aspects for this master thesis are explained in the following.

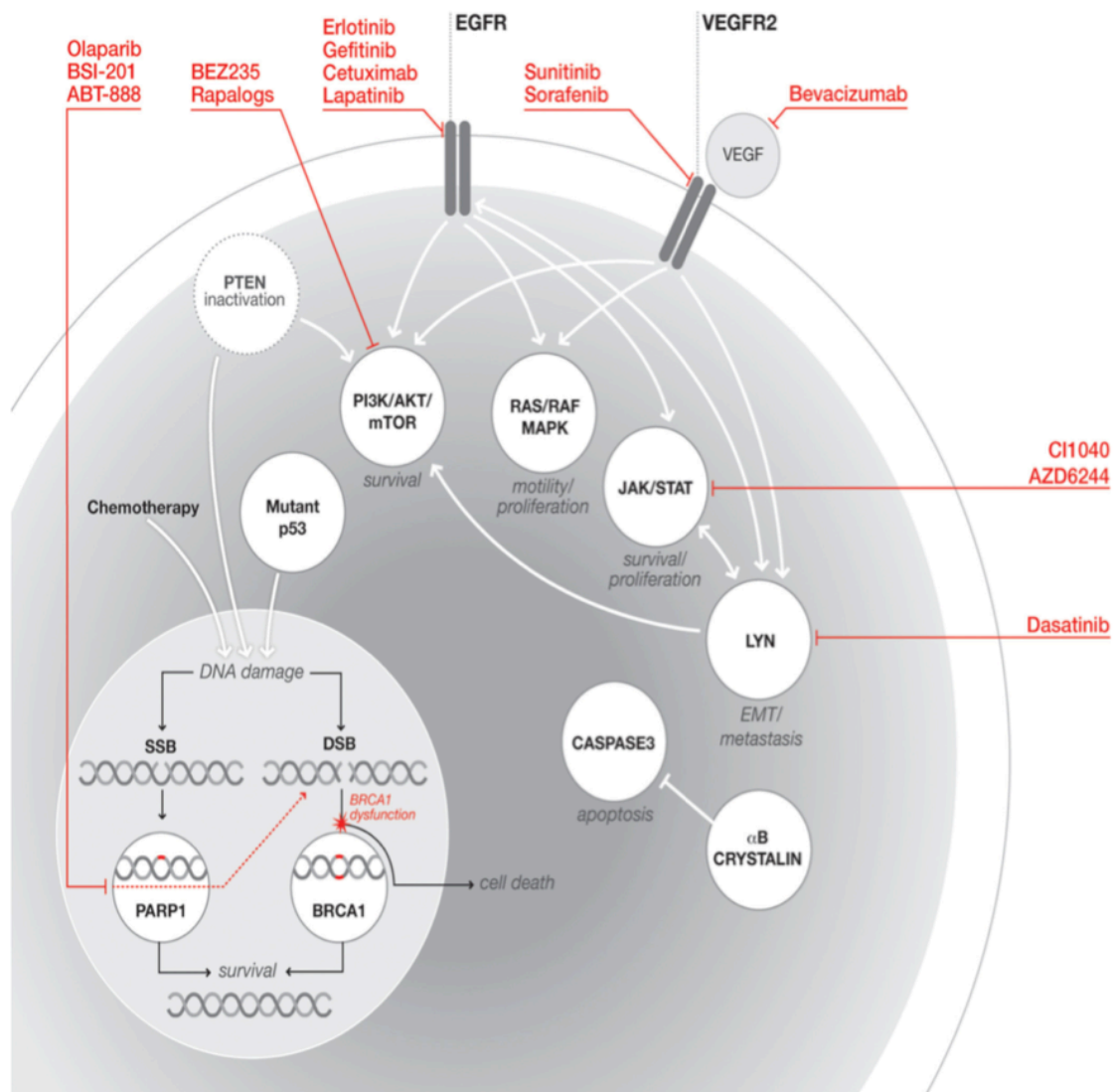


Figure 1. Schematic overview of key signal transduction pathways involved in the pathogenesis of BLBC and suggested targeted therapies. Commonly dysregulated pathways and their biological effects are specified. The suggested targeted therapies inhibiting pathways involved in cell survival, angiogenesis and proliferation are marked in red, DSB, double-strand break; SSB, single-strand DNA break; LYN, Lck/Yes novel tyrosine kinase; PTEN, Phosphatase and tensin homolog; JAK, Janus family of tyrosine kinases; PI3K, phosphatidylinositol-3-kinase; STAT, signal transducer and activator of transcription. From Toft *et al.* 2011, with permission (23).

1.2 Phospholipase A₂ (PLA₂) enzymes

Phospholipase A₂ (PLA₂) enzymes are part of a large superfamily of catalytic enzymes and are associated with several inflammatory conditions such as rheumatoid arthritis (RA), asthma and atherosclerosis, and also different types of cancers (see next section) (25-29).

The PLA₂ enzymes are sorted into 16 groups and several subgroups based on their biochemical properties and mechanisms (30). There are 6 different types of PLA₂ enzymes; cytosolic PLA₂ (cPLA₂), calcium-independent PLA₂ (iPLA₂), secreted PLA₂ (sPLA₂), platelet-activating factor acetyl-hydrolase (PAF-AH), lysosomal PLA₂ (LPLA₂) and adipose PLA₂ (ad-PLA₂) (30). PLA₂ enzymes catalyse the hydrolysis of an ester bond at the *sn*-2 position of fatty acids from membrane phospholipids and provide polyunsaturated fatty acids (PUFAs) and lysophosphatidylcholine (LPC), which are important precursors of various bioactive lipid mediators (see figure 2) (30-32).

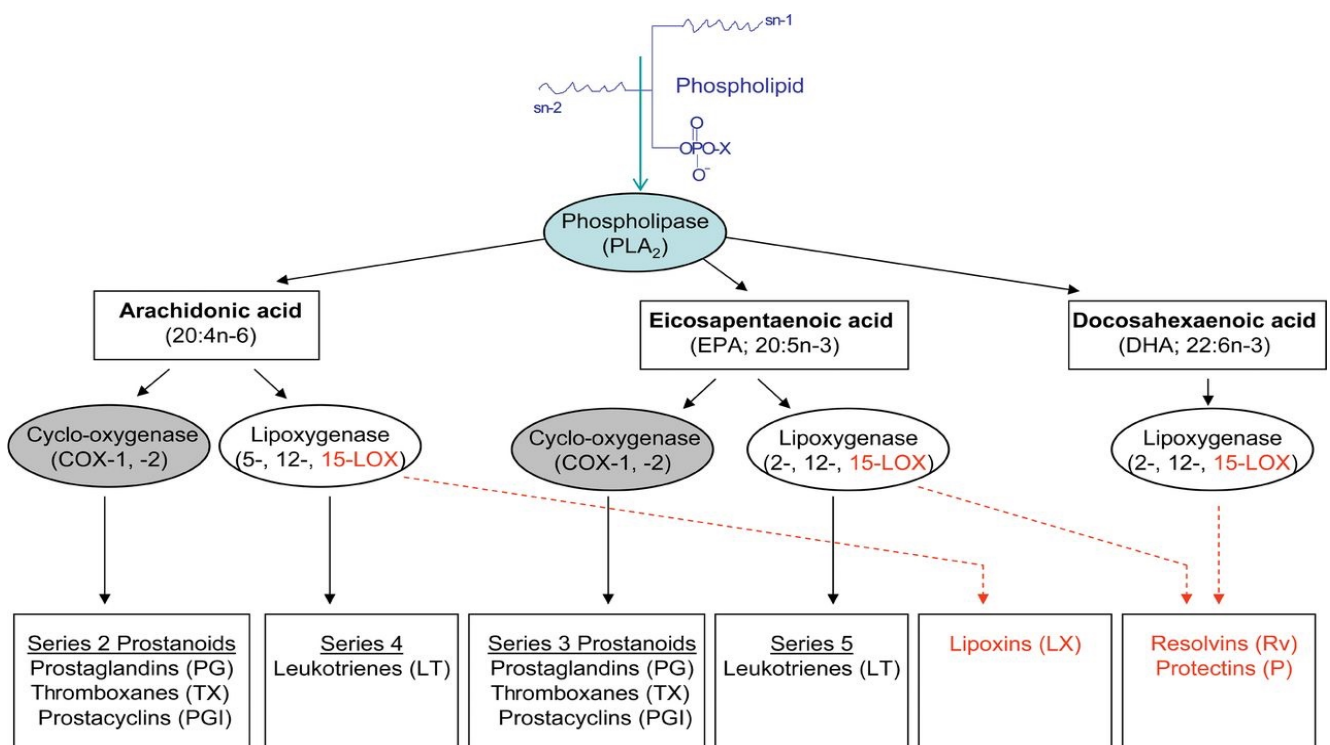


Figure 2: An overview of lipid mediator pathway. PLA₂ enzymes represent the first step in the lipid-signalling pathway. PLA₂ enzymes hydrolyse membrane phospholipids at the *sn*-2 position and liberate arachidonic acid (AA) as well as other polyunsaturated fatty acids (PUFAs). AA is metabolized through cytochrome p-450 (CYP450) (not shown here), lipoxygenase (LOX) and cyclooxygenase (COX) pathway that produces different lipid mediators called eicosanoids. This includes leukotrienes (LTs), lipoxins (LXs) and prostanoids such as prostaglandins (PGs), prostacyclins (PGIs) and thromboxanes (TXs). Ultimately, these lipid mediators will react on its G-protein coupled receptors (GPCRs) on target cell membranes and activate different signalling cascades in the cell. From Flachs *et al.* 2009, with permission (33).

1.2.1 Cytosolic phospholipase A₂ α and role of lipid mediators in cancer

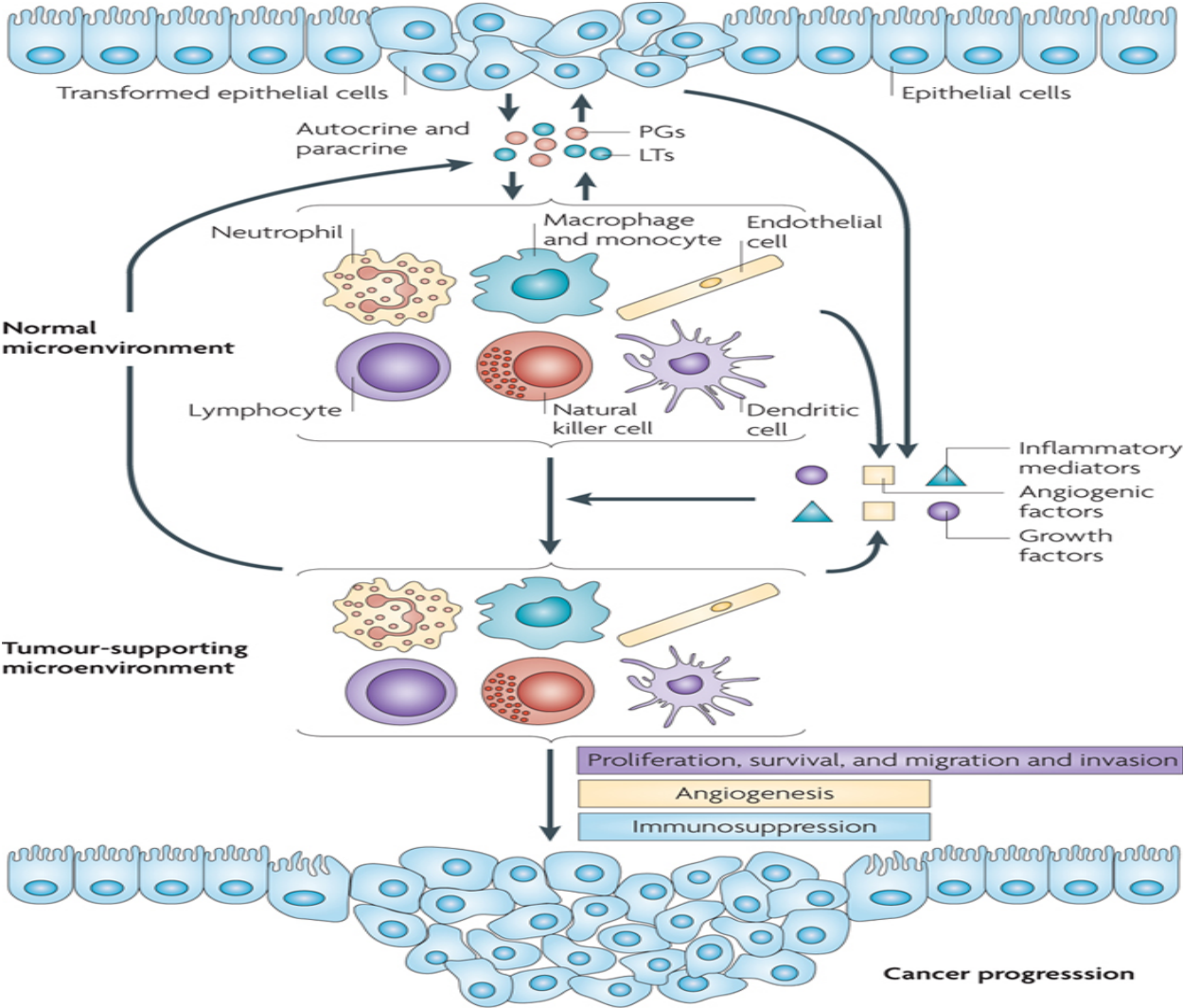
Different groups of cPLA₂s exist, and the most studied of them is GIVA cPLA₂ enzyme (or cPLA₂ α), due to its high specificity to liberate arachidonic acid (AA) and subsequent production of various eicosanoids involved in several pathological and physiological processes (30). This enzyme consists of 749 amino acids, have a molecular weight of kDa 85.2, and is found in a broad range of tissues except lymphocytes (27, 34).

The activity of cPLA₂ α is regulated by an increase in intracellular Ca²⁺ influx, and by phosphorylation. The cPLA₂ α requires Ca²⁺ for translocation from the cytosol to perinuclear membranes, such as the golgi, endoplasmic reticulum (ER) and nuclear envelope. The release of AA from membrane phospholipids, is however, facilitated by phosphorylation of cPLA₂ α on specific serine residues, which is Ser505, Ser727 and Ser515 (30). The enzymes responsible for the phosphorylation of cPLA₂ α on Ser505, Ser727, and Ser515 are mitogen activated protein kinases (MAPKs) such as p38, p42/44, MAPK-interacting kinase (MKK1), and calmodulin kinase II (CamKII) (30, 35). Other kinases involved in the activation of cPLA₂ α and its subsequent release of AA are PI3K through other downstream protein kinases and c-Jun N-terminal kinase (JNK) (36, 37).

AA is metabolised through the lipoxygenases (LOX), cyclooxygenases (COX), and cytochrome p50 pathway after its release. This reaction is further continued by a panel of terminal synthases that transforms the intermediary mediators into various eicosanoids with different physiological effects. Accordingly, these generated lipid mediators, will act on their specific G-protein coupled receptors (GPCRs) on target cell membranes and activate different signalling cascades in the cells (38). The metabolic pathway of AA conversion is reviewed in figure 2.

Eicosanoids, including prostaglandins and leukotrienes are biologically active lipid mediators that have been implicated in various pathological conditions such as inflammation and cancer (39). Prostaglandins and leukotrienes can stimulate tumour progression through several different mechanisms. They can activate their specific receptors on tumour epithelial cells to regulate cell proliferation, apoptosis, migration and invasion. In addition, these lipid mediators can directly stimulate epithelial cells and their surrounding stromal cells (cells in the tumour microenvironment) to secrete growth factors, pro-inflammatory mediators and

angiogenic factors, which change their microenvironment from a normal state to a tumour supporting environment (39). This pathway is demonstrated in figure 3.



Nature Reviews | Cancer

Figure 3: An overview of the events by which prostaglandins and leukotrienes promote cancer progression. Transformed epithelial cells and cells in their microenvironment (stromal cells) play a key role in cancer progression. Tumour epithelial cells and their surrounding stromal cells secrete pro-inflammatory prostaglandins and leukotrienes, which are central mediators in promoting cancer progression and metastasis through different mechanisms. These pro-inflammatory mediators can directly induce epithelial cell proliferation, survival, metastasis and invasion in autocrine and paracrine manners. In addition, these pro-inflammatory lipids can also stimulate epithelial cells and their surrounding stromal cells to generate growth factors, pro-inflammatory mediators and angiogenic factors which turn the cells from a normal state to tumour supporting environment. This tumour microenvironment, in turn, recruits immune cells and endothelial cells (tumour-infiltrating cells), which further produce additional pro-inflammatory mediators, such as eicosanoids, growth factors and angiogenic factors. All these factors contribute in tumour progression and stimulate metastasis through an autocrine loop by inducing angiogenesis and invading attack from the immune system. From Dingzhi and Raymond, with permission (39).

In the last years, several studies have shown dysregulated cPLA₂α activity and induction of downstream AA metabolizing enzymes in many types of cancers. This includes colon cancer (40), prostate cancer (41), lung cancer (42), brain cancer (42), breast cancer, especially BLBC (43), and other cancer types (44). cPLA₂α contribute to the first step of eicosanoid production. As stated earlier, eicosanoids play a central role in tumour progression and therefore cPLA₂α has been suggested as a pharmacological drug target against several cancer types, including breast cancer (44).

Recently, it has been demonstrated that BLBC overexpress the gene PLA2G4A, encoding the cPLA₂α enzyme (45, 46). In the study of Kim *et al.*, the specific cPLA₂α inhibitor, AVX235 (Avexxin AS, Trondheim, Norway) was tested in patient derived xenograft model of BLBC (47). Findings from this study revealed significant tumour reduction upon exposure of AVX235 and show that cPLA₂α inhibition with AVX235 in patient derived BLBC xenografts has anti-angiogenic effects. In this study, AVX235 was able to reduce vessel volume fraction, density and caliber. It was also observed that treated tumours had fewer mature blood vessels and decreased endothelial cell proliferation. Interestingly, these findings indicate that the effects may be due to reduced downstream metabolites of cPLA₂α, such as PGE₂ and lysophosphatidylcholine (LPC) (47).

Because of the multivariate effect of such lipid mediators (38), there is a possibility that the effects produced by the activity of cPLA₂α may also be caused by other mechanisms. More research is however necessary to understand the mechanism(s) behind it and investigate whether other inhibitory pathways, such as cellular apoptosis, also contribute to this context.

1.2.2 Role of cPLA₂α in cell-cycle arrest and apoptosis

As previously mentioned, cPLA₂α is involved in regulating and producing many justified effects in cells. In the last years, researchers have also reported that cPLA₂α plays an important role in regulating the cell cycle (48, 49).

Cells divide by a tightly regulated sequence of events, which leads to formation of two daughter cells. This process consists of four distinct phases where each one has a specific function (G₀-G₁, S, G₂ and M). In the initial phase, G₀, the cells are in a resting stage and are not involved in the cell division process. The process of cell division starts when a cell enters G₁ phase from G₀. During this phase, cells increase in size and proteins required for DNA duplication and transcription are synthesized. After the synthesis of elementary proteins and other factors, cells transit into the S phase (synthesis phase) where DNA is duplicated. This process is followed by an entry into the G₂ phase where cells produce other proteins, increase further in size and prepare for mitosis (M phase, cell division). During the M phase, cell growth stops, and cells start to divide by a coordinated sequence of events, leading to the formation of two daughter cells. Cyclic proteins, called cyclins, cyclin-dependent kinases (CDKs) and their inhibitors (CDK-inhibitors, CKIs, such as p15, p16^{INK4a}, p21 and p27) drive the progression of cell cycle process. To activate or increase the kinase activity of CDKs, cyclins must form a complex with CDKs. When CDKs is activated, they can phosphorylate serine/threonine residues of target proteins, which regulate the progression of the cell cycle (50). In each phase, cells must go through multiple checkpoints before entering the next phase. These checkpoints make sure that each task in each phase is correctly accomplished before further progression of the cell cycle. During these checkpoints, the cells ensure that their size is large enough, DNA damage is repaired and replication is done correctly, and that chromosomes are all well aligned on the spindle before entering the mitosis, as illustrated in figure 4. If the cells cannot repair these problems, cell proliferation stops and the cell cycle progression discontinues, leading to cell cycle arrest (50).

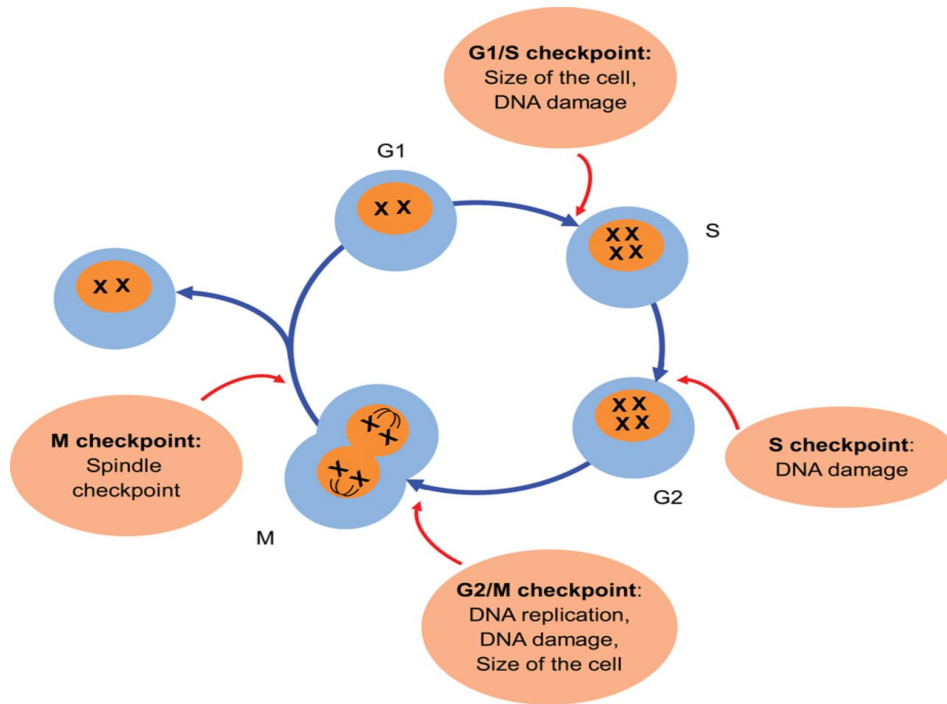


Figure 4. Cell cycle process and checkpoints. Cells divide by a tightly regulated sequence of events, giving rise to two daughter cells. The cell cycle comprises of four phases (G₀-G₁, G₂, S and M), each one with specific tasks. Cyclic proteins, called cyclins, cyclin-dependent kinase (CDKs) and their inhibitors drive the progression of the cell cycle. From Canaud *et al.* 2015, with permission (50).

In the study of Naini *et al.*, cPLA₂ α was found to regulate G₁ progression via PGE₂, signalling (48). PGE₂, an important bioactive lipid mediator and a product of cPLA₂ α activation, acts on the specific receptor, EP₄. Activation of this receptor leads to induction of the PI3K/AKT pathway, which are shown to increase phosphorylation of the transcription factor (TF) and tumour suppressor protein forkhead box O1 (FOXO1) (51). The phosphorylation of this protein promotes its nuclear export, which in turn mediate G₁ progression of the cell cycle. When FOXO1 is not phosphorylated, however, it remains in the nucleus where it can facilitate cell cycle arrest, DNA repair, and apoptosis (51). An important issue to address is that FOXO1 is capable of inducing apoptosis in some cell types, but in other cell types, activated FOXO1 may induce cell cycle arrest with low level of cellular death (52).

Moreover, another study of Movahedi *et al.*, have revealed that cPLA₂ α regulates the G₂-M transition of the cell cycle (49). This mechanism is mediated through inhibition of the activity of the tumour suppressor sirtuin 2 (SIRT2). The SIRT2 plays a significant role in controlling the G₂-M transition checkpoint under cellular stress. However, cPLA₂ α can through

phosphorylation of SIRT2 antagonize the checkpoint function of this protein and promote cell proliferation (49).

1.3 A new targeted treatment: specific cPLA₂α inhibitors

Lately, several specific cPLA₂α inhibitors have been developed. The cPLA₂α enzyme has been proposed as a medicinal target for BLBC as described earlier. Therefore, it is of big interest to investigate the role of this enzyme in BLBC/TNBC to find out whether selective inhibitors of cPLA₂α may be a therapeutic option for BLBC/TNBC. In this subchapter, a number of specific cPLA₂α inhibitors used in this master's project, are briefly introduced.

The trifluoromethyl ketone analogue of ω-6-polyunsaturated fatty acid AA, AACOCF₃ (or ATK) was the first cPLA₂α inhibitor to be reported (30). ATK has been proven to have intermediate specificity towards cPLA₂α and also shown to inhibit the activity of other enzymes, such as cyclooxygenases (53). In various cell based *in vitro* assays, ATK was found to inhibit the activity of cPLA₂α in concentrations ranging from 1-30 μM (54-56).

The Norwegian company Avexxin AS has developed novel selective cPLA₂α inhibitors, which have been studied in *in vitro* and *in vivo* model systems. Results from these studies show effective inhibition of cPLA₂α and further reduction of its downstream metabolites that are implicated in different pathological conditions (57). A specific cPLA₂α inhibitor, AVX002 is a derivate of the ω-3-polyunsaturated fatty acid docosahexaenoic acid (DHA) and has a molecular structure similar to ATK. AVX002 differs from ATK in the way that the methylene group β to the carbonyl group of the ketone in ATK are substituted by a sulphur atom in AVX002 (58). This substitution creates a more electrophilic molecule, assuming to give a more potent inhibitor. In the study of Huwiler and co-workers, AVX002 was shown to inhibit the activity of cPLA₂α in concentrations as low as 126 nM in rat mesangial cells (54). In contrast, ATK blocked the action of cPLA₂α in concentrations from 300 nM, indicating that AVX002 is a more potent inhibitor of cPLA₂α (54). Also, in the study of Sommerfelt and co-workers, SW892 cells were treated with AVX002 in various concentrations and the result showed that AVX002 inhibited tumour necrosis factor (TNF)-induced AA release in a dose-dependent manner with an estimated IC₅₀ (half maximum inhibitory concentration) value of 0.9 ± 0.3 μM. In addition, AVX002 reduced the basal level of AA in concentrations ranging from 0.63-5 μM (59). Later, Sommerfelt and co-workers reported that AVX002 reduced AA and subsequent production of PGE₂ in synoviocytes with 5 μM concentration (60).

In 2013, the company Avexxin modified a new cellular selective cPLA₂ α inhibitor (AVX235) with a different molecular chemistry than AVX002 and ATK. This compound belongs to the group of chemical compounds called thiazolyl ketones. Thiazolyl ketones has two heteroatoms in the heterocyclic ring of the molecule that ensures the activation of the carbonyl group. Moreover, the oxygen atom at the β -position in the molecular structure enforces the activation of this molecule further. AVX235 has been tested in concentrations ranging from 0-20 μ M in synoviocytes *in vitro* models and results shows that AVX235 strongly inhibited the activity of cPLA₂ α from 5 μ M (57).

AVX420 is a further modification of AVX235 and also a thiazolyl ketone. The modification in AVX420 is believed to give a more electronegative atom, which gives a higher specificity to cPLA₂ α (manuscript in progression). The molecular structures of ATK, AVX002, AVX235 and AVX420 are illustrated in figure 5.

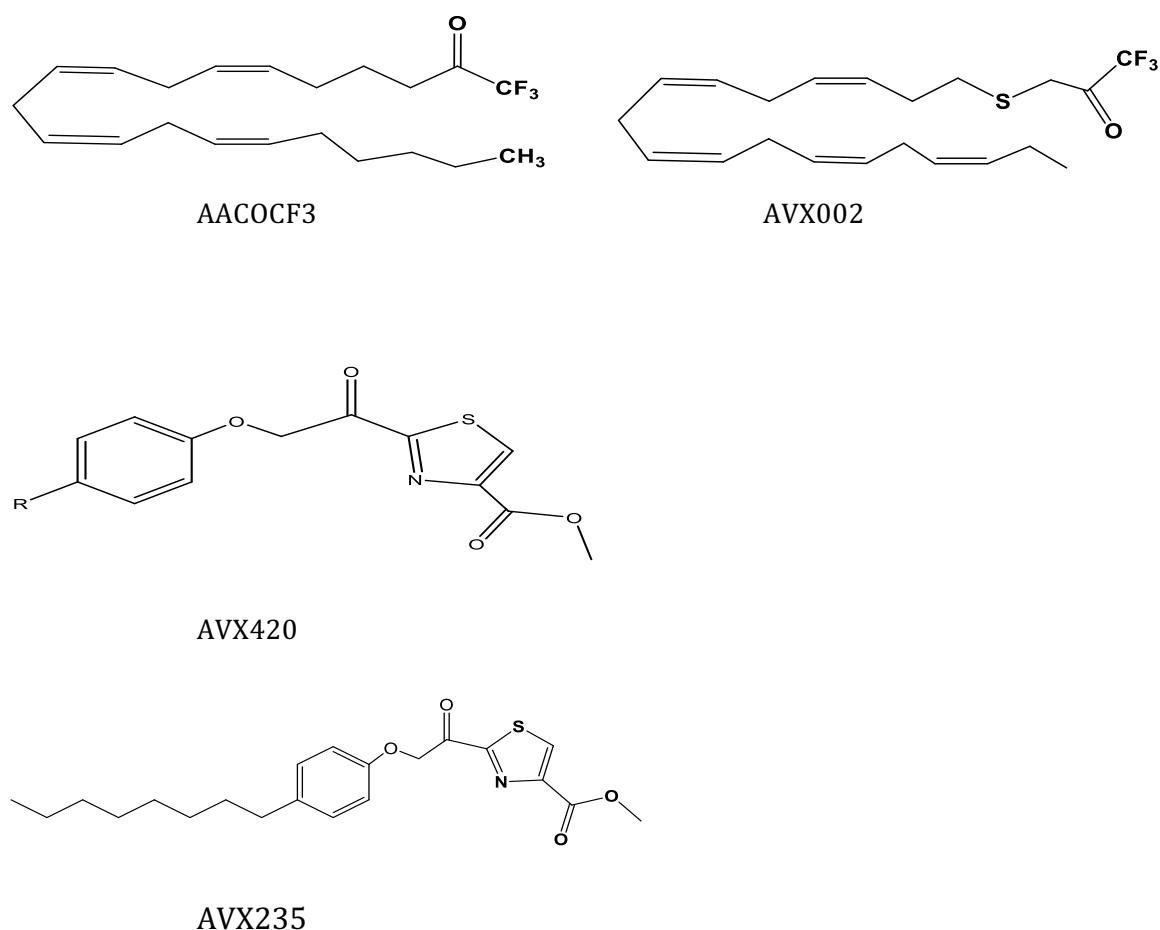


Figure 5: Molecular structure of AACOCF3 (ATK), AVX002, AVX420 and AVX235

1.4 The MDA-MB-468 cell line as an *in vitro* model for BLBC

The MDA-MB-468 cell is a basal-like breast cancer cell line and originates from a 51-year-old black female with metastatic adenocarcinoma of the breast. The MDA-MB-468 cell line was isolated in 1977 by R. Cailleau, *et al.*(61), from a pleural effusion and can be purchased from the American Type Culture Collection (ATCC), which is a private, non-profit biological resource center (BRC) and research organization.

Human cancer cell lines have been established for more than 50 years and the first cancer cell line grown in culture were HeLa cells in 1951 (62). Cancer cell lines have since then been a useful tool for studying molecular biology, genetics and cancer therapy. The advantages of using established cell lines are that they represent the same morphological and molecular features of the tissue they were derived from. Use of cancer cell line to study therapeutic effects, however have also their disadvantages, due to the fact that cultured cells lack the optimal cell growth conditions, such as their surrounding microenvironment (63).

MDA-MB-468 cells overexpress EGFR and transforming growth factor alpha (TGF α) receptor (64). Usually, in many normal and malignant cells, activation of EGFR by EGF results in increased cell proliferation and resistance to cell death. However, exposure of EGF in MDA-MB-468 cells leads to apoptosis and growth inhibition (65, 66). These effects are mainly evident in cells treated with EGF in serum free media, which means that all growth factors are removed from their cultivation medium. A possible explanation for this phenomenon is that EGF activates its receptor, but in the absence of other essential growth factors, such as in serum free media, the cells cannot complete cell proliferation. Instead, these cells activate their apoptotic machinery and commit suicide (66). Another important issue is that MDA-MB-468 cells have a high frequency (44-82%) of p53 mutations, which make the cells highly resistant to apoptosis (23, 67). Defects in the apoptotic cell death mechanism are central in the pathogenesis of many cancers (23). As stated earlier, damage in double-stranded DNA usually results in cell cycle arrest and cell death by apoptosis. However, in the presence of p53 loss of function mutations, this protein has no longer the ability to induce apoptotic cell death. The cells therefore become resistant to cell cycle arrest and apoptosis (23).

The MDA-MB-468 cell line is a BLBC cell line that lack the expression of ER, PR and HER2 (EGFR2) and can therefore be used as a model for studying the effects of TNBC and BLBC *in vitro*.

1.5 The aims of this thesis

BLBC is an aggressive type of breast cancer with limited therapeutic options due to the complexity of this disease and the fact that these patients do not respond to any available targeted treatments such as ER-, PR- antagonists and antibodies against HER2-receptor. Currently, there are no established targeted therapies against BLBC/TNBC (13). Although many agents that specifically aim to target this breast cancer subgroup are suggested, there are many adverse side effects related to these compounds (68, 69). Moreover, some of these compounds have had limited response in the overall survival in BLBC/TNBC patients, with tendency of developing resistance towards the treatments (23). Therefore, there is still urgent need for new compounds that can offer these patients better optional choices with less harmful effects (7).

Given the important effects of $cPLA_2\alpha$ and its downstream metabolites in cancer and angiogenesis, it is of great interest to investigate this phenomenon further and explore the possibility of $cPLA_2\alpha$ as a therapeutic target for BLBC/TNBC (47). To our knowledge, few researchers have investigated the exact role of $cPLA_2\alpha$ in cell proliferation in BLBC/TNBC. Hence, the main objective of this master project was to investigate whether $cPLA_2\alpha$ inhibitors affects cell proliferation and/or cell viability in the MDA-MB-468 cells. If so, were the effects on cell proliferation and viability due to apoptosis and/or cell cycle arrest?

Another goal of this master project was to evaluate the possible synergistic or additive effects of combining $cPLA_2\alpha$ inhibitors with selective mTOR/PI3K inhibitors, such as dactolisib (BEZ235), alpelisib (BYL719) and buparlisib (BKM120), which themselves represent a promising treatment strategy for BLBC/TNBC(70-72). This co-treat strategy of combining two specific inhibitors that target different cellular pathways may in turn open for more effective treatment, possibly reduce adverse effects and lower resistance problems.

Based on the information given in this chapter and the above statements, the aims of this project are to:

- 1) Establish the MDA-MB-468 cell line as a BLBC/TNBC cell model**
- 2) Investigate cell proliferation of the MDA-MB-468 cells when treated with different cPLA₂ α inhibitors and other comparative drugs/inhibitors**
- 3) Study whether cPLA₂ α -inhibitors and/or other comparative drugs/inhibitors affects apoptosis and/or the cell cycle of MDA-MB-468 cells**

2 MATERIALS AND METHODS

2.1 Reagents solution and materials

All equipment such as reagents, solutions, pipettes and other materials used in this master thesis are listed in the following section.

Cell cultivation, growth curve and cell experiments:

The MDA-MB-468 cell line was obtained from ATCC. The cells were cultivated and maintained in 75 cm² vented flasks, from Sarstedt. Similarly, 25 cm² flasks were used to make growth curves. Roswell Park memorial institute medium (RPMI-1640), L-glutamine, Gentamycin, dimethyl sulfoxide (DMSO) was from Sigma-Aldrich. Fetal bovine serum (FBS) and trypsin-EDTA 0.05 % was from Gibco. The phosphate buffered saline (PBS) was from Oxoid. For the viability assays, Resazurin from R&D Systems were used. The different cPLA₂α inhibitors and comparative drugs used in cell experiments are listed in table 2.1 along with their supplier.

Inhibitor	Supplier	Target
AVX235	Prof. George Kokotos, University of Athens, Greece	cPLA ₂ α
AVX420	Prof. George Kokotos, University of Athens, Greece	cPLA ₂ α
AVX002	Synthetica AS, Oslo, Norway	cPLA ₂ α
ATK (AACOCF3)	Cayman chemicals, USA	cPLA ₂ α
EGF	Sigma-Aldrich, Norway	EGFR
Etoposide	Sigma-Aldrich, Norway	Topoisomerase II
Doxorubicin	Cayman Chemicals, USA	Topoisomerase II
Methotrexate	Sigma-Aldrich, Norway	Dihydrofolate reductase
BEZ235	Cayman Chemicals, USA	mTOR/PI3K
BKM120 (Buparlisib)	Selleck Chemicals, USA	Selective PI3K-inhibitor of p110α/β/δ/γ
BYL719 (Alpelisib)	Selleck Chemicals, USA	PI3Kα

Apoptosis Assay:

For the apoptosis assay, the Caspase-GLO® from promega and a digital plate shaker from IKA® MS3 were used. The plate reader from Biotek was used for luminescence analysis. White 96-well plate with a flat and clear bottom was from Corning.

Cell-cycle assay:

Methanol 100 % solution was from VWR, RNase 200 µg/mL from Sigma-Aldrich and Propidium Iodide 40 µg/mL from Fluka. The 6-well plate was from Corning.

2.2 Cell culture and cell experiments:

The MDA-MB-468 cells were cultured using 75 cm² cell culture flasks. The cells were grown in RPMI-1640 growth medium with 10 % FBS, 3 % L-glutamine and 0.1mg/mL gentamycin added. RPMI-1640 containing 10 % FBS is referred to as RPMI/10 % FBS in the following chapters.

The cells were maintained and split at sub-confluent state every 3-4 days in a sterile LAF-cabinet. Cells were counted and 1000 000 cells were transferred to the cultivation flask each time cells were split. The cells were split by washing the cells twice with 10 mL room tempered PBS, adding 1.5 mL of preheated (37 °C) 0.05 % trypsin-EDTA and incubating the cells for 4-5 minutes at 37 °C. To loosen the cells from the surface of the flask, the flask was gently tapped against the lab bench. Trypsin was deactivated by adding RPMI/10 % FBS approximately 4 times the volume of trypsin. The solution was then transferred to a 15 mL centrifuge tube and centrifuged at 700 rpm and 25 °C for 5 minutes. After centrifugation, the supernatant was discarded and cells were re-suspended in fresh growth media. The cells were then counted by using Bürcher chamber or automatized cell counter from Biorad. Cells were transferred to a tissue flask with 9 mL fresh preheated (37 °C) RPMI/10 % FBS growth media and incubated thereafter in a humidified 5 % CO₂ incubator at 37 °C.

For the cell experiments, the remaining cells were diluted using preheated (37 °C) fresh RPMI/10 % FBS medium until the desired cell concentration was obtained. Experiments were conducted using both serum-free RPMI (SF-RPMI) i.e. media containing only gentamycin and L-glutamin without FBS and RPMI/10 % FBS.

2.3 Establishing the growth curve of MDA-MB-468 cell:

A growth curve is an empirical model for characterizing the development of cell growth over time. Cells in culture grow either in adherent way i.e. they grow attached to a surface (anchorage dependent), or in suspensions (anchorage independent). The MDA-MB-468 cells are adherent cells and grow only when attached to the surface of the flask. The characteristic growth pattern of most adherent cells consists of four phases: lag, log, stationary or plateau and decline phase. The lag phase indicates the initial phase after seeding of the culture vessel. During this phase, the cells grow slowly due to the stress that they are introduced to in sub-culturing, or due to the fact that they are very few in numbers and lack cell-cell communication. In the lag-phase cells use their energy to attach to the surface and other basal metabolic activities. As the cells recover from the stress caused by sub-cultivation and increase in numbers, they enter the log phase. During the log-phase cells starts to grow exponentially until the growth surface is entirely covered with cells. When cells occupy all surface area, cell proliferation reduces and stops and the cells enter the stationary phase. During the decline phase, the cells lose viability and their number decreases. To maintain cell viability, genetic stability and phenotypic stability, the cells need to be sub-cultured in the log phase i.e. when cells grow exponentially (73).

Determining cell density of the culture flask is also important to define the growth surface area of cells. Confluence is often used to describe this phenomenon and refers to the proportion of the surface area that is covered by cells. In the lag phase, the confluency is very low and the surface area covered with cells range from 0-40 %. In sub-confluence state, there is available space for the cells to grow. At this stage the cell growth is exponentially and the confluency is between 50-85 %. When cells cover the entire surface area i.e.100 %, the available growth area is utilized and all the cells will be in contact with other cells. At this stage the cells have reached stationary phase and are confluent. Cells that are confluent stops dividing due to contact inhibition and may start to express specific features of the differentiated mature cells.

Cells were seeded at 50 000, 250 000 and 750 000 cells per culturing flask in RPMI/10 % FBS at day 0. The cells were then observed daily for 8 days. For each cell concentration, 8 culturing flasks were used, one flask for each day. Culturing flasks were labeled with the different cell numbers and marked from 1-8 for each counting day. The 3 flasks with different cell seedings were counted using a Bürcher chamber for each day with 3 technical repeats. At

day 3 the growth medium of flasks numbered from 6-8 were changed. Prior to counting, confluency of the cells in different flasks containing different initial cell number was determined for each day. Confluency below 40 % is referred as C<40 %. The growth curve experiment was repeated 2 times and the last experiment is presented as a representative for all experiments.

2.4 Dose-Response:

A dose-response experiment has the intention to determine the relation between the doses that induces a visual/measurable effect and the doses that does not. The purpose of the experiment was to validate the minimal dose of the inhibitors/comparative drugs that induces effects on MDA-MB-468 cells. Visual effects such as cellular death, phenotypic changes, morphologic changes and reduced cell proliferation were used to validate the effects. Moreover, resazurin was used as a viability assay to determine the viability of MDA-MB-468 cell when treated with different inhibitors/comparative agents/ and or marketed drugs.

Resazurin, also known as Alamar blue, is a redox dye that is often used as an indicator in cell viability assays. The assay is based on metabolically active cells that can reduce resazurin to pink resorufin and dihydroresorofin, which can be measured colorometrically or fluorometrically. Viable cells have high metabolic activity and are capable of reducing resazurin to resorufin and this reduction is directly proportional to the number of viable cells present in the medium. Hence, resazurin can provide us information about cell proliferation/viability in a sample (74).

The dose-response experiment was performed for each therapeutic agent in a similar setup. The choice of concentration range was taken from earlier studies reported in the literature, which was carried out in similar cell lines or in the MDA-MB-468 cells. Relevant papers used as basis for the dose-response experiments conducted in this master's project, along with their mechanism of action, are listed in table 2.2.

MDA-MB-468 cells were seeded in a 96-well plate with 5000-7000 cells per well. The cells were incubated for 24-48 hours to adhere and until the confluency of the cells reached ~60 %, i.e in a sub-confluent state where the cells grow exponentially. The 96-well plate were divided in half where 48 wells contained SF-RPMI and the 48 other wells contained RPMI/10 % FBS. 4-5 columns of the 96-well plate were treated with different concentrations of compounds,

starting from high to low concentrations. 1-2 columns in each plate were used as control for cells treated in RPMI/10 % FBS and 1-2 columns with SF-RPMI. The columns used as controls were not treated with any inhibitor-/inducer/comparative drug and contained only growth media. Cells were observed in the microscope after 6 hours, 12 hours, 24 hours, 48 hours and 72 hours exposure of the test compounds. Each set of experiment was repeated independently 3-4 times. The observed results were noted each day of the experiment. In the end of each experiment (i.e 72 hours after exposure), cells were treated with 10 μ L/well i.e. final concentration 10 % ($C_f=10$ %) resazurin and incubated for 2-3 hours in a humidified CO₂ incubator at 37 °C. Most inhibitors/inducers used in this master thesis were dissolved in DMSO, thus one 96-well plate were treated with 10 μ L of DMSO in each well (equals the highest volume of agent added in each well) and compared to a control with no treatment. The fluorescence reading was recorded with excitation (λ_{ex}) wavelength of 544 nm and emission (λ_{em}) wavelength of 590 nm. The duration, stock concentrations, and the different concentrations of inhibitor used in the dose-response experiment are listed in table 2.3.

Table 2.2: List of inhibitors/inducers with their mechanism of action, documentation from different studies were these compounds have been tested in different assays and in various cell types.

Cell line	Compound	Mechanism of action/target protein	References
MDA-MB-468	EGF	Targets EGFR; EGF is a growth factor that stimulate proliferation, cell growth and differentiation (75). Normally activated EGFR leads to increased cell proliferation, cell survival and inhibition of apoptosis. In MDA-MB-468 cells, high levels of EGF in serum free media leads to apoptosis (66).	10-100 ng/mL of EGF have induced programmed cell death in MDA-MB-468 cells (66, 76)
MDA-MB-468 HL-60: human progranulocytic leukemia	Etoposide	Etoposide is a DNA topoisomerase II inhibitor. Inhibition of topoisomerase II induces the production of DNA breaks that stimulates programmed cell death or apoptosis. Etoposide acts in the S-phase and G-phase of the cell cycle and prevents the cells from going in the mitosis phase (77).	Have shown to induce apoptosis from 0.2 -100 μ M (78-80)
MDA-MB-468	Doxorubicin	Doxorubicin intercalates between DNA base pairs, inhibits topoisomerase II and induces steric obstruction, which lead to inhibition of DNA and RNA synthesis. Doxorubicin interacts at points of local uncoiling of the double helix and also binds to iron and produce iron-doxorubicin complex. The iron-doxorubicin complex can bind DNA and cell membranes and produce free radicals (81). Doxorubicin is a well-known cytotoxic drug and are commonly used chemotherapy in breast cancer.	Induces apoptosis in range 0.1- 25 μ M (82, 83)
ZR-75 (human breast cancer cells)	Methotrexate	Folic-acid antagonist: Methotrexate irreversibly binds to and inhibits dihydrofolate reductase and inhibits formation of reduced folate and thymidylate synthetase. This leads to inhibition of purine and thymidylic acid synthase, which interacts with DNA synthesis, repair and cell replication. Methotrexate act specifically in the S-phase of the cell cycle (84).	Induces apoptosis in range 10-100 μ M with maximum inhibition at 100 μ M (85)
MDA-MB-468	Alpelisib/-BYL719	Inhibits PI3K α , an important protein kinase in cell proliferation signaling. Several studies point to this protein as a central enzyme in cell proliferation and survival signaling in cancer (86). This compound are currently under clinical trials in solid tumors.	IC50:>10 μ M (86)
MDA-MB-468	Buparlisib/-BKM120	Selective PI3K-inhibitor of p110 $\alpha/\beta/\delta/\gamma$: Aberrant PI3K- signaling has been implicated in the pathogenesis of many cancers and therefore is highly requested molecular target against several types of cancers (86). This compound are currently under clinical trials in solid tumors.	IC50: <1 μ M (86)
MDA-MB-231	Dactolisib/-BEZ235	mTOR/PI3K- inhibitor: Is a dual inhibitor of PI3K/mTOR. A dysregulation of the PI3K/mTOR pathway is frequently observed in many types of tumours. Hence, targeting this pathway is of big interest in cancer therapy (86).	Tested in concentrations ranging from 0.1-100 μ M in growth inhibition assays (87)
-	AVX420	cPLA ₂ α -inhibitor: Inhibits the cPLA ₂ α enzyme by blocking its active site, leading to reduced release of AA from membrane phospholipids.	Currently, no data are available
SW982	AVX235	cPLA ₂ α ; inhibits the cPLA ₂ α enzyme by blocking its active site, leading to reduced release of AA from membrane phospholipids.	Is shown to inhibit cPLA ₂ α in doses from 0.3-20 μ M <i>in vitro</i> assays (57)
Mesangial cells	AVX002	cPLA ₂ α -inhibitor: inhibits the cPLA ₂ α enzyme by blocking its active site, leading to reduced release of AA from membrane phospholipids.	Have shown to inhibit cPLA ₂ α in doses from 0.1-10 μ M with maximum effect shown at 10 μ M (54, 59, 76)
SW982 Mesangial cells	ATK	cPLA ₂ α -inhibitor; inhibits the cPLA ₂ α enzyme by blocking its active site, leading to reduced release of AA from membrane phospholipids. This compound also inhibit COX-enzymes.	Is shown to inhibit cPLA ₂ α from 0.3-20 μ M (54)

Table 2.3: Overview of tested compounds, concentration range and duration of exposure time in dose-response experiments.

Agents	Stock concentration	Concentration	Duration (hours)
AVX002	20 mM diluted in DMSO	1-100 μ M	72 hours
AVX235	20 mM diluted in DMSO	1-100 μ M	72 hours
AVX420	20 mM diluted in DMSO	1-100 μ M	72 hours
ATK	20 mM diluted in DMSO	1-50 μ M	72 hours
Etoposide	50 mM diluted in Chloroform	10-120 μ M	72 hours
Doxorubicin	10 mM diluted in DMSO	0.5-10 μ M	72 hours
Methotrexate	20 mM diluted in DMSO	1-100 μ M	72 hour
EGF	200 ug/mL diluted in PBS	10-100 ng/mL	72 hours
BEZ235	5 mM diluted in DMSO	1-100 μ M	72 hours
BKM120 (Buparlisib)	20 mM diluted in DMSO	0.5-20 μ M	72 hours
BYL719 (Alpelisib)	20 mM diluted in DMSO	1-100 μ M	72 hours

2.4.1 Combination treatment of cPLA₂ α and selective PI3K inhibitors

To assess the effects of cPLA₂ α inhibitors and PI3K inhibitors on the viability of the MDA-MB-468 cells, several combination treatments were conducted. The experiment setup was similar as the dose-response experiment, except that the cells were treated in SF-RPMI for 24 hours before adding resazurin and using the plate-reader. Cells were treated with various types of selective cPLA₂ α inhibitors or a selective PI3K-inhibitor (one column for each treatment). In addition, each selective cPLA₂ α inhibitor, were combined with one selective PI3K-inhibitor. For each treatment, 6-8 parallels were used. The different concentrations of the inhibitors used in this experiment are listed in table 2.4 below.

Table 2.4: Overview of the concentrations used in the combo-treatment experiment.

Mono-treatment	Concentration	Combo-treatment Buparlisib/ BKM120	Combo-treatment Dactolisib/BEZ235	Combo-treatment Alpelisib/BYL719
AVX002	5 – 7.5 μ M	5 μ M + 2 μ M	5 μ M + 5 μ M	5 μ M + 5 μ M
ATK	5 – 7.5 μ M	7.5 μ M + 2 μ M		
AVX235	5-20 μ M	10-20 μ M + 2 μ M	5 μ M + 5 μ M	5 μ M + 5 μ M
AVX420	7.5- 20 μ M	10-20 μ M + 2 μ M	5 μ M + 5 μ M	5 μ M + 5 μ M
Buparlisib/BKM120	2 μ M			
Dactolisib/BEZ235	5 μ M			
Alpelisib/BYL/719	5 μ M			
Doxorubicin	1-5 μ M			
DMSO	4-6 μ L			

2.4.2 Caspase-3 and -7 assay

Caspase-Glo® 3/7 assay is a luminescent assay that measures caspase-3 and 7-activities in cultured cells and purified enzyme formulations. The caspase-3 and caspase-7 are members of cysteine aspartic acid-specific proteases (Caspase) family of proteolytic enzymes that plays a central role in apoptosis (88). This assay will provide information about apoptosis by measuring the caspase activity of the cells, which is proportional to the amount of apoptotic cells in a sample. When using this assay, a proluminescent caspase 3/7 substrate is produced, which contains the tetrapeptide sequence of DEVD (Aspartic acid- Glutamine- Valine – Aspartic acid). This substrate is cleaved to release aminoluciferin, which is a substrate of luciferase used in the production of light. Adding the Caspase-Glo® reagent mix to the cells results in cell lysis followed by caspase cleavage of this substrate and production of a luminescent signal, produced by luciferase. This luminescence signal is proportional to the amount of caspase activity present in the sample (89).

The main objective of this caspase assay was to investigate whether different agents induce apoptosis or other inhibitory mechanisms such as necrosis in MDA-MB-468 cells. A combination of buparlisib/BKM120 with different cPLA₂α inhibitors was used to investigate whether cPLA₂α alone is involved in apoptosis and if combined with PI3K inhibitors there is a possible synergistic/additive effect. Caspase assay was performed on MDA-MB-468 cells in sub-confluent state plated in white 96-well plates at 7000 cells per well in 100 μL RPMI/10 % FBS. Due to the risk of edge effects, only the inner 60 wells of the plates were used. Instead, 100 μL of PBS was added to the uttermost wells of the plates. After seeding, the cells were incubated over night to adhere. Next day, the media from the cells was replaced with SF-RPMI containing different concentrations of single inhibitors/agents and combination of two inhibitors: cPLA₂α inhibitor and buparlisib/BKM120 (pan-PI3K inhibitor). After treatment, the cells were incubated for 5 hours in 37 °C. The concentration of the inhibitors is listed in table 2.5. The cells were treated with AVX002 in mono treatment and combined with buparlisib/BKM120. The same goes for AVX235 and AVX420 were one column was used for mono treatment and one for combination treatment. One column of the 96-well plate was used as a apoptosis control, these cells were treated with 5 μM doxorubicin, which is a commonly used apoptosis inducer. Also, 4 μL of DMSO (equals the highest volume of inhibitors added to each solution) was dissolved in SF-RPMI and added to one column. In addition, one column was used as control with no treatment in this experiment. After 5 hours of incubation, the cells were treated with Caspase-Glo®. The Caspase-GLO was taken out from freezer -20 °C and equilibrated to room temperature. Thereafter the content of Caspase-GLO® 3/7 buffer was mixed with the Caspase-GLO® substrate and 70 μL of the solvent was added to each well. When the assay was performed, one well was used as a blank reaction which contained only SF-RPMI and no cells. Also, one well was used as a negative control which contained cells with SF-RPMI. The blank reaction was used to measure the background luminescence associated with the cell culture system. The cells were thereafter read in a plate reader equipped for chemiluminescence detection. When the results were analysed the values of the blank reaction was subtracted from the experimental values.

Table 2.5: Concentration of the inhibitors used in the caspase assay.

Mono treatment concentration	Combo-treatment Buparlisib/ BKM120 concentration
AVX002 5 μ M	5 μ M + 5 μ M
AVX235 20 μ M	20 μ M + 5 μ M
AVX420 20 μ M	20 μ M + 5 μ M
Buparlisib/BKM120 5 μ M	
Doxorubicin 1 μ M	

2.5 Cell-cycle assay

Flow cytometry is a rapid method used to measure the optical and fluorescence characteristics of cells. It includes measurements of different characteristics such as cell size, cytoplasmic complexity, DNA or RNA content and also a broad variety of other proteins in the cells. Flow cytometry can also be used to analyse blood samples, bone marrow, serous cavity fluids, cerebrospinal fluid, urine and solid tissues. To be able to measure these characteristics, the samples must be pre-treated with certain fluorescent dyes that can bind and intercalate to different cell components such as DNA or RNA. The dyes commonly used for these purposes, include propidium iodide, phycoerythrin and fluorescein (90).

Cells were plated at 150 000 cells per well in a 6-well plate and incubated at 37 °C for 24 hours to adhere and to reach ~60 % confluency. After 24 hours, the cells were treated with 8.0, 5.0 and 2.0 μ M AVX002, 3.0 μ M buparlisib/BKM120 (pan PI3K-inhibitor) and 1 μ M doxorubicin diluted in SF-RPMI. Moreover, the 8.0 μ M, 5.0 μ M and 2.0 μ M AVX002 were combined with 3.0 μ M BKM120 and cells were incubated for 24 hours in 37 °C. The experiment was performed with six technical repeats for each condition and two biological replicates.

2.5.1 Fixing and permeabilizing cells

After 24 hours of treatment, the cells were detached from their surface by removing the media and adding ~0.5 mL 0.05% trypsin-EDTA to each well and incubated for ~7 minutes. The trypsin was deactivated by adding RPMI/10 % FBS 4 times the volume of trypsin (i.e 2 mL) to the cells and transferred to 15 mL centrifuge tubes. Next, the cells were resuspended and centrifuged for 5 min at 1500 rpm and the supernatant was thereafter discarded. The cells were then resuspended in ice cold methanol (-20 °C) very gently, due to the risk of clumping and fragile condition of the cells. Next, the tubes were labeled and frozen at -20 °C until further processing.

2.5.2 Removal of RNA

After fixation, the cells were centrifuged at 1500 rpm for 5 minutes, the supernatant was removed and the cells were resuspended in 2 mL of 200 µg/mL RNase. Thereafter, the cells were left at room temperature for 30 minutes.

2.5.3 Staining the cells and analysis by using flow cytometer

After removal of the RNA, the cells were again centrifuged at 1500 rpm for 5 minutes and resuspended in propidium iodide 40 µg/mL. The samples were analysed by using the Beckman Coulter flow cytometer at the Department of Physics at NTNU.

2.6 Statistical analysis

Student's t test was used to determine a significant difference between two groups for the viability assays. *P* values <0.05 were considered statistically significant. Significance levels are indicated in the figures and tables. The error bars represent mean values with ± standard deviation (SD). Cell cycle profiles were created using the Kaluza 1.1 software program. The Excel program was used to determine the slope and the log phase of the entire growth curve experiment.

3 RESULTS

3.1 MDA-MB-468 cells do not enter stationary and decline phase

Cells grown in culture have generally four distinct growth phases: lag, log, stationary and decline phase. In each phase the frequency of mitosis differs due to several factors influencing the growth of the cells, such as metabolic activity, cell-cell contact, protein synthesis and the presence of serum in the culturing media. The purpose of the growth curve experiment was to investigate the proliferative rate of different cell seeding densities of the MDA-MB-468 cells in culture, which is a major factor when conducting experiments to study cell proliferation.

MDA-MB-468 cells were seeded at 50 000, 250 000 and 750 000 cells per culturing flask in RPMI/10 % FBS. Cells seeded at 50 000 cells per flask never entered the log phase, and continued in the lag phase during the whole 8-day experiment. Cells seeded at 250 000 cells per flask, on the other hand, reached the log phase at day 4 and stayed in this phase the remaining days of the experiment. Cells seeded at 750 000 cells per culturing flask reached the log phase at day 2 and also continued in this phase throughout the whole experiment. None of the flasks containing different cell concentrations reached the plateau and/or stationary phase. The cells seeded at 250 000 cells per flask and 750 000 cells per flask continued to grow exponentially even though the total growth surface area was occupied (figure 6). Also, the flasks with the highest cell density had more cells floating in their growth medium and for each day this trend increased gradually. The flasks that had their growth media replaced with fresh media had higher growth rate compared to the first days (figure 6). The growth curve experiment conducted in this master thesis is similar to the ATCC growth curve for MDA-MB-468 cells (91). It was observed that the MDA-MB-468 cells grow multilayers when the cells became denser in the flasks. This was observed under high microscope magnification where it was possible to see the cells grow on top of each other.

Growth curve 1

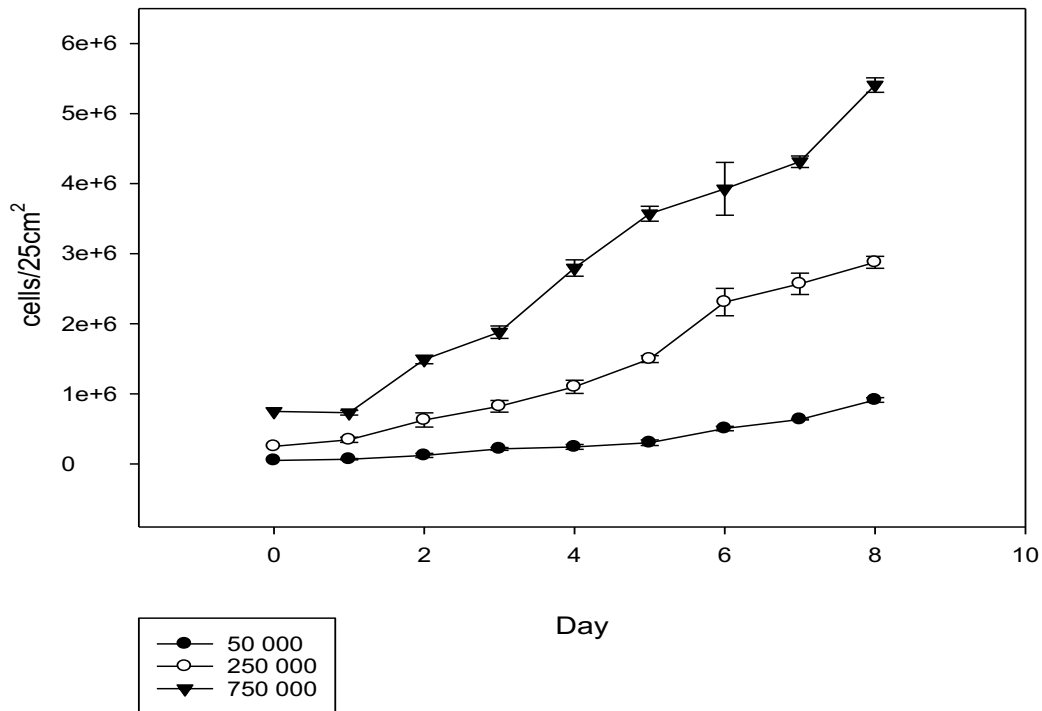


Figure 6: Growth curve of MDA-MB-468 cells that were plated in 25 cm² tissue flasks with different cell densities. The y-axis indicates the average number of cells per flask for each day of the experiment. The last experiment is shown as representative of two independent growth curve experiments. The error bars show standard deviation after three technical counts.

The population doubling time (PDT) for cells seeded at 250 000 cells per flask and 750 000 cells per flask was calculated by using formula (1). Cells seeded at 50 000 cells per flask did not reach the exponential growth phase and therefore the PDT was not calculated for these cells.

$$DT = T \ln(2) / \ln(X_e / X_b) \quad (1)$$

T = the incubation time at the beginning in any unit

X_b = the beginning of the incubation time

X_e = the cell number at the end of the incubation time (73).

The PDT was considerably higher in the highest initial cell seeding (750 000 cells per flask) and lower in cells seeded at 250 000 cells per flask (table 3.1). The PDT after the cells had reached the log-phase was calculated to be approximately 42 hours for cells seeded at 250 000 cells per flask and 46 hours for cells seeded at 750 000 cells per flask.

Table 3.1: The population doubling time (PDT) of the growth curve experiment.

<i>Primary cell number</i>	<i>Population doubling time (PDT)(hours)</i>
50 000	-
250 000	~ 42
750 000	~ 46

Cell confluency is a term used to estimate the total surface area of the tissue flask that is covered with cells. It is often designated as the percentage of available growth area that is occupied by cells.

Cells plated at 50 000 cells per flask, never reached the log phase and the confluency remained $C < 40\%$ during the whole 8-day experiment. At this seeding density, cells grew in “patches” or colonies and were not evenly spread in the flasks. In addition, cells at this cell density had low proliferative progress in contrast to the other cell densities. The highest confluency of the flask with initial seeding at 50 000 cells, barely reached 35 % confluency. Cells seeded at 250 000 cells per flask reached 40 % confluency at day 2 and had a large increase in confluency the day after and continued in this process until the end of the experiment. The last day of the experiment, cells seeded at 250 000 cells per flask had become 100 % confluent and the total culturing flask was covered with cells. Cells seeded at 750 000 cells per culturing flask had 60 % confluency day 1 of the experiment and reached 100 % confluency at day 5 (figure 7). Even though cells seeded at this density were 100 % confluent and the total flask was covered with cells, cells kept increasing in numbers (figure 6).

Cells confluency

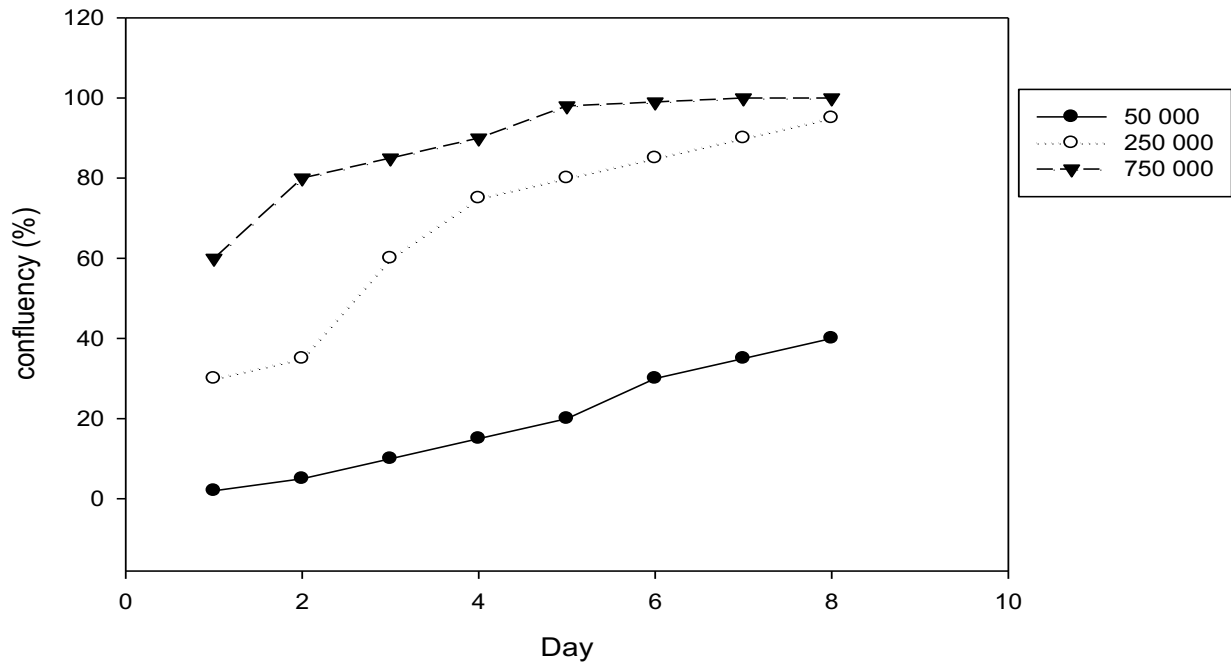


Figure 7: Progression of cell confluency each day of the 8-day experiment. The graph shows one curve for each cell number plated in different 25 cm² tissue flasks. Following the 8-day growth curve experiment, cells with the highest cell seeding density reached 100 % confluency during the first 4-5 days, while the lowest cell seeding density barely reached ~35 % confluency. The figure shows the last experiment as a representative of two independent growth curve experiments.

In summary, cell density of 250 000 and 750 000 cells per 25 cm² tissue flask are optimal cell densities for conducting experiments for cells in exponential proliferative growth. These results are important to address when performing experiments where cell confluency and cell density are essential.

3.2 Methotrexate, doxorubicin, etoposide and EGF as apoptosis-inducing agents

Doxorubicin, etoposide and methotrexate are well-known chemotherapeutic drugs used for treatment of many types of cancers (92). EGF, which is known to increase proliferation has also shown to induce apoptosis in the MDA-MB-468 cells due to their over expression of EGFR (76). Therefore, the purpose of this experiment was to study their effects on the viability of the MDA-MB-468 cells using the resazurin viability assay. EGF was included to compare the effects of this growth factor and commonly used chemotherapies/or apoptosis inducing agents.

DMSO is frequently used for dissolving compounds/agents/inhibitors and for making stock solutions in different concentrations in our lab. DMSO is however toxic for cells in high concentrations. Therefore, we tested the highest DMSO load that equalled the highest amount of the inhibitors/agents/compounds used in our experiments. This was done in order to exclude the possible cytotoxic effects of DMSO on the viability of the MDA-MB-468 cells.

Cells were seeded in 96-well plates at desired cell density and incubated in 37 °C for 24 hours to adhere. Next, cells were treated with different drugs/or compounds in SF-RPMI and RPMI/10% FBS for 72 hours. The viability of the cells was observed after 6, 12, 24, 48 and 72 hours of exposure. One plate was treated with 10 µL/mL DMSO in SF-RPMI for 24 hours and compared with the viability of cells with no treatment.

EGF did not reduce the viability of the MDA-MB-468 cells considerably in RPMI/10 % FBS compared to SF-RPMI. In addition, cells treated with 100-200 ng/mL EGF in SF-RPMI had much lower viability compared to cells treated with the same concentrations in RPMI/10% FBS. Cells treated with EGF in RPMI/10 % FBS reduced the viability of the cells by ~20-30 % regardless of the dose. After 6 hours of treatment, cells treated with the highest concentration of EGF had a round appearance and this trend gradually decreased with lower concentrations of EGF (figure 8-A). The effect of EGF gradually increased over time (exposure time 6,12, 24, 48 and 72 hours).

Doxorubicin and etoposide showed similar effects with increasing apoptotic cell death for each day (figure 8-B, C). Following 6, 12, 24, 48 and 72 hours exposure, the cells showed the characteristic signs of apoptosis, such as blebbing, small dots, gradually breakdown of the membrane etc. (microscopy observations, results not shown). Cells treated with etoposide

showed slightly higher metabolic activity (viability) in SF-RPMI treated cells. Yet, these effects were insignificant (figure 8-B).

For methotrexate, clear effects were also observed, however not in a dose-dependent manner; the effects in the viability of the cells were similar in all concentrations. Again, the effects did not differ between cells treated in SF-RPMI and RPMI/10 % FBS. Increasing the dosage of methotrexate did not give any higher response on the viability of the MDA-MB-468 cells (figure 8-D).

Cells treated with 10 μ L/mL DMSO show no significant difference in viability compared to the control. The DMSO-load in these experiments represents 2-6 μ L/mL in media and is safely under the limit where DMSO shows toxic effects. Therefore, we excluded the possible cytotoxic effects of DMSO on the MDA-MB-468 cells in 1 % concentration as shown in figure 8-E. The IC₅₀ value of each inhibitor was defined by using sigmoidal plots and is demonstrated in table 3.2.

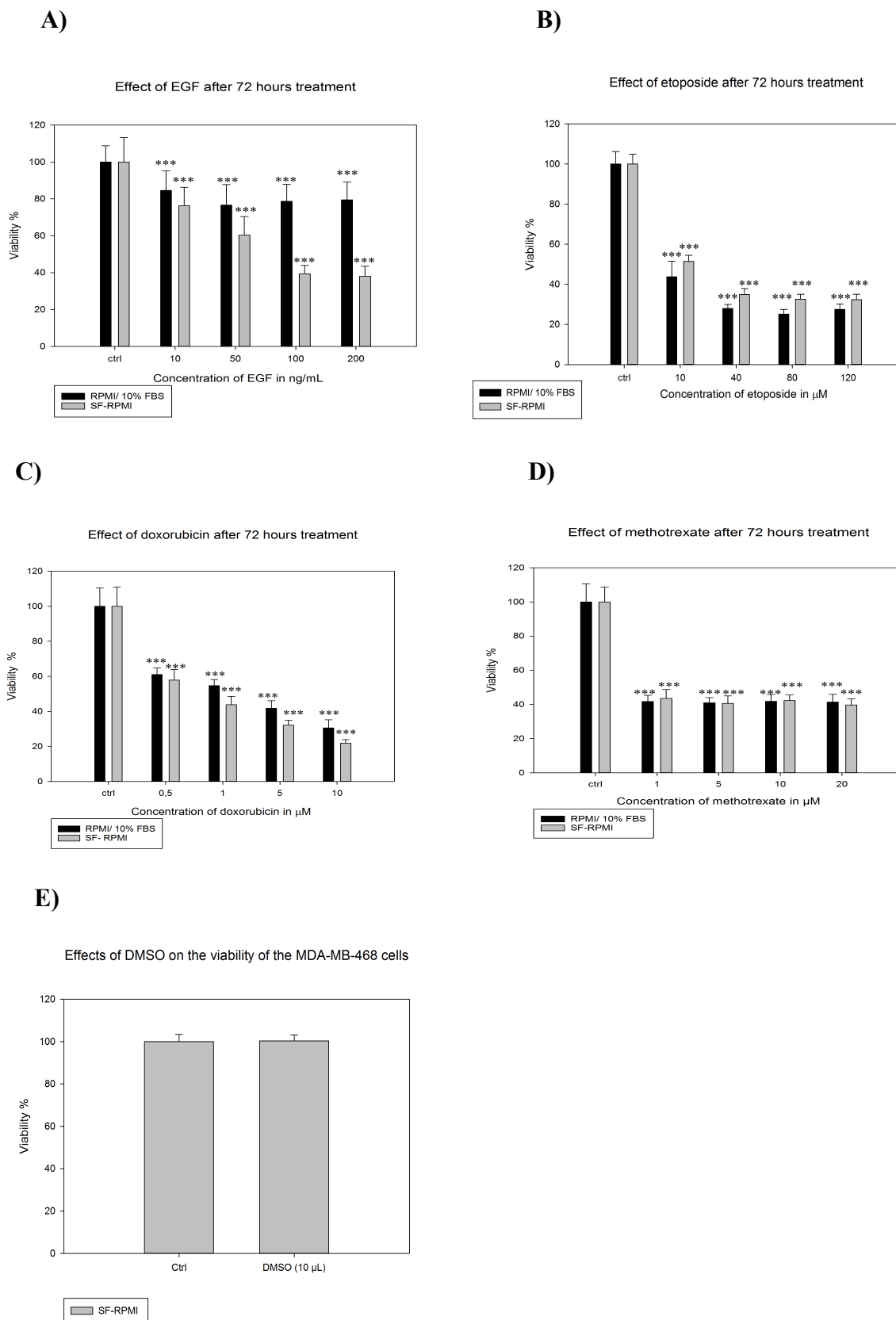


Figure 8: Results represent the average of three biological replicates after 72 hours of treatment where the \pm SD is presented in appendix A. **A)** EGF reduced the viability of the MDA-MB-468 cells in the concentration range from 10-200 ng/mL in both SF-RPMI and RPMI/10% **B)** Etoposide reduced the viability of the cells from 10-120 μ M. **C)** Doxorubicin showed almost no difference between SF-RPMI and RPMI/10 % FBS treated cells. **D)** Methotrexate did not reduce the viability of the MDA-MB-468 cells in a dose-dependent manner. **E)** DMSO-load in these experiments is safely below the limit where DMSO has effect and shows no cytotoxic effects in 10 μ L/mL concentration. The data is represented as mean \pm SD where ctrl is set to 100 % viability (n=3). ***($p < 0.001$), versus untreated cells. Ctrl, untreated cells

Table 3.2: Effects of apoptosis inducing agents on the viability of MDA-MB-468, IC50-values show the half maximum inhibitory concentration of the compounds.

Inhibitor	Target	IC50 72 hours, RPMI 10%/FBS	IC50 72 hours, SF-RPMI
Etoposide	Topoisomerase II	<10 μ M	<10 μ M
Doxorubicin	Topoisomerase II	1.0 μ M	0.7 μ M
Methotrexate	Dihydrofolate reductase	a	b
EGF	EGFRs	a	60 ng/mL

^a 50% reduction in viability not achieved in concentration range 10-200 ng/mL; ^b no dose-response;

To summarize, EGF was not found to be strong inducer of apoptosis in the MDA-MB-468 cells. A dose-response was not achieved for cells treated with methotrexate and cells showed no difference between the various concentrations tested in this experiment. The DMSO-load of the inhibitors used in this study is considered to be non-toxic.

Cells treated with drugs/agents in SF-RPMI and RPMI/10% FBS showed no significant difference in reducing the viability of the MDA-MB-468 cells. Both doxorubicin and etoposide induced apoptosis in the MDA-MB-468 cells in a dose-dependent manner. This shows that etoposide and doxorubicin, which are commonly used chemotherapies in cancer treatment, also is effective in this cell line. Moreover, this finding strengthens the validity of the cell model system.

3.3 Selective cPLA₂α inhibitors affect the viability of the MDA-MB-468 cells

The cPLA₂α-enzyme regulates several cellular effects in various types of tissues by controlling the release of AA and the subsequent conversion of lipid mediators called eicosanoids. In cancer cells, an increased cPLA₂α expression have been associated with high proliferation rate, invasion, metastasis and reduced apoptosis (44). In this study the possible role of selective cPLA₂α inhibitors on proliferation/viability of the MDA-MB-468 cells was evaluated.

A dose-response experiment was conducted for each agent in order to investigate the effects of each inhibitor. Cells were treated with selective cPLA₂α inhibitors in SF-RPMI and RPMI/10 % FBS and followed for 72 hours. Moreover, the effects were compared between different culturing media.

AVX235 and AVX420 belong to the group of compounds called thiazolyl ketones and exerted similar inhibitory effects on the MDA-MB-468 cells. In this experiment, AVX235 and AVX420 reduced the viability of the MDA-MB-468 cells with similar concentrations in a dose-dependent manner. The inhibitory effects of the compounds were clearly stronger in cells treated with SF-RPMI compared to cells treated in RPMI/10 % FBS. After 6 hours of treatment with > 25 μM AVX235 and AVX420, cellular stress/death was clearly seen (figure 9-A, B). Moreover, these cells had a morphological appearance that differed from cells treated with lower concentrations of the same inhibitors. These cells were swollen and had a transparent “balloon” like appearance around each cell when observed under the microscope (results not shown). Following 12 hours of treatment, cells treated with AVX235 and AVX420 in concentrations > 25 μM showed stronger effects with further visible signs of stress/cellular death in a larger quantity of cells. After 24 hours of treatment, maximal effect was seen in all inhibitors. Following 48 and 72 hours post treatment, no further signs of cell death/stress was observed in cells treated with AVX235 and AVX420 in all concentrations.

In contrast to AVX235 and AVX420, AVX002 reduced viability of the MDA-MB-468 cells in the same concentrations (>25 μM), but showed more potent inhibition in 50 μM and 100 μM concentration both in SF-RPMI and RPMI/10% FBS treated cells (figure 9-C). Cells treated with 25 μM AVX002 in RPMI/10 % FBS displayed similar effects on the viability of the MDA-MB-468 cells as AVX235 and AVX420. Intriguingly, MDA-MB-468 cells treated with 1 μM and 5 μM of AVX002, showed ~10 % higher metabolic activity (p value <0.05).

Following these cells for 6, 12, 24, 48 and 72 hours, the same trends as for AVX235 and AVX420 were observed with the same concentrations in both SF-RPMI and RPMI/10 % FBS.

Since all AVX-inhibitors showed approximately no difference in effects on viability of the cells in 100 μ M and 50 μ M, the 100 μ M concentration was excluded in the dose-response experiment with ATK. Also in this context, ATK showed similar effects in the dose-response experiments, except lower inhibition in 25 μ M both in SF-RPMI and RPMI/10% FBS compared to all AVX-inhibitors. Cells treated with 25 μ M ATK in SF-RPMI showed 30 % inhibition in viability compared to 40-50 % inhibition with AVX235 and AVX420, and ~ 90 % inhibition with AVX002 in SF-RPMI (figure 9-A-D). The IC₅₀ value of each inhibitor is demonstrated in table 3.3.

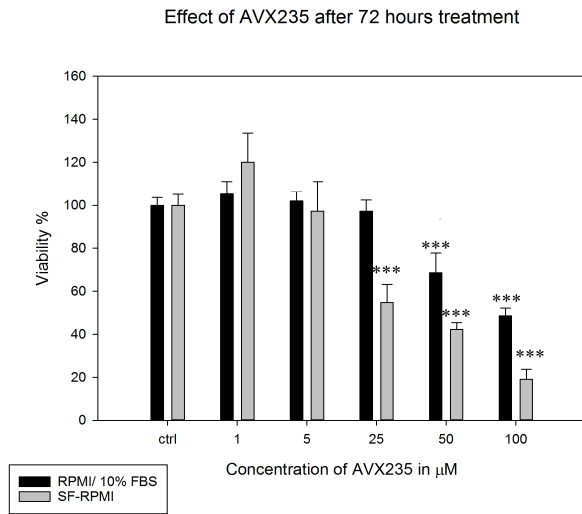
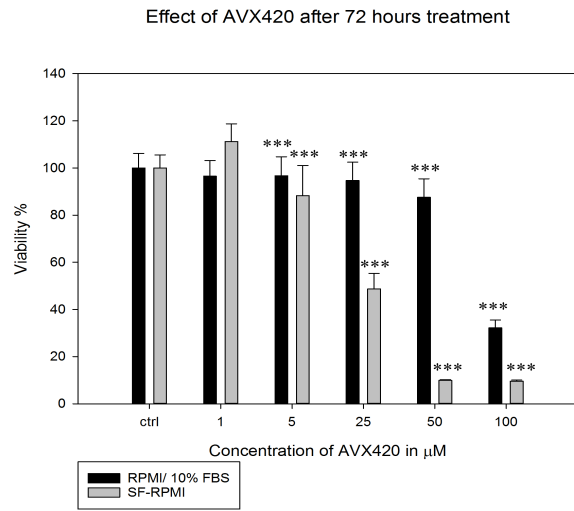
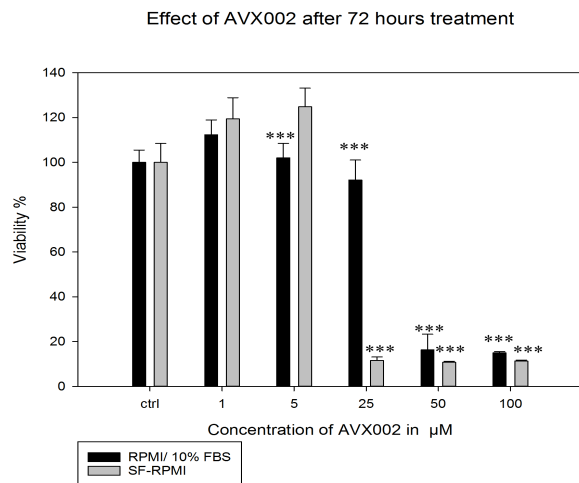
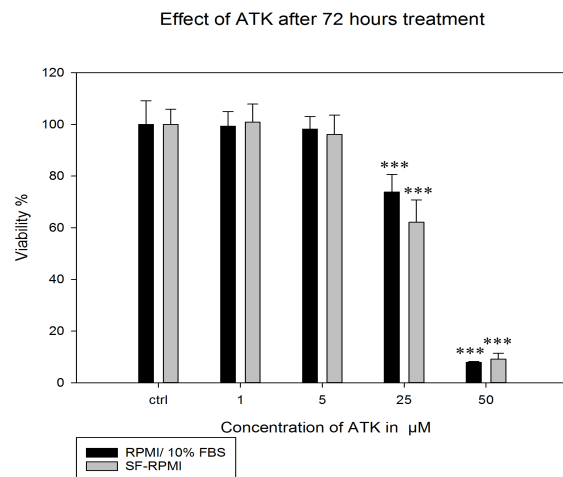
A)**B)****C)****D)**

Figure 9: Dose-response experiments of MDA-MB-468 cells treated with selective cPLA₂α inhibitors in a concentration range from 1-100 μM (1-50 μM for ATK) in SF-RPMI and RPMI/10 % FBS. The results are based on the average of three biological replicates, where the SD is presented in appendix B. **A)** AVX235 **B)** AVX420 **C)** AVX002 **D)** ATK. The data is represented as mean ± SD where ctrl is set to 100 % viability (n=3). *** (p<0.001) versus untreated cells. Ctrl, untreated cells.

Table 3.3: Effects of selective cPLA₂α inhibitors on the viability of MDA-MB-468 cells, IC₅₀-values show the half maximum inhibitory concentration of the compounds.

Inhibitor	Target	IC ₅₀	IC ₅₀
		72 hours, RPMI/ 10% FBS	72 hours, SF-RPMI
ATK	cPLA ₂ α/COX	36 μM	32 μM
AVX002	cPLA ₂ α	34 μM	7 μM
AVX235	cPLA ₂ α	83 μM	34 μM
AVX420	cPLA ₂ α	90 μM	25 μM

In summary, selective cPLA₂α inhibitors affect the proliferation/viability of the MDA-MB-468 cells in a dose-dependent manner. The effects were clearly significant with all selective cPLA₂α inhibitors, however AVX002 showed more potent inhibition than AVX235 and AVX420 in both SF-RPMI and RPMI/10 % FBS for concentrations > 50 μM.

3.4 PI3K/mTOR-inhibitors reduce viability of MDA-MB-468 cells in a dose-dependent manner

Since the PI3K-pathway has been proposed as a therapeutic alternative for BLBC/TNBC (22), the next step was to investigate the impact of various selective PI3K inhibitors on the viability of the MDA-MB-468 and compare it with the effects seen in cPLA₂α treated cells. In addition, the purpose of this experiment was to assess the efficacy/potency of distinctive types of PI3K inhibitors with different selectivity towards specific isoforms of PI3K.

A dose-response experiment was conducted as described earlier with each agent in order to evaluate the effects of each inhibitor. Cells were treated with selective PI3K inhibitors in SF-RPMI and RPMI/10 % FBS, and the effects were compared between the different culturing media. The results were also compared with various types of PI3K inhibitors.

All the PI3K inhibitors tested in this experiment reduced the viability of the MDA-MB-468 cells in a dose-dependent manner as shown for the cPLA₂α inhibitors (subchapter 3.3). However, each compound tested in this experiment showed a unique response in decreasing the viability of the MDA-MB-468 cells both in SF-RPMI and RPMI/10% FBS. Furthermore, the effects of the inhibitors did not differ by much in SF-RPMI and RPMI/10 % FBS in contrast to cells treated with the cPLA₂α inhibitors. For example, the difference in IC₅₀-values of buparlisib/BKM120 between cells treated in SF-RPMI and in RPMI/10% FBS was only 1.2 μM (table 3.4) compared to 65 μM for AVX420 (table 3.3). Also, following the cells for 6, 12, 24, 48 and 72 hours post-treatment showed increasing effect on the viability of the cells. After 24 hours exposure, no additional signs of cellular stress/death were observed for each inhibitor.

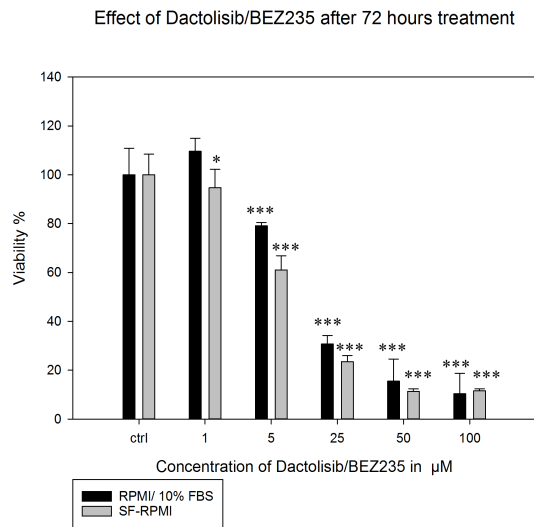
The dual mTOR/pan PI3K inhibitor dactolisib/BEZ235 inhibited the viability of the cells in SF-RPMI and RPMI/10 % FBS from ≥ 5 μM in a dose-dependent manner (figure 10-A). Alpelisib/BYL719 (PI3Kα inhibitor) did not affect the viability of the cells significantly in 1 μM and cells treated with 100 μM alpelisib/BYL719 in SF-RPMI had a higher viability compared to cells treated with alpelisib/BYL719 in RPMI/10 % FBS in the same concentration. Maximum viability was up to 30 % in cells treated in 100 μM alpelisib/BYL719 in both growth media (figure 10-B). As for the pan PI3K inhibitor, buparlisib/BKM120, the inhibitory effects of this compound was similar for almost all concentrations. In addition, cells treated with 10 μM and 20 μM buparlisib/BKM120 in SF-

RPMI, showed higher viability compared to cells treated in RPMI/10 % FBS. Although buparlisib/BKM120 showed variable effects in different culturing media, this compound was the most potent inhibitor in reducing the viability of cells from 1 μ M in both SF-RPMI and RPMI/10 % FBS (figure 10-C).

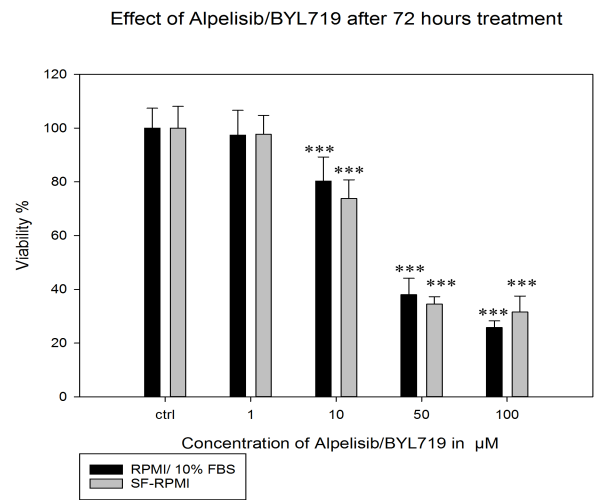
Table 3.4: Effects of selective PI3K inhibitors on the viability of MDA-MB-468 cells, IC50-value show the half maximum inhibitory concentration of the compounds.

Inhibitor	Target	IC50	IC50
		72 hours, RPMI 10%/FBS	72 hours, SF-RPMI
BEZ235/Dactolisib	panPI3K/mTOR	13 μ M	7 μ M
Alpelisib/ BYL719	PI3K α	32 μ M	20 μ M
Buparlisib /BKM120	panPI3K	6.7 μ M	5.5 μ M

A)



B)



C)

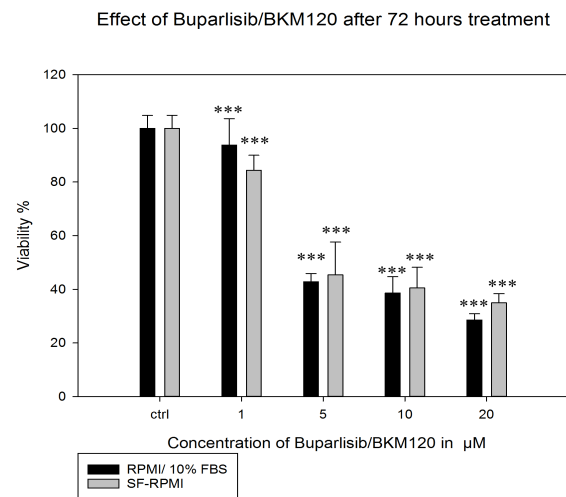


Figure 10: Dose-response experiment of MDA-MB-468 cells treated with selective mTOR/PI3K inhibitors in a concentration range from 1-100 μM (1-20 μM for Buparlisib/BKM120) in SF-RPMI and RPMI/10% FBS based on the average of three biological replicates of all inhibitors where the SD is presented in appendix C. **A)** Dactolisib/BEZ235. **B)** Alpelisib/BYL719 **C)** Buparlisib/BKM120. The data is represented \pm SD as mean where Ctrl is set to 100 % viability (n=3). *(p<0.05), ***(p<0.001), versus untreated cells. Ctrl, untreated cells.

In summary, selective (mTOR)/PI3K inhibitors reduced the proliferation/viability of the MDA-MB-468 cells in a dose-dependent manner. Buparlisib/BKM120 was the most potent inhibitor and reduced the viability of cell in all tested concentrations with IC₅₀ value 5.5 μM in SF-RPMI and 6.7 μM in RPMI/10 % FBS. The difference between cells treated with inhibitors in SF-RPMI and RPMI/10 % FBS was not significant.

3.5 Combination of buparlisib/BKM120 with cPLA₂α inhibitors demonstrated additive effects

Having found that cPLA₂α inhibitors and (mTOR)/PI3K inhibitors affect the viability of the MDA-MB-468 cells, the next step was to assess the effects of this occurrence by combining cPLA₂α inhibitors with different selective PI3K inhibitors. The PI3K pathway and cPLA₂α pathway both play a major role in cancer cell growth, survival, angiogenesis and proliferation (23, 47). Therefore, our intention for conducting a combination treatment was to investigate the possible additive/synergistic effects of cPLA₂α inhibitors when combined with selective PI3K inhibitors. Also, the purpose of the experiments was to investigate the effects of combination treatment in lower concentrations. Additivity describes the effect of two compounds that produces the same effects of one compound in a lower concentration than the required concentration of only one compound. Synergistic effects, on the other hand means that the effect of two compounds together is greater than the total effect of each compound individually in the same dose (93).

The combination treatments were performed in a period of 24 hours and all the cells were treated in SF-RPMI. This choice was made to exclude other factors that may influence our results. Also, since the effects on the viability of the cells did not differ by much from 24 -72 hours post-treatment (as described in subchapter 3.3 for the cPLA₂α inhibitors), cells were treated for 24 hours in this experiment. The plate was read after 24 hours of treatment in a plate reader. The concentrations of each treatment was chosen based on the IC₅₀ values found for the inhibitors. In order to study whether the compounds have additive effects on the MDA-MB-468 cells when combined together, a sub-optimal dose close to the IC₅₀ values was chosen.

The result from this study revealed additive effects upon combining dactolisib/BEZ235 with AVX002. In this experiment, AVX002 showed most promising result on reducing the viability of the MDA-MB-468 cells when combined with selective (mTOR)/PI3K inhibitors (figure 11-A, C). AVX235 and AVX420 demonstrated lower additive effects in combination with dactolisib/BEZ235 and showed no synergistic effects (figure 11-A).

When alpelisib/BYL719 was combined with selective cPLA₂α inhibitors, no additive effects were observed in any biological replicate (figure 11-B). Buparlisib/BKM120, on the other hand, showed most potent inhibition and also showed additive effects in almost all combination treatments (figure 11-C). In this experiment, it was discovered that combining

two inhibitors that target different pathways could provide a new treatment strategy for BLBC/TNBC.

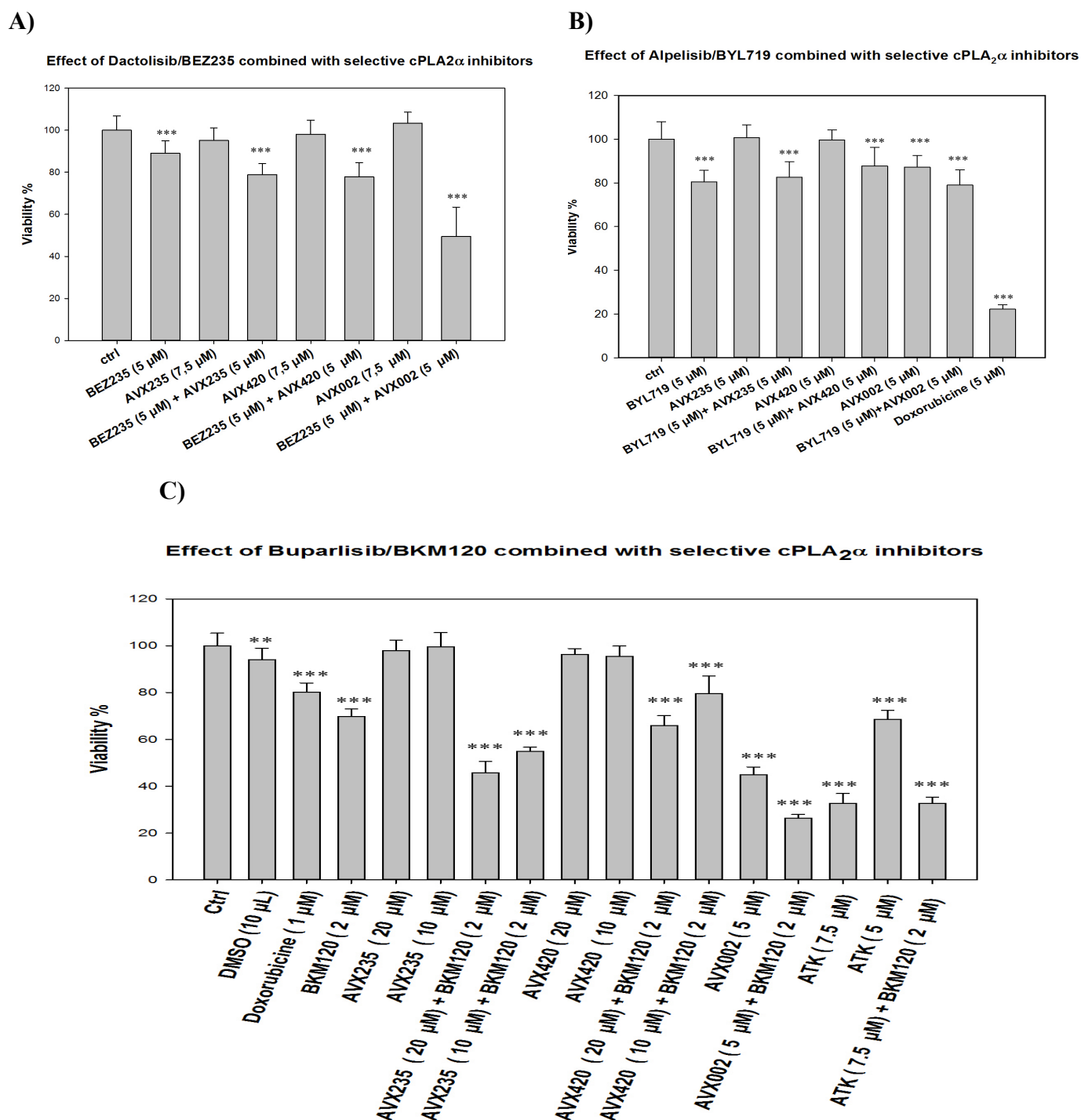


Figure 11: Viability assay of combining two selective inhibitors with different working mechanisms, one that inhibits the activity of cPLA₂α and the other targeting the (mTOR)/PI3K-pathway, which are associated with cancer progression and proliferation. The result is based on the average of three biological replicates after 24 hours of treatment where SD is presented in appendix D. **A)** Dactolisib/BEZ235 combined with selective cPLA₂α inhibitors **B)** Alpelisib/BYL719 combined with selective cPLA₂α inhibitors **C)** Buparlisib/BKM120 combined with selective cPLA₂α inhibitors. The data is presented as mean ± SD where ctrl is set to 100 % viability (n=3). ***(p<0.001), versus untreated cells. Ctrl, untreated cells.

In conclusion, the combination of selective PI3K inhibitors and selective cPLA₂α inhibitors that targets proliferation pathways of the MDA-MB-468 cells in different ways may offer alternative treatments for BLBC/TNBC. Alpelisib/BYL719 was not a good combination candidate and showed no additive effects in combo-treatment. Buparlisib/BKM120, on the other side, showed additive effects in all combo-treatments and may offer a new treatment strategy for BLBC/TNBC.

3.6 Buparlisib/BKM120 and cPLA₂α inhibitors increase the caspase activity of the MDA-MB-468 cells

The caspases are a central group of enzymes that play a major role in the apoptotic pathway by regulating different processes in the cells which leads to cell death. Caspase 3- and 7 functions as the last step of apoptosis and work by cleaving a number of different substrates in the nucleus or cytoplasm. The cleavage of different substrates in the cells leads to the general morphological features of apoptosis (DNA fragmentation, blebbing and cell shrinkage) (88, 94).

The caspase assay was performed to investigate whether the effects of selective PI3K and cPLA₂α-inhibitors shown in previous experiments, was due to apoptosis or other inhibitory mechanism such as necrosis. The caspase assay was used as a method to determine the caspase activity of the MDA-MB-468 cells, which reflects the amount of apoptotic cells in a cell population.

Based on the previous performed resazurin experiments, buparlisib/BKM120 showed best effects in combination treatment. Therefore, buparlisib/BKM120 was chosen in this assay to be combined with AVX235, AVX420 and AVX002 in different concentrations. The choice of the concentrations of the inhibitors used in this experiment was determined based on previous data from the dose-response experiments and the calculated IC₅₀ values for the inhibitors.

The results show that single treatment of selective inhibitors increases the caspase activity of the MDA-MB-468 cells in a similar fashion as doxorubicin, which was chosen as a control for apoptosis. In contrast, cells treated with combination treatment had a higher caspase activity (figure 12). This highlights that combining two inhibitors with different cellular targets, namely cPLA₂α and PI3K, increases the caspase activity of the MDA-MB-468 cells significantly. As expected, the control treatment, which only contained SF-RPMI, did not increase the caspase activity at all.

Caspase activity of the MDA-MB-468 cells treated in different compounds

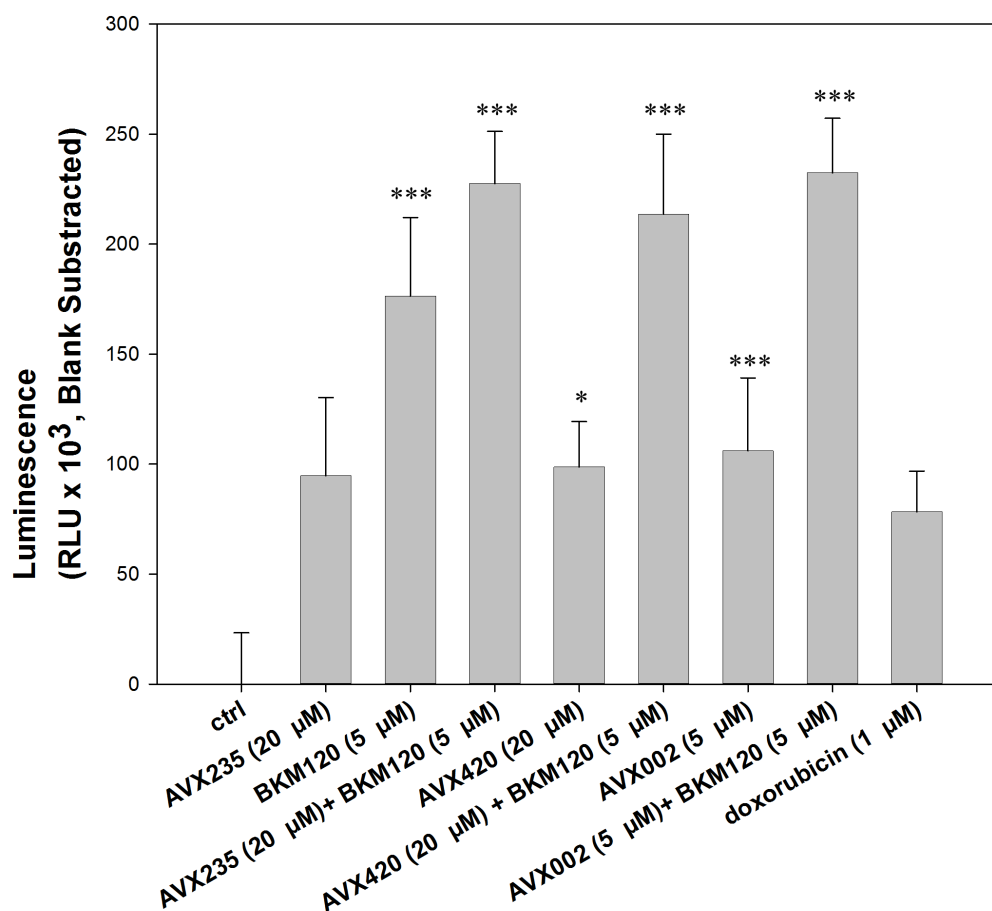


Figure 12: The figure represents the relative light units (RLU) obtained from the average of two biological replicates of MDA-MB-468 cells treated with different types of cPLA₂α inhibitors and buparlisib/BKM120. The values are blank-subtracted (blank= no caspase activity). The units and SD of each treatment is presented in appendix E. *** indicate (p < 0.001) and * indicate (p < 0.05)

To conclude, the compounds tested in the caspase 3/7 experiment showed a significant increase in caspase activity, and the increase was higher than what was observed for doxorubicin which is was used as an apoptosis control. Also, combining the cPLA₂α and the pan-PI3K inhibitor buparlisib/BKM120 targeting different pathways resulted in a two-fold additive effect. This indicates that induction of apoptosis is one possible mechanism to explain reduced viability of MDA-MB-468 cells in response to cPLA₂α- and PI3K inhibitors alone and in combination.

3.7 AVX002 and buparlisib/BKM120 induce cell cycle arrest in the MDA-MB-468 cells

The previous data obtained from the caspase assay showed increased caspase activity of the MDA-MB-468 cells when treated with selective cPLA₂ α inhibitors and the pan PI3K inhibitor buparlisib/BKM120. Moreover, combining these two type of inhibitors showed significantly higher caspase activity compared to mono-treatment.

To investigate whether the cell cycle of the cells is also affected when inhibiting these two cellular pathways, flow cytometry was utilized. In this experiment, the effects of AVX002 and buparlisib/BKM120 in MDA-MB-468 cells cell cycle phase distribution were analysed. Cells were treated with 2 μ M, 5 μ M and 8 μ M AVX002, 3 μ M buparlisib/BKM120 and 1 μ M doxorubicin in SF-RPMI for 24 hours. Also, different concentrations of AVX002 was combined with 3 μ M buparlisib/BKM120. The results of these treatments were compared with untreated cells (control).

Doxorubicin, at 1 μ M induced cell cycle arrest in the G2+M phase significantly (G2+M 84.26 %) ($p < 0.001$) (figure 13-B and table 3.4) in contrast to the control (G2+M 35.18 %) (figure 13-A and table 3.4). Treating the cells with 3 μ M buparlisib/BKM120 also arrested the cells significantly in the G2+M phase similar to doxorubicin, however to a lower extent; (84.26 % for doxorubicin vs. 59.02 % for buparlisib/BKM120), (figure 13-B,C and table 3.4).

The lowest concentration of AVX002 (2 μ M) did not alter the cell cycle phase distribution of cells significantly (figure 13-D and table 3.4). In addition, the same applies for the cells treated with 5 μ M AVX002, even though a possible indication of cell cycle arrest in the G1 phase was observed (figure 13-E and table 3.4). However, increasing the dose of AVX002 to 8 μ M gradually altered the cell cycle phase distribution of the MDA-MB-468 cells significantly and arrested the cells in the G1 phase ($p < 0.03$) (figure 13-F and table 3.4). When 2 μ M AVX002 was combined with 3 μ M buparlisib/BKM120, the effects of buparlisib/BKM120 were more evident (figure 13-G and table 3.4). Moreover, increasing the dose of AVX002 to 5 μ M showed higher amount of cells in G1 phase compared to the combination treatment with 2 μ M concentration of AVX002 (figure 13-H and table 3.4). MDA-MB-468 cells treated with 8 μ M AVX002 combined with 3 μ M buparlisib/BKM120 showed more cells arrested in the G1 phase. This observation was made by comparing the data from the cell cycle phase distribution of mono-treatment with buparlisib/BKM120 and AVX002. Increasing the dose of AVX002 to 5 μ M in combo-treatment, neutralized the effects of

buparlisib/BKM120 to a certain level by shifting the cell cycle phase distribution towards G1. Moreover, cells were also more gathered in the G2+M phase compared to the control even though the effects of AVX002 were increasing (figure 13-I and table 3.4).

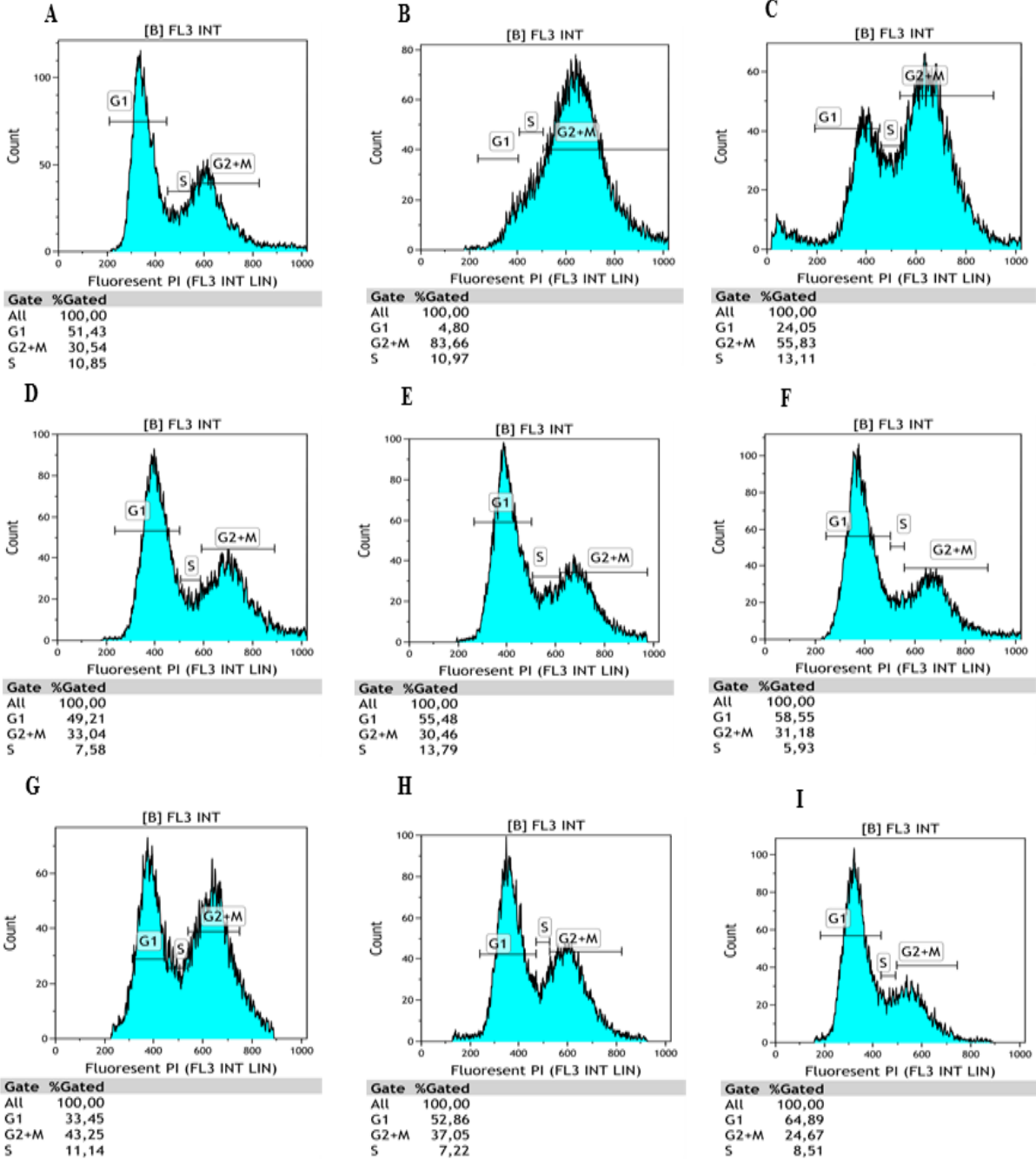


Figure 13: Histograms of cell cycle phase distribution of the MDA-MB-468 cells treated with different inhibitors after 24 hours in SF-RPMI. One figure was selected to represent the results of each treatment. The figure shows the gated cells on the fluorescent (FL3) histogram where the fluorescence intensity was detected at channel FL3 for propidium iodide. Count, cell number **A)** Control **B)** Doxorubicin (1 μ M) **C)** Buparlisib/BKM120 (3 μ M) **D)** AVX002, (2 μ M) **E)** AVX002 (5 μ M) **F)** AVX002 (8 μ M) **G)** AVX002 (2 μ M) and buparlisib/BKM120 (3 μ M) **H)** AVX002 (5 μ M) and buparlisib/BKM120 (3 μ M) **I)** AVX002 (8 μ M) and buparlisib/BKM120(3 μ M)

The total gated phases were setup to exclude cell debris and/or aggregates of cells from the final flow cytometry analysis. Moreover, the total gated phases were defined to 100 % in each trial and each phase was calculated relative to that. Hence, the total percentage of G1, S and G2+M adds up to 100 % in each trial. The percentages of cell cycle phase distribution of each treatment are presented in table 3.4.

Table 3.4: Effects of different treatments on cell cycle phase distribution of the MDA-MB-468 cells.

Treatment	G1 (%)	S (%)	G2+M (%)
Ctrl	54.102 ± 2.41	10.67 ± 1.07	35.183 ± 2.9
Doxorubicin (1 µM)	5.704 ± 3.66 ***	10.038 ± 1.65	84.26 ± 2.87 ***
Buparlisib/BKM120 (3 µM)	27.72 ± 2.26 ***	12.95 ± 2.37	59.02 ± 2.81 *
AVX002 (2 µM)	51.85 ± 2.41	11.68 ± 3.03	35.00 ± 1.65
AVX002 (5 µM)	56.20 ± 0.93	11.03 ± 3.07	32.88 ± 2.69
AVX002 (8 µM)	59.17 ± 2.77 **	7.045 ± 1.41***	33.89 ± 2.81
AVX002 (2 µM) + buparlisib/BKM120 (3 µM)	42.08 ± 3.46 ***	6.2 ± 0.55 ***	51.99 ± 4.18***
AVX002 (5 µM) + buparlisib/BKM120 (3 µM)	52.57 ± 1.60	7.60 ± 1.46**	39.47 ± 2.40**
AVX002 (8 µM) + buparlisib/BKM120 (3 µM)	60.66 ± 4.52 *	8.99 ± 1.72	29.30 ± 4.67*

The data represent the percentage of SD ± (%) of one representative experiment with 6 technical repeats. The asterisks denote the significance level from untreated cells (ctrl). *(p<0.05), **(p<0.03), ***(p<0.001)

In summary, doxorubicin and buparlisib/BKM120 clearly showed cell cycle arrest in the G2+M phase. This shows that these compounds/inhibitors regulate the progression of G2-M phase and prevent the MDA-MB-468 cells from undergoing mitosis. Cells treated with 8 µM AVX002 arrested the cells in G1 phase and inhibited the progression of G1 to S phase. The combination treatment of AVX002 with buparlisib/BKM120 showed variable effects on the cell cycle phase distribution of the MDA-MB-468 cells depending on the concentrations of the inhibitors. Increasing the dose of AVX002 clearly increased the amount of cells in the G1 phase.

4 DISCUSSION

This master project addresses the effects of cPLA₂α on MDA-MB-468 cells viability. Proliferation, apoptosis and the cell cycle of the MDA-MB-468 cells were investigated by using selective cPLA₂α inhibitors alone, comparative drugs, and/or combined with selective PI3K inhibitors. During this master project various methods and instruments were used to investigate the effects of cPLA₂α inhibition on the MDA-MB-468 cells and whether the viability and/or the cell cycle of these cells were affected when treated with different concentrations of various inhibitors. The aim was to evaluate whether selective inhibitors of cPLA₂α alone or combined with other recommended targeted treatments could offer a promising targeted treatment for BLBC/TNBC.

The effects of different treatments on the viability of the MDA-MB-468 cells were measured by using resazurin as an indicator of cell proliferation and metabolic activity. Since resazurin measures the metabolic conversion of resazurin to dihydroresorufin, a reduction in the conversion of resazurin may indicate less viable cells (74).

A caspase assay was performed in order to determine whether the effects of the inhibitors on the viability of the cells were caused by apoptosis. In order to assess the effects of cPLA₂α inhibition alone and in combination with buparlisib/BKM120 on the MDA-MB-468 cells cell cycle, flow cytometry was utilized.

All the experiments performed on the MDA-MB-468 cells were conducted in sub-confluent state at the time of treatment. Cells in this stage grow exponentially and characterize the natural proliferative state of BLBC/TNBC cells in the tumour.

4.1 Different seeding numbers affects the growth of the MDA-MB468 cells

The knowledge and experience of senior researchers in the PLA2 lab were essential in defining the different seeding concentrations at the beginning of the experiment. Three different concentrations were selected to differentiate between too low initial cell density and too high initial cell density. The purpose of the experiment was also to compare the growth rates of different cell seeding densities and to determine the optimal seeding density in later experiments.

The MDA-MB-468 cells were seeded at 50 000, 250 000 and 750 000 cells in 25 cm² tissue flasks and were followed for 8 days. Cells seeded at 50 000 cells per flask never reached exponential growth phase and stayed in the lag phase the remaining days of the experiment. Moreover, cells in the lowest initial cell seeding density grew in patches or colonies. Beside these cells showed different morphologies with different shapes and sizes in contrast to the higher cell seeding densities, where most cells were aligned tightly next to each other and had a round shape. Due to the fact that cells growing in culture is dependent on cell-cell contact, low initial cell seeding density may limit cell-cell contact and therefore inhibit the growth progression of these cells. In addition, cells seeded at 50 000 cells per flask were able to adapt to their environment and make cell-cell contact with nearby cells, which can explain why cells grew in patches/colonies and why the cells were not evenly spread in the flasks. Cell at the lowest seeding concentration had challenges in growth during the total 8-day experiment, which was not unexpected. Cells seeded at the highest density on the other hand, reached exponential growth early after seeding and continued in this state until the last day of the experiment. These results reveals that cell-cell contact is a major factor for cell proliferation and that seeding density plays an important role in this context.

Cells seeded at 250 00 cells per flask reached exponential growth at day 4 in contrast to cells seeded at 750 000 cells per flask, which reached exponential phase at day 2. However, when calculating the PDT, the time required for cells to double were higher for cells seeded at 750 000 cells per flask compared to the cells seeded at 250 000 cells per flaks. A possible explanation for this may be that more cells require more growth factors and consume more serum, which can lead to starvation of cells and a decrease in cell growth (95). The PDT was calculated only for cells that had reached exponential growth phase. This choice was made due to the fact that cell growth, during the exponential phase, is relatively constant and reproducible for various types of growth conditions (73). Calculating the PDT of cells in the

lag phase, however, may not be reliable or reproducible since these cells grow in much lower rate. Cells seeded at the highest density had a steep rise in cell numbers at day 6. This can confirm that cancer cells can proliferate regardless of cell density but needs sufficient amounts of growth factors to complete mitosis (95).

4.2 Cells keep growing even though the total surface of the flask are occupied

Cells seeded in the highest density continued to grow exponentially even though the total tissue flask was covered with cells. This may be related to the fact that tumour cells *in vitro*, unlike other cell lines, have a wide range of morphological appearances and other growth related properties. This includes alterations in cell motility and shape, adhesive properties, loss of density dependent growth, changes in cell surface properties and loss of anchorage dependence growth. These properties have been associated directly or indirectly with the cytoskeleton (96).

The MDA-MB-468 cells never reached the stationary phase or decline and continued to grow exponentially during the whole experiment period. A possible explanation may be, that the media was changed at day 4, which supplemented the cells with more serum that contains various types of growth factors. Also, these cells are cancer cells and may not be affected by contact inhibition. The cells kept proliferating in multilayer as observed in our case, which is supported by a study showing that MDA-MB-468 cells grow in multi layers (97). On the other hand, the ATCC guide line for this cell line has a similar growth curve, which reveals that these cells enter the stationary phase at day 10 (91). It suggests that even though the cells evade density dependent growth, the access of serum may limit cell growth and further development. In addition, the limited time course of the experiment may also affect the observed results. If the experiment was prolonged for a longer period or if the cells was seeded in a higher concentration, we might have observed the stationary phase of these cells. Cells seeded in the highest seeding density reached 100 % confluency at day 5 and even though the flask where 100 % confluent, the cells kept growing exponentially. However, these cells had a rounder shape and were smaller in size which may correlate to adaption towards the limited growth space to further facilitate cell proliferation.

For experimental purposes, a seeding density of 50 000 cells in a 25 cm² culturing flask is not desired. Low seeding densities limit cell proliferation and reduce cell-cell contact. Therefore,

when conducting experiments on cell proliferation it should be taken into account that cell seeding density play a major role in this context and should be considered carefully.

4.3 Comparison of EGF, methotrexate, etoposide and doxorubicin

Methotrexate, etoposide and doxorubicin are commonly used cytotoxic drugs in cancer therapy. These drugs act directly or indirectly on the DNA or on the cell proliferation machinery and induce apoptosis (92). EGF is generally known to induce proliferation in several cell types, but in MDA-MB-468 cells, increased apoptosis are reported in response to EGF (66).

In this research, EGF was found to inhibit viability of MDA-MB-468 cells in a dose-dependent manner. The anti-proliferative effects or apoptosis inducing effects of EGF were rather limited in RPMI/10% FBS compared to the other apoptosis inducing drugs. In addition, the anti-proliferative effects of EGF were stronger in SF-RPMI. In earlier studies, it has been reported that MDA-MB-468 cells, in response to EGF in growth arrested cells, activates EGFR (66). However, instead of initiating a cascade of events that leads to cell proliferation, these cells react by activating other kinases, leading to cellular apoptosis (76). This phenomenon is believed to be more evident in serum free media. Serum containing media comprises other growth factors besides EGF, which might compensate for the growth inhibition of EGF. Serum free media on the other hand, lack these growth factors and can initiate apoptosis in response to EGFR activation in MDA-MB-468 cells (66).

Doxorubicin and etoposide exerted similar response on the viability of the MDA-MB-468 cells. It was not observed considerable better effects in SF-RPMI compared to RPMI/10% FBS. This can be supported by the fact that these drugs act mainly in highly proliferative cells (77, 81). Therefore, removing serum from their growth media may not increase their cytotoxic effects substantially. Even though a slightly lower metabolic activity was found in cells treated with doxorubicin in SF-RPMI, these results were insignificant.

A dose-response was not achieved for methotrexate in our viability assay. This is in line with the fact that these cells are resistant to methotrexate therapy. In the study of de Almagro *et al.*, one possible reason behind methotrexate resistance was found to be caused by the induction of UDP-glucuronosyltransferase 1A6 (UGT1A6) (98). This enzyme is involved in phase II metabolism where a glycosyl group from uridine diphosphoglucuronic acid (UDPGA) is

added to methotrexate. This addition transforms methotrexate to a more hydrophilic drug so it can be eliminated via the bile and urine. It has been suggested that methotrexate induce the transcription level of UGT1A6, which leads to increased conversion of methotrexate to inactive form by UGT1A6 (98). This is in line with what was observed in our study where increased methotrexate dose did not induce higher cytotoxic effects.

4.4 Comparison of different cPLA₂α inhibitors

The cPLA₂α enzyme is considered as an important enzyme and play a essential role in the pathogenesis of many inflammatory diseases including cancer as mentioned earlier. Hence, selective inhibitors of cPLA₂α have been investigated for a long time, and several types of inhibitors that target the active site of this enzyme have been developed (30). In our case, the effect of selective cPLA₂α inhibitors on the viability of the MDA-MB-468 cells showed promising results where growth inhibition was successful in all the tested compounds.

The dose-response experiment of the cPLA₂α inhibitors revealed that AVX002 was the most potent inhibitor. Nevertheless, all four selective inhibitors of cPLA₂α suppressed proliferation of the MDA-MB-468 cells significantly and to a certain degree in a dosage-dependent manner.

Firstly, AVX002 is a derivative of the ω-3-PUFA DHA and are known to be stable in cell based assays (54). The reason behind this may relate to its molecular structure where the ketone on the molecule is reduced. This reduction renders the molecule to its active form where it can bind to cPLA₂α and block the activity of it.

It should also be mentioned that ATK is a slow inhibitor of cPLA₂α and need more time to bind to its target (99). Also, in this context, the same may apply for AVX002 due to the fact that this compound displays similar structural properties as ATK. Another issue to address is the lipophilic properties of these compounds. Lipophilic compounds such as AVX002 and ATK are derivatives of PUFA and such molecules are believed to interact with membrane phospholipids before entering into the cytoplasm where they exert their effects. Therefore, due to these factors, the effect of such compounds may be delayed in comparison to the other compounds (54). In this project, similar observations were made in the dose-response experiments with AVX002 and ATK where the effects were observed after 4-5 hours compared to 2 hours after exposure with AVX235 and AVX420 in the highest concentration. Cells treated in the highest concentration showed a morphological change where enlargement

of the plasma membrane and bursting after a couple of hours were observed. The same observation was made with these inhibitors in HaCaT keratinocytes (personal communication Nur Mahammad, Avexxin AS). These findings may indicate necrosis, since it illustrates the general morphological characteristics of necrosis (100).

In low concentrations of the inhibitors, however, it appeared that the cells had a morphological appearance that resembles cells undergoing apoptosis, which was membrane blebbing, pores in the membrane and small black dots which may be an indicative of cell debris (100).

These observations highly support that cPLA₂α inhibitors at high concentrations may induce necrosis and apoptosis at low concentrations of inhibitors. More research is still needed to confirm these findings and the possible reasons behind these observations.

Secondly, ATK was the least effective inhibitor of cPLA₂α. A possible explanation of this may be due to the fact that ATK is rapidly oxidized in contact with oxygen (101), which also concerns AVX002. Therefore, when working with this compound it should be dissolved and applied rapidly. In addition, when performing experiments with such compounds, the compounds should always be stored at -80 °C to minimize oxidation, which is common practice in the PLA₂ lab. Further explanation for this topic is discussed in subchapter 4.10 that mention technical variations of the experiments.

Thirdly, AVX235 and AVX420 have different chemical structure, which are also in high risk of getting reduced metabolically. The reduction of the ketone group of these compounds, in contrast to what is the case for AVX002, are not beneficial due to the fact that these compounds are inactivated when reduced (102). Furthermore, the half-life of these compounds is believed to be shorter because of this rapid reduction.

In our study, we discovered that the potency of these two compounds differed significantly compared to ATK and AVX002. Indeed, these findings may suggest that the effects of these inhibitors may be due to shorter half-life.

Also, it should be mentioned that even though AVX002 was found to be the most potent inhibitor in this experiment, we can not conclude that AVX002 is the most potent cPLA₂α inhibitor of the tested compounds. However, it is speculated that adding AVX235 and AVX420 to cell culture experiments every 6-12 hours may show similar potency as AVX002 on the MDA-MB-468 cells. In addition, the study of Mete *et al.* suggested that adding a

methyl-group in the α -position of the ketone group of the molecule could stabilize the structure of these compounds. This modification, can in turn inhibit the enzymatic reduction of such compounds and increase their biological effects (102). The reduction site of each inhibitor and suggested modification of AVX235 and AVX420 are shown in figure 14.

Also, the exposure time of the inhibitors were chosen from earlier studies with viability assays on similar cell lines and compounds. Yet, the exposure time was not optimal due to the fact that cells already after 24 hours showed maximal effects on the viability of the MDA-MB-468 cells.

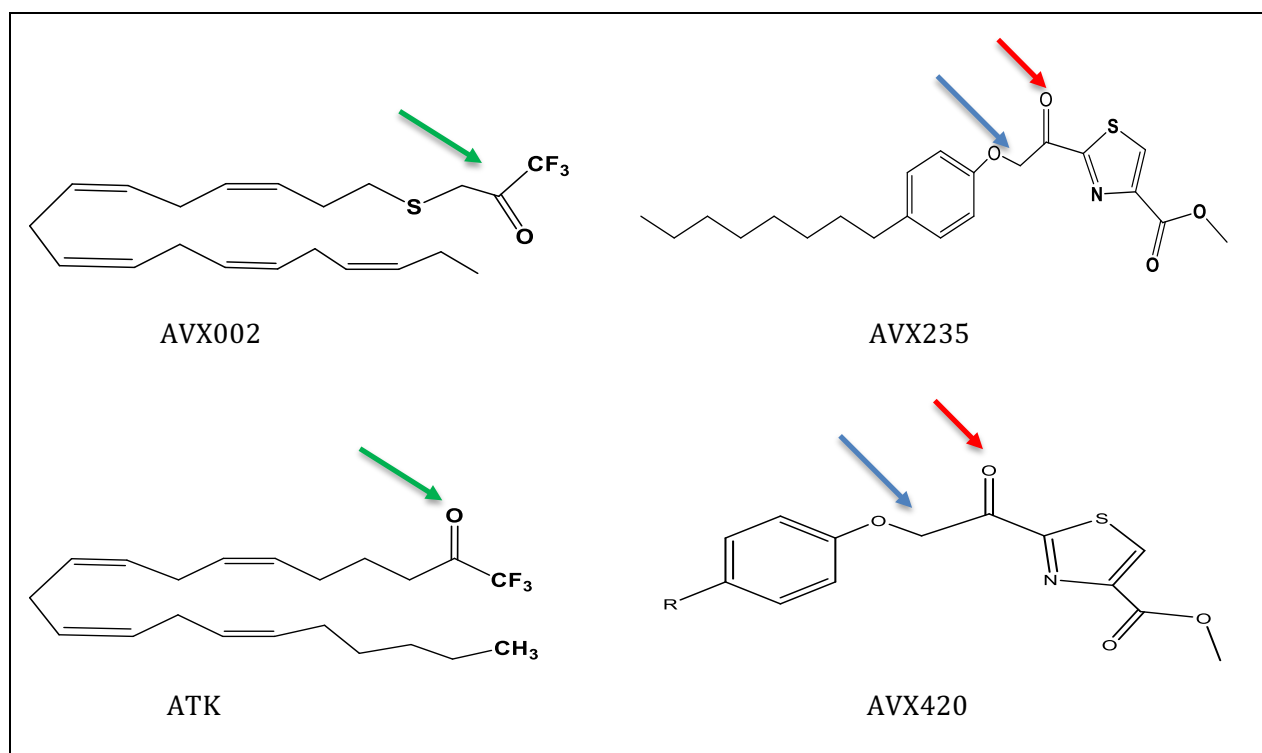


Figure 14: The chemical structure of AVX002, AVX235, ATK and AVX420. The ketone group of ATK and AVX002 is reduced to its active form where it can bind to the active site of the cPLA₂ α enzyme. AVX235 and AVX420 have a different structure and are also metabolically reduced by other enzymes, but this reduction inactivates these molecules. The red arrows point to the ketone group that can be reduced to inactive form and the green arrows points at the ketone group of AVX002 and ATK that are reduced to their active form. The blue arrows on AVX235 and AVX420 shows the possible substitution of the hydrogen-atom by a methyl-group in α -position to the ketone which can stabilize these structures and reduce metabolic inactivation of the ketone.

4.5 Comparison of selective PI3K/(mTOR) inhibitors

Three different types of inhibitors that are shown to be central in BLBC/TNBC signalling pathway were tested on MDA-MB-468 cells.

The results of the dose-response experiments revealed excellent inhibition in all the tested compounds with different IC₅₀ values depending on the type of inhibitor. All the inhibitors showed small differences in effects between compounds dissolved in SF-RPMI and RPMI/10 % FBS. The difference between the two different media was not as big as for the cPLA₂ α inhibitors. This finding can indicate that these compounds target cells where the proliferation rate is high. Also, in this context, serum starvation is known to decrease cell proliferation rate (103), and therefore reduced proliferation rate may suppress the effect of such inhibitors. Even though all compounds showed positive anti-proliferative effects on MDA-MB-468 cells, the potency varied between different compounds. Alpelisib/BYL719 was the least potent inhibitor with an IC₅₀ value of 20 μ M in SF-RPMI compared to dactolisib/BEZ235 and buparlisib/BKM120, which had an IC₅₀ value of 7 μ M and 5.5 μ M, respectively. A possible explanation for this observation may be due to the fact that alpelisib/BYL719 only targets one specific isoform of the many existing isoforms of PI3K-enzymes (104). It is not surprising that targeting several isoforms of PI3K involved in cancer signalling give better anti-proliferative effects compared to targeting only one isoform. Also, it has been found that this inhibitor is most effective in tumours with altered PI3K α (104). This can indicate that targeting PI3K α is not relevant in MDA-MB-468 cells, and the reason behind it can be due to the fact that not all isoforms of PI3K occurs to be important in all cancer cells signalling pathways (104). Alpelisib/BYL719 may thus have excellent anti-proliferative effects in some tumours and limited response in others. More research is however needed to find whether PI3K α can benefit all BLBC/TNBC patients or only a selection of these patients.

The dual PI3K/mTOR inhibitor dactolisib/BEZ235, targets four different isoforms of PI3K, namely p110 α / γ / δ / β and mTOR. The advantages of using inhibitors targeting different isoforms of PI3K are that they inhibit several types of enzymes involved in cancer cell survival, metastasis and angiogenesis (105). This can in turn increase their efficacy in tumour cells, but it should also be mentioned that using such inhibitors have their disadvantages as well. Lately, the study of Netland *et al.*, discovered that using dactolisib/BEZ235 in brain

tumour was associated with high toxicity and intolerable side-effects (106). Therefore, this compound is not recommended to be used as a therapeutic drug.

The pan PI3K inhibitor buparlisib/BKM120 targets the p110 α / β / δ / γ . This compound has shown great anti-proliferation and apoptosis activity in several *in vivo* and *in vitro* studies (86, 107).

4.6 Comparison of combo-treatment with selective PI3K inhibitors and cPLA₂ α inhibitors

In the combination experiment we aimed to investigate additive and/or synergistic effects of selective cPLA₂ α and PI3K inhibitors. Each cPLA₂ α inhibitor was combined with one specific PI3K inhibitor.

Overall, combining these two types of inhibitors did not show synergistic effect, but rather additive effects. Additive effects were also observed in the caspase assay (figure 12).

In our results, the combination treatment with buparlisib/BKM120 was the most successful treatment. The reason behind this can be due to better concentration choice of the inhibitors and to the fact that a higher concentration of the cPLA₂ α inhibitors was chosen.

Combining alpelisib/BYL719 with selective cPLA₂ α inhibitors did not show any additive or synergistic effects. Again, the reason behind this might be the concentration choice of alpelisib/BYL719 and cPLA₂ α inhibitors, which was not optimal. The calculated IC₅₀ value of alpelisib/BYL719 was 20 μ M in SF-RPMI and in the combination experiment, a concentration much below this limit was used (5 μ M). This also applies for the cPLA₂ α inhibitors where 5 μ M of each inhibitor were used, which was also below the IC₅₀ value limits of the inhibitors. Therefore, it is questioned that choosing a concentration closer to the IC₅₀ limit of this compound may also show similar inhibitory effects as the buparlisib/BKM120 combination treatment. Due to the limited time of this master project, this experiment was not repeated beside the three biological replicas. Thus, optimizing the concentration of the inhibitors in the combination treatment is an issue to be addressed in future studies.

Similarly, the combination treatment of dactolisib/BEZ235 did not show any additive or synergistic effects on the MDA-MB-468 cells. The reason behind this is believed to be caused by the concentration choice of the cPLA₂ α -inhibitors only, and not concentration of

dactolisib/BEZ235. This is highly supported by the fact that 5 μ M AVX002 in combination with 5 μ M dactolisib/BEZ235 (which was around the limit of the IC₅₀ values for each compound) induced additive effects. Also, in this context, an additive effect can not be ruled out and optimizing the concentration of the inhibitors could confirm this suggestion.

In summary, even though selective cPLA₂ α and PI3K/mTOR inhibitors have had positive response on reducing the viability of MDA-MB-468 cells, rational combination of these two inhibitors that targets different signalling pathways in cancer are important. This can substantially increase the therapeutic outcome and overcome the resistance problem for these patients.

4.7 Selective cPLA₂ α inhibitors increase caspase activity

Caspases are responsible for many of the morphological and biochemical alterations of cells during apoptosis. Activated caspase 3 and 7 cleave and activate other caspases and proteins involved in apoptosis. An increase in caspase activity is highly correlated with a high apoptosis signal (88).

The activity of caspase 3 and 7 were investigated by caspase assay. Here, selective cPLA₂ α inhibitors and buparlisib/BKM (pan PI3K inhibitor) increased the caspase activity of MDA-MB-468 cells in a similar way as doxorubicin. In addition, when selective cPLA₂ α inhibitors were combined with buparlisib/BKM120 a further increase in the caspase activity was observed. This can indicate that both inhibitors induce caspase activity in MDA-MB-468 cells. However, in the study of Basu *et al.*, a selective COX-2 inhibitor, celecoxib, that targets a downstream enzyme of cPLA₂ α , showed no induction in the caspase activity and did not increase apoptotic death in the MDA-MB-468 cells (108). In the same study, MDA-MB-231, a more aggressive cancer cell line, both increased caspase-activity and induced apoptotic death. The COX-2 enzymes are responsible for the conversion of AA to various lipid mediators, including PGE₂ that is implicated in cancer signalling (109). The cPLA₂ α on the other hand, regulates the release of AA which can metabolically be converted through other enzymes than COX-2 to several types of lipid mediators (44). It is therefore considered that other metabolites of AA (such as thromboxanes) also may play important role in the caspase activation. However, further studies are needed to examine whether other metabolites may be involved in this process. Also in the study of Basu *et al.*, Dulbecco's modified eagle medium

(DMEM) was used to culture the cells and cells were 80 % confluent at time of the treatment (108). Such elements have shown to play a fundamental role in order to obtain reproducible results. For example, the study of Kim *et al.*, discovered the importance of these factors and showed that alterations in these elements changes the gene expression levels of cancer cells substantially (110). Therefore, we cannot rely on the fact that the results of this study also apply for these cells.

4.8 Cells arrested at different cell cycle phases in response to AVX002 and buparlisib/BKM120

The cPLA₂α enzyme has been found to regulate cell cycle progression of murine cells by controlling the production of PGE₂, which leads to activation of the PI3K/AKT pathways. This in turn increases phosphorylation of FOXO1 that mediate G1 progression of the cell cycle (48). It has also been found that cPLA₂α can control the G2-M transition of the cell cycle through phosphorylation of SIRT2 (49).

In this experiment, cPLA₂α was not found to regulate G2-M arrest in the MDA-MB-468 cells. However, 8 μM AVX002 was shown to induce G1 arrest to a certain level. This can indicate that cPLA₂α seems to play a greater role in controlling the G1 phase in the MDA-MB-468 cells cycle than the transition of G2-M phase.

Doxorubicin, on the other hand, induced cell cycle arrest in the G2-M phase. This finding is highly supported by the study of Lüpertz R *et al.*, that also showed similar findings in Hct-116 human colon carcinoma cells (111). Yet, in this study, doxorubicin was found to induce cell cycle arrest in the G2-M phase at 1 μM concentration after 24 hours and G1-arrest in 5 μM concentration. Simultaneously, buparlisib/BKM120 also arrested the MDA-MB-468 cell in the G2-M phase of the cell cycle. These observations were similar to the observations made for doxorubicin, beside the fact that the percentage of cells in the G2-M phase in response to buparlisib/BKM120 was significantly lower. Also here, our findings are in correlation with the study of Koul *et al.* where buparlisib/BKM120 also arrested cells in the G2-M phase (112). Although in this study, the effects were seen in glioma cells and the exposure time were 72 hours, same observations were made in this context.

When 3 μM buparlisib/BKM120 and 8 μM AVX002 was combined, an increasing number of cells in the G1 phase of the cell cycle were observed. This may suggest that low concentration

of AVX002 did not affect the cell cycle phase distribution of the cells and the effects of buparlisib/BKM120 here were more visible. Increasing the dose of AVX002 in the combination treatment increased the effects of AVX002 and induced cell cycle arrest in the G1 phase.

In order to truly conclude that these observations are due to the effects of AVX002 and buparlisib/BKM120, protein expression level and phosphorylation levels of proteins involved in the regulation of cell cycle phase needs to be assessed.

4.9 cPLA₂α may regulate pathways such as PI3K and RAF/MEK/ERK in BLBC/TNBC

Here we present the possible signalling pathways of the cPLA₂α inhibition that can affect BLBC/TNBC survival, apoptosis, angiogenesis and proliferation. An overview of the possible signalling pathways of cPLA₂α in BLBC/TNBC is demonstrated in figure 15. In the figure, the blue arrows points at the possible pathways which may be affected when inhibiting the cPLA₂α enzyme. The detailed information about signalling proteins and other enzymes were not investigated in this project, and are mostly based on suggestions and confirmed knowledge. Studying the downstream signalling proteins in the MDA-MB-468 cells or other BLBC/TNBC cells with high expression of cPLA₂α could be an issue to be addressed in future research.

The cPLA₂α enzyme is known to regulate the activity of the PI3K/AKT pathway by regulating the production of PGE₂, as described earlier. Also, cPLA₂α is shown to regulate the RAF/MEK/ERK signalling by its phospholipase activity (48). Inhibiting these pathways is thus associated with cell cycle arrest and/or apoptosis. Also, this enzyme plays a crucial role in other cancer signalling pathways that leads to metastasis, survival and angiogenesis (44). Hence, cPLA₂α inhibition may be beneficial in regulating the expression and the activity of these pathways. Therefore, this enzyme could introduce a novel targeted therapy that may benefit BLBC/TNBC patients, which have a different survival prognosis compared to other breast cancer patients.

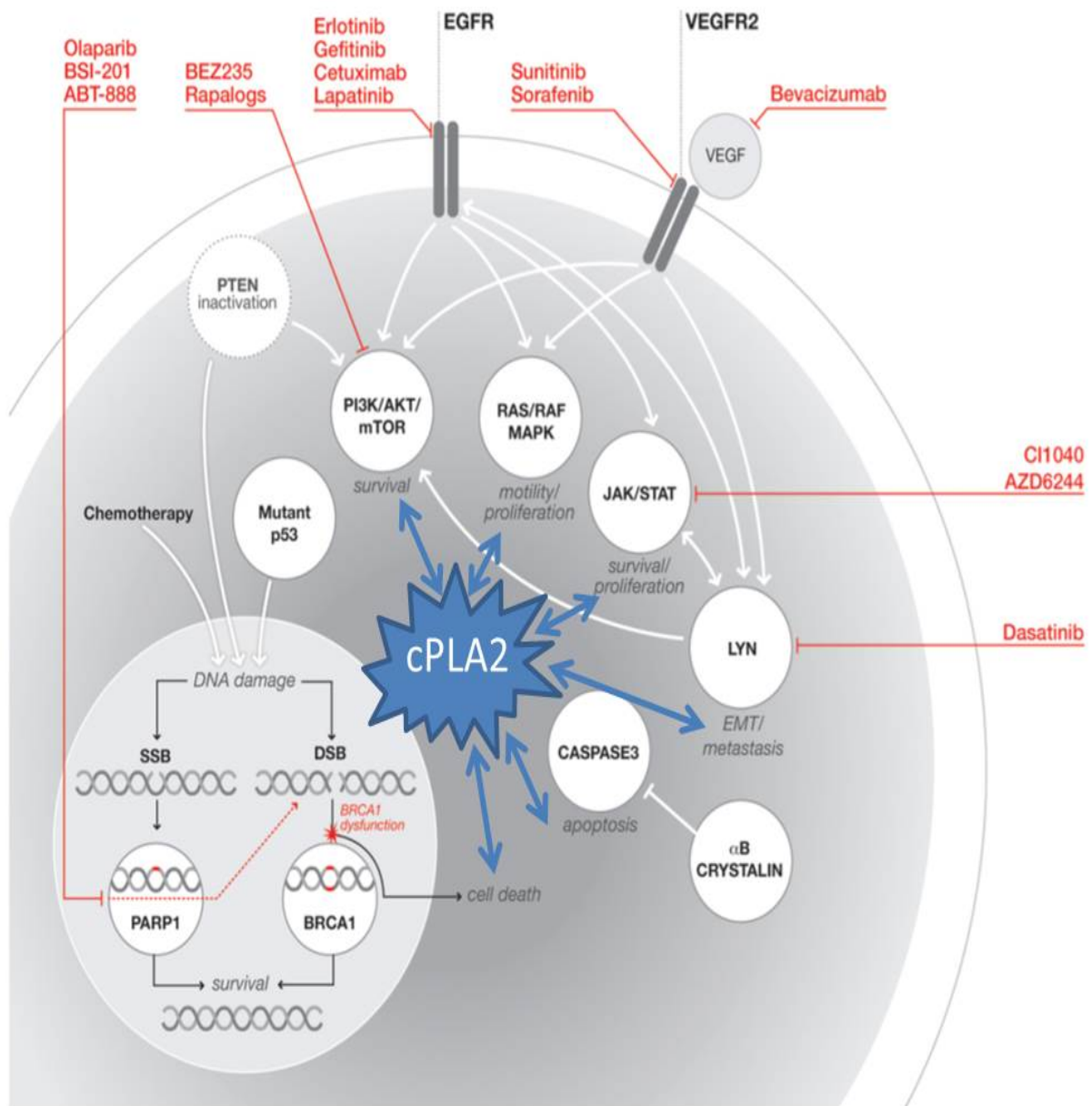


Figure 15: Suggested mechanism of action where cPLA₂α may target different pathways in BLBC/TNBC. The blue arrows indicate possible pathways where PLA₂α may target cell proliferation, survival, metastasis and apoptosis. PTEN, phosphatase and tensin homolog; PI3K/AKT/mTOR, phosphatidylinositol-3-kinases-/akt/mammalian target of rapamycin; RAS/RAF/MAPK, RAS/rapidly accelerated fibrosarcoma/mitogen activated protein kinases; JAK/STAT, Janus family of tyrosine kinase; LYN, Lck/Yes novel tyrosine kinase; CASPASE3, cysteine-aspartic acid proteases-3; PARP, Poly (ADP) ribose polymerase-1; BRCA1, Breast cancer 1; SSB, single-strand DNA break; DSB, double-strand DNA break

4.10 Technical variations in cell experiments

An important factor that affects the results of the experiments is technical variations. Technical variations can be cell confluency, use of various batches of inhibitors and the passage numbers of cells. All these factors can play an essential role in the results obtained from the experiments. To make sure that approximately the same number of cells was seeded in all wells, a multi-channel pipet was used. In this project, all the wells in the 96-well plate were utilized, except for the caspase assay where the edges were not used. However, when the results were analysed, values that differed from the general average of all the parallels were excluded. The experiments were conducted in healthy, viable cells in sub-confluent state. Also, cells were always split in sub-confluent state to exclude the possible effects of cells in post-confluent state.

In all the dose-response experiments of the AVX-inhibitors, an increase in metabolic activity of cells treated in low concentrations was observed. These effects were mostly seen in cells treated with inhibitors in SF-RPMI. Also, the same observations were made by a former master student, Madina Akan (MSc thesis, NTNU, June 2016). However, since the resazurin assay mainly measures the metabolic activity of cells (74), an increase in signal is not synonymous with increased viability. Another possible explanation for these effects can be due to the location of the treated cells. Cells treated with the lowest concentration of inhibitors was cultured on the edges and therefore, the observed effects of these inhibitors may be caused by edge effects. Also, the results of AVX002 and ATK differed between the dose-response experiments and in the combination treatment with selective PI3K inhibitors. As described in subchapter 4.3, these compounds are rapidly oxidized. Even though the vials were kept in -80 °C and taken out quickly before applying them to the cells, it is a possibility that the reduced response of these inhibitors in the first experiments were due to oxidation. Also, different batches of inhibitors were used between different experiments which may have affected the results.

After gaining some experience and knowledge about the inhibitors, the vials were kept on ice during the whole experiment to reduce further oxidation. These changes can support the increased effect of AVX002 and ATK in the combination experiments as demonstrated in figure 11-C.

4.11 Future research

The experiments conducted in this master's project were done in the MDA-MB-468 cells, where the cPLA₂α expression level are unknown (reports not found). To evaluate the possibility of using selective cPLA₂α inhibitors as a targeted treatment against BLBC/TNBC, the same experiments should also be performed in other BLBC/TNBC cell lines with higher and lower expression of the cPLA₂α-enzyme. This may reveal whether expression levels of the cPLA₂α enzyme in various cell lines affects their proliferation rates.

Due to time restraints, the cell cycle experiment was repeated only once with 6 technical repeats and with no biological replicates. Therefore, these results were preliminary and should be repeated with more biological replicas.

Even though cPLA₂α inhibition was found to reduce the viability of the MDA-MB-468 cells, both alone and combined with other agents/ compounds/therapies, it should be kept in mind that most of the experiments were performed in serum free growth media. When using serum free growth media, the cells are starved from serum, which contains several essential growth factors that cells need to accomplish important tasks such as proliferation. Therefore, starving the cells may affect the progression of the cell cycle and arrest cells in a specific cell cycle phase. Also, starved cells may express other features when it comes to the expression of essential proteins and enzymes. All these elements may play a substantial role in cell experiments and therefore limit the physiological relevance of our results. Therefore, to be able to evaluate the physiological relevance of using cPLA₂α inhibitors as a therapeutic target, additional cancer cell lines, primary cells and more animal studies should be utilized in future studies.

Furthermore, future studies should also include other combination treatments with selective cPLA₂α inhibitors that targets BLBC/TNBC via different pathways, such as chemotherapies or other targeted therapies suggested for BLBC/TNBC.

Lastly, dactolisib/BEZ235 is excluded from other preclinical studies due to serious unwanted side effects. Hence, a combination treatment of dactolisib/BEZ235 and a selective cPLA₂α inhibitor may not be a clinically relevant combination for treating BLBC/TNBC.

5 Conclusion

This thesis addresses the effects of cPLA₂α inhibition alone and combined with selective PI3K inhibitors in the MDA-MB-468 cells, which is an *in vitro* model for BLBC/TNBC. Several aspects of cPLA₂α and PI3K inhibition were investigated separately and combined together, such as viability, apoptosis and cell cycle phase distribution.

Selective cPLA₂α and PI3K inhibitors were found to have anti-proliferative effects in the MDA-MB-468 cells in a dose-dependent manner. The results from the dose-response experiments were variable and are correlated with variable potency of the inhibitors. However, the observed lower response of AVX235 and AVX420 in contrast to AV002 in the viability assay may be caused by increased enzymatic reduction of these compounds.

Combination treatment of selective cPLA₂α with buparlisib/BKM120 revealed additive effects with improved anti-proliferative effects compared to mono-treatment in the same concentrations. The selective PI3Kα inhibitor alpelisib/BYL719 did not show any additive effects, while mTOR/PI3K inhibitor dactolisib/BEZ235 induced a two-fold additive effect only in combination with AVX002. The lack of additive effects upon combining these inhibitors with selective cPLA₂α inhibitors are believed to be caused by the fact that a concentration much lower than the IC₅₀ values were used. Optimizing the doses of these combo-treatments in the future are believed to give the same additive effects as buparlisib/BKM120. Selective cPLA₂α inhibitors are believed to cause apoptosis in low concentration and possibly also cell cycle arrest at G1 phase in the MDA-MB-468 cells, but the underlying mechanism of these effects are yet to be explored. Further studies are necessary to confirm these findings.

Taken together, the use of selective cPLA₂α inhibitors in mono-therapy could offer a novel targeted therapy for BLBC/TNBC which otherwise have low survival prognosis. Furthermore, combining selective cPLA₂α inhibitors with selective PI3K inhibitors could potentially balance the side effect profile of each inhibitor and reduce resistance problems. Further studies need to be conducted to reject or accept these observations.

6 REFERENCES

1. Jemal A, Bray F, Center MM, Ferlay J, Ward E, Forman D. Global cancer statistics. *CA: A Cancer Journal for Clinicians*. 2011;61(2):69-90.
2. Ferlay J, Soerjomataram I, Dikshit R, Eser S, Mathers C, Rebelo M, et al. Cancer incidence and mortality worldwide: Sources, methods and major patterns in GLOBOCAN 2012. *International Journal of Cancer*. 2015;136(5):E359-E86.
3. Youlten DR, Cramb SM, Dunn NAM, Muller JM, Pyke CM, Baade PD. The descriptive epidemiology of female breast cancer: An international comparison of screening, incidence, survival and mortality. *Cancer Epidemiology*. 2012;36(3):237-48.
4. Berry DA, Inoue L, Shen J, Venier D, Cohen M, Bondy R, et al. Modeling the impact of treatment and screening on U.S. breast cancer mortality: a Bayesian approach. *Journal of the National Cancer Institute Monographs*. 2006(36):30-6.
5. Key TJ, Verkasalo PK, Banks E. Epidemiology of breast cancer. *Lancet Oncol*. 2001;2(3):133-40.
6. Giordano SH, Buzdar AU, Smith TL, Kau SW, Yang Y, Hortobagyi GN. Is breast cancer survival improving? *Cancer*. 2004;100(1):44-52.
7. Alvarez RH, Valero V, Hortobagyi GN. Emerging targeted therapies for breast cancer. *Journal of clinical oncology : official journal of the American Society of Clinical Oncology*. 2010;28(20):3366.
8. Senkus E, Kyriakides S, Ohno S, Penault-Llorca F, Poortmans P, Rutgers E, et al. Primary breast cancer: ESMO Clinical Practice Guidelines for diagnosis, treatment and follow-up. *Annals of Oncology*. 2015;26(suppl 5):v8-v30.
9. Sobin LH, Wittekind C, Gospodarwicz MK, International Union Against C. TNM : classification of malignant tumours. 7th ed. ed. Oxford: Wiley-Blackwell; 2010.
10. Schott AF. Systemic treatment of metastatic breast cancer in women: Chemotherapy 2015 [updated 21 August, 2015; cited 2016 27 January]. Available from: [http://www.uptodate.com/contents/systemic-treatment-of-metastatic-breast-cancer-in-women-chemotherapy?source=see link - H196667394](http://www.uptodate.com/contents/systemic-treatment-of-metastatic-breast-cancer-in-women-chemotherapy?source=see_link-H196667394).
11. Rosa GM, Gigli L, Tagliasacchi MI, Di Iorio C, Carbone F, Nencioni A, et al. Update on cardiotoxicity of anti-cancer treatments. *European journal of clinical investigation*. 2016.
12. Charles S. Targeted cancer therapy. *Nature*. 2004;432(7015):294.
13. Mohamed A, Krajewski K, Cakar B, Ma CX. Targeted Therapy for Breast Cancer. *The American Journal of Pathology*. 2013;183(4):1096-112.
14. Pritchard KI. Adjuvant endocrine therapy for non-metastatic, hormone receptor-positive breast cancer 2015 [updated 13 October. 2015; cited 2016 27 January]. Available from: [http://www.uptodate.com/contents/adjuvant-endocrine-therapy-for-non-metastatic-hormone-receptor-positive-breast-cancer?source=see link - H2110938219](http://www.uptodate.com/contents/adjuvant-endocrine-therapy-for-non-metastatic-hormone-receptor-positive-breast-cancer?source=see_link-H2110938219).
15. Burstein HM. Adjuvant medical therapy for HER2-positive breast cancer 2015 [updated January 18, 2016. Available from: [http://www.uptodate.com/contents/adjuvant-medical-therapy-for-her2-positive-breast-cancer?source=related link](http://www.uptodate.com/contents/adjuvant-medical-therapy-for-her2-positive-breast-cancer?source=related_link).
16. B N. Treatment of breast cancer Norway 2016 [updated 26.03.14; cited 2015 07.09.15]. Available from: <http://oncolex.org/Breast-cancer/Procedures/TREATMENT/RadiationTherapy?lg=procedureGroup>.
17. Sørlie T, Perou CM, Tibshirani R, Aas T, Geisler S, Johnsen H, et al. Gene Expression Patterns of Breast Carcinomas Distinguish Tumor Subclasses with Clinical Implications. *Proceedings of the National Academy of Sciences of the United States of America*. 2001;98(19):10869-74.
18. Vuong D, Simpson P, Green B, Cummings M, Lakhani S. Molecular classification of breast cancer. *The European Journal of Pathology*. 2014;465(1):1-14.

19. Engstrom MJ, Opdahl S, Hagen AI, Romundstad PR, Akslen LA, Haugen OA, et al. Molecular subtypes, histopathological grade and survival in a historic cohort of breast cancer patients.(PRECLINICAL STUDY). *Breast Cancer Research and Treatment*. 2013;140(3):463.
20. Cheang M, Voduc D, Bajdik C, Leung S, McKinney S, Chia S, et al. Basal-like breast cancer defined by five biomarkers has superior prognostic value than triple-negative phenotype. *Clin Cancer Res*. 2008;14(5):1368-76.
21. Edling CE, Hallberg B. c-Kit—A hematopoietic cell essential receptor tyrosine kinase. *International Journal of Biochemistry and Cell Biology*. 2007;39(11):1995-8.
22. Pazaiti A, Fentiman I. Basal phenotype breast cancer: implications for treatment and prognosis. London: Future Medicine Ltd; 2011. p. 181-202.
23. Toft DJ, Cryns VL. Minireview: Basal-Like Breast Cancer: From Molecular Profiles to Targeted Therapies. *The Journal of Clinical Endocrinology & Metabolism*. 2010;95(10):4781-2.
24. Elias AD. Triple-Negative Breast Cancer: A Short Review. *American Journal of Clinical Oncology*. 2010;33(6):637-45.
25. Linkous A, Yazlovitskaya E. Cytosolic phospholipase A2 as a mediator of disease pathogenesis. *Cellular Microbiology*. 2010;12:1369-77.
26. Rosenson RS, Hurt-Camejo E. Phospholipase A enzymes and the risk of atherosclerosis. *European Heart Journal*. 2012;33(23):2899-909.
27. Laye JP, Gill JH. Phospholipase A 2 expression in tumours: a target for therapeutic intervention? *Drug Discovery Today*. 2003;8(15):710-6.
28. Masuda S, Murakami M, Komiyama K, Ishihara M, Ishikawa Y, Ishii T, et al. Various secretory phospholipase A 2 enzymes are expressed in rheumatoid arthritis and augment prostaglandin production in cultured synovial cells. *FEBS Journal*. 2005;272(3):655-72.
29. Pniewska E, Pawliczak R. The Involvement of Phospholipases A2 in Asthma and Chronic Obstructive Pulmonary Disease. *Mediators of Inflammation*. 2013;2013:12.
30. Dennis EA, Cao J, Hsu Y-H, Magrioti V, Kokotos G. Phospholipase A(2) Enzymes: Physical Structure, Biological Function, Disease Implication, Chemical Inhibition, and Therapeutic Intervention. *Chemical reviews*. 2011;111(10):6130-85.
31. Mouchlis VD, McCammon JA, Dennis EA, Bucher D. Membranes serve as allosteric activators of phospholipase a 2 , enabling it to extract, bind, and hydrolyze phospholipid substrates. *Proceedings of the National Academy of Sciences of the United States of America*. 2015;112(6):E516-E25.
32. Burke J, Dennis E. Phospholipase A 2 Biochemistry. *Cardiovascular Drugs and Therapy*. 2009;23(1):49-59.
33. Flachs P, Rossmeisl M, Bryhn M, Kopecky J. Cellular and molecular effects of n-3 polyunsaturated fatty acids on adipose tissue biology and metabolism. *Clin Sci*2009. p. 1-16.
34. Jia-Jia H, Gang T, Ning Z. Cytosolic Phospholipase A2 and Its Role in Cancer. *Cancer Biology & Medicine*. 2011;8(2):71.
35. Kramer RM, Roberts EF, Um SL, Börsch-Haubold AG, Watson SP, Fisher MJ, et al. p38 Mitogen-activated Protein Kinase Phosphorylates Cytosolic Phospholipase A2 (cPLA2) in Thrombin-stimulated Platelets: EVIDENCE THAT PROLINE-DIRECTED PHOSPHORYLATION IS NOT REQUIRED FOR MOBILIZATION OF ARACHIDONIC ACID BY cPLA2. *Journal of Biological Chemistry*. 1996;271(44):27723-9.
36. Myou S, Leff AR, Myo S, Boetticher E, Meliton AY, Lambertino AT, et al. Activation of group IV cytosolic phospholipase A2 in human eosinophils by phosphoinositide 3-kinase through a mitogen-activated protein kinase-independent pathway. *Journal of immunology (Baltimore, Md : 1950)*. 2003;171(8):4399.
37. Casas J, Meana C, Esquinas E, Valdearcos M, Pindado J, Balsinde J, et al. Requirement of JNK-mediated phosphorylation for translocation of group IVA phospholipase A2 to phagosomes in human macrophages. *Journal of immunology (Baltimore, Md : 1950)*. 2009;183(4):2767.
38. Murakami M. Lipid Mediators in Life Science. *Experimental Animals*. 2011;60(1):7-20.
39. Dingzhi W, Raymond ND. Eicosanoids and cancer. *Nature Reviews Cancer*. 2010;10(3):181.

40. Parhamifar L, Jeppsson B, Sjölander A. Activation of cPLA2 is required for leukotriene D4-induced proliferation in colon cancer cells. *Carcinogenesis*. 2005;26(11):1988-98.
41. Patel MI, Singh J, Niknami M, Kurek C, Yao M, Lu S, et al. Cytosolic phospholipase A 2- α : A potential therapeutic target for prostate cancer. *Clinical Cancer Research*. 2008;14(24):8070-9.
42. Linkous AG, Yazlovitskaya EM, Hallahan DE. Cytosolic Phospholipase A2 and Lysophospholipids in Tumor Angiogenesis. *Journal of the National Cancer Institute*. 2010;102(18):1398-412.
43. Caiazza F, Mccarthy NS, Young L, Hill ADK, Harvey BJ, Thomas W. Cytosolic phospholipase A2- α expression in breast cancer is associated with EGFR expression and correlates with an adverse prognosis in luminal tumours. *British Journal of Cancer*. 2010;104(2):338.
44. Nakanishi M, Rosenberg DW. Roles of cPLA2 α and arachidonic acid in cancer. *Biochimica et Biophysica Acta (BBA) - Molecular and Cell Biology of Lipids*. 2006;1761(11):1335-43.
45. Grinde MT, Skrbo N, Moestue SA, Rødland EA, Borgan E, Kristian A, et al. Interplay of choline metabolites and genes in patient-derived breast cancer xenografts. *Breast Cancer Research : BCR*. 2014;16(1):R5-R.
46. Moestue SA, Borgan E, Huuse EM, Lindholm EM, Sitter B, Børresen-Dale A-L, et al. Distinct choline metabolic profiles are associated with differences in gene expression for basal-like and luminal-like breast cancer xenograft models. *BMC Cancer*. 2010;10(1):1-12.
47. Kim E, Tunset HM, Cebulla J, Vettukattil R, Helgesen H, Feuerherm AJ, et al. Anti-vascular effects of the cytosolic phospholipase A2 inhibitor AVX235 in a patient-derived basal-like breast cancer model. *BMC Cancer*. 2016;16:191.
48. Naini SM, Choukroun GJ, Ryan JR, Hentschel DM, Shah JV, Bonventre JV. Cytosolic phospholipase A2 α regulates G1 progression through modulating FOXO1 activity. *FASEB journal : official publication of the Federation of American Societies for Experimental Biology*. 2016;30(3):1155.
49. Movahedi Naini S, Sheridan AM, Force T, Shah JV, Bonventre JV. Group IVA Cytosolic Phospholipase A2 Regulates the G2-to-M Transition by Modulating the Activity of Tumor Suppressor SIRT2. *Molecular and cellular biology*. 2015;35(21):3768.
50. Canaud G, Bonventre JV. Cell cycle arrest and the evolution of chronic kidney disease from acute kidney injury. *Nephrology, dialysis, transplantation : official publication of the European Dialysis and Transplant Association - European Renal Association*. 2015;30(4):575.
51. Burgering BMT, Kops GJPL. Cell cycle and death control: long live Forkheads. *Trends in Biochemical Sciences*. 2002;27(7):352-60.
52. Birkenkamp KU, Coffey PJ. Regulation of cell survival and proliferation by the FOXO (Forkhead box, class O) subfamily of Forkhead transcription factors. *Biochemical Society Transactions*. 2003;31(1):292-7.
53. Leis HJ, Windischhofer W. Inhibition of cyclooxygenases 1 and 2 by the phospholipase-blocker, arachidonyl trifluoromethyl ketone. *Br J Pharmacol*. 2008;155(5):731-7.
54. Huwiler A, Feuerherm AJ, Sakem B, Pastukhov O, Filipenko I, Nguyen T, et al. The ω 3-polyunsaturated fatty acid derivatives AVX001 and AVX002 directly inhibit cytosolic phospholipase A(2) and suppress PGE(2) formation in mesangial cells. *British Journal of Pharmacology*. 2012;167(8):1691-701.
55. Andreis PG, Buttazzi P, Tortorella C, De Caro R, Aragona F, Neri G, et al. The inhibitor of phospholipase-A2, AACOCF3, stimulates steroid secretion by dispersed human and rat adrenocortical cells. *Life Sciences*. 1999;64(15):1287-94.
56. Riendeau D, Guay J, Weech PK, Laliberte F, Yergey J, Li C, et al. Arachidonyl trifluoromethyl ketone, a potent inhibitor of 85-kDa phospholipase A2, blocks production of arachidonate and 12-hydroxyeicosatetraenoic acid by calcium ionophore-challenged platelets. *J Biol Chem*. 1994;269(22):15619-24.
57. Kokotos G, Barbayianni E, Magrioti V, Feuerherm AJ, Sæther M, Nguyen T, et al. Inhibition of group IVA cytosolic phospholipase A 2 by thiazolyl ketones in vitro, ex vivo, and in vivo. *Journal of Medicinal Chemistry*. 2014;57(18):7523-35.

58. Holmeide AK, Skattebol L. Syntheses of some polyunsaturated trifluoromethyl ketones as potential phospholipase A2 inhibitors. *Journal of the Chemical Society, Perkin Transactions 1*. 2000(14):2271-6.
59. Sommerfelt RM, Feuerherm AJ, Jones K, Johansen B. Cytosolic Phospholipase A2 Regulates TNF-Induced Production of Joint Destructive Effectors in Synoviocytes. *PLoS ONE*. 2013;8(12):e83555.
60. Sommerfelt RM, Feuerherm AJ, Skuland T, Johansen B. Cytosolic phospholipase A2 modulates TLR2 signaling in synoviocytes. *PLoS ONE*. 2015;10(4).
61. Cailleau R, Olivé M, Cruciger Q. Long-term human breast carcinoma cell lines of metastatic origin: Preliminary characterization. *In Vitro*. 1978;14(11):911-5.
62. Masters JR. HeLa cells 50 years on: the good, the bad and the ugly. *Nat Rev Cancer*. 2002;2(4):315-9.
63. Chavez KJ, Garimella SV, Lipkowitz S. Triple Negative Breast Cancer Cell Lines: One Tool in the Search for Better Treatment of Triple Negative Breast Cancer. *Breast disease*. 2010;32(1-2):35-48.
64. Bates SE, Valverius EM, Ennis BW, Bronzert DA, Sheridan JP, Stampfer MR, et al. Expression of the transforming growth factor-alpha/epidermal growth factor receptor pathway in normal human breast epithelial cells. *Endocrinology*. 1990;126(1):596-607.
65. Kai-Yun C, Li-Ming H, Hsing-Jien K, David KA, Hsiu-Ming S. The role of tyrosine kinase Etk/Bmx in EGF-induced apoptosis of MDA-MB-468 breast cancer cells. *Oncogene*. 2003;23(10):1854.
66. Armstrong DK, Kaufmann SH, Ottaviano YL, Furuya Y, Buckley JA, Isaacs JT, et al. Epidermal growth factor-mediated apoptosis of MDA-MB-468 human breast cancer cells. *Cancer research*. 1994;54(20):5280.
67. Hernandez-Alcoceba R, Fernandez F, Lacal JC. In vivo antitumor activity of choline kinase inhibitors: a novel target for anticancer drug discovery. *Cancer Res*. 1999;59.
68. McLean BA, Zhabyeyev P, Pituskin E, Paterson I, Haykowsky MJ, Oudit GY. PI3K Inhibitors as Novel Cancer Therapies: Implications for Cardiovascular Medicine. *Journal of Cardiac Failure*. 2013;19(4):268-82.
69. Robert C, Soria J-C, Spatz A, Le Cesne A, Malka D, Pautier P, et al. Cutaneous side-effects of kinase inhibitors and blocking antibodies. *The Lancet Oncology*. 2005;6(7):491-500.
70. Mayer I, Singer C, Fasching PA, Holmes FA, Gnant M, Estevez L, et al. A Phase II study of the safety and efficacy of alpelisib or buparlisib plus letrozole in neoadjuvant treatment of postmenopausal women with HR+/HER2-, PIK3CA mutant or wild-type breast cancer. *J Clin Oncol*. 2015;33(15).
71. Geuna E, Milani A, Martinello R, Aversa C, Valabrega G, Scaltriti M, et al. Buparlisib , an oral pan-PI3K inhibitor for the treatment of breast cancer. *Expert opinion on investigational drugs*. 2015;24(3):421-31.
72. Paplomata E, O'Regan R. The PI3K/AKT/mTOR pathway in breast cancer: targets, trials and biomarkers. *Therapeutic Advances in Medical Oncology*. 2014;6(4):154-66.
73. ATCC@ ANIMAL CELL CULTURE GUIDE tips and techniques for continuous cell lines: ATCC; 2014 [cited 2016 22.03.2016]. Available from: <http://www.lgcstandards-atcc.org/en/Guides/Guides.aspx>.
74. Anoopkumar-Dukie S, Carey JB, Conere T, O'Sullivan E, van Pelt FN, Allshire A. Resazurin assay of radiation response in cultured cells. *The British journal of radiology*. 2005;78(934):945.
75. Harris RC, Chung E, Coffey RJ. EGF receptor ligands. *Exp Cell Res*. 2003;284(1):2-13.
76. Schaeferli P, Jaggi R. EGF-induced programmed cell death of human mammary carcinoma MDA-MB-468 cells is preceded by activation of AP-1. *Cellular and Molecular Life Sciences CMLS*. 1998;54(2):129-38.
77. Montecucco A, Zanetta F, Biamonti G. Molecular mechanisms of etoposide. *EXCLI Journal*. 2015;14:95-108.
78. Badinloo M, Esmaeili-Mahani S. Phosphatidylinositol 3-kinases inhibitor LY294002 potentiates the cytotoxic effects of doxorubicin, vincristine, and etoposide in a panel of cancer cell lines. *Fundamental & clinical pharmacology*. 2014;28(4):414.

79. Marzec KA, Lin MZ, Martin JL, Baxter RC. Involvement of p53 in insulin-like growth factor binding protein-3 regulation in the breast cancer cell response to DNA damage. *Oncotarget*. 2015;6(29):26583.
80. Kaufmann SH. Induction of endonucleolytic DNA cleavage in human acute myelogenous leukemia cells by etoposide, camptothecin, and other cytotoxic anticancer drugs: a cautionary note. *Cancer research*. 1989;49(21):5870.
81. Doxorubicin: Drug information. Mechanism of Action 2016 [updated January 27, 2016; cited 2016 22.03.216]. Lexicomp]. Available from: http://www.uptodate.com/contents/doxorubicin-conventional-drug-information?source=see_link&utdPopup=true.
82. Patil R, Portilla-Arias J, Ding H, Konda B, Rekechenetskiy A, Inoue S, et al. Cellular Delivery of Doxorubicin via pH-Controlled Hydrazone Linkage Using Multifunctional Nano Vehicle Based on Poly(β -L-Malic Acid). *International Journal of Molecular Sciences*. 2012;13(9):11681-93.
83. Shafiee F, Sadeghi-aliabadi H, Hassanzadeh F. Evaluation of cytotoxic effects of several novel tetralin derivatives against Hela, MDA-MB-468, and MCF-7 cancer cells. *Advanced Biomedical Research*. 2012;1:76.
84. Methotrexate: Drug information. Mechanism of action 2016 [updated 12.May.2016; cited 2016 12. may]. Available from: http://www.uptodate.com/contents/methotrexate-drug-information?source=search_result&search=Methotrexate%3A+Drug+information&selectedTitle=1%7E150-F194514.
85. Cowan KH, Jolivet J. A methotrexate-resistant human breast cancer cell line with multiple defects, including diminished formation of methotrexate polyglutamates. *The Journal of biological chemistry*. 1984;259(17):10793.
86. O'Brien NA, McDonald K, Tong L, von Euw E, Kalous O, Conklin D, et al. Targeting PI3K/mTOR overcomes resistance to HER2-targeted therapy independent of feedback activation of AKT. *Clin Cancer Res*. 2014;20(13):3507-20.
87. Kong D, Yamori T. JFCR39, a panel of 39 human cancer cell lines, and its application in the discovery and development of anticancer drugs. *Bioorganic & Medicinal Chemistry*. 2012;20(6):1947-51.
88. McIlwain DR, Berger T, Mak TW. Caspase functions in cell death and disease. *Cold Spring Harbor perspectives in biology*. 2013;5(4):a008656.
89. Caspase-Glo® 3/7 Assay Promega: Promega; [cited 2016 25.05]. Protocoll. Available from: https://no.promega.com/~media/files/resources/protocols/technical_bulletins/101/caspase-glo_3_7_assay_protocol.pdf.
90. Brown M, Wtttwer C. Flow cytometry: Principles and clinical applications in hematology.(Beckman Conference). *Clinical Chemistry*. 2000;46(8):1221.
91. MDA-MB-468 (ATCC® HTB-132™) United states of America: American Type Tissue Culture; [updated 21.02.2014; cited 2015 10.09.2015]. Available from: http://www.lgcstandards-atcc.org/products/all/HTB-132.aspx?geo_country=no-characteristics.
92. Lind MJ. Principles of cytotoxic chemotherapy. *Medicine*. 2008;36(1):19-23.
93. Shafer SL, Hendrickx JF, Flood P, Sonner J, Eger EI, 2nd. Additivity versus synergy: a theoretical analysis of implications for anesthetic mechanisms. *Anesthesia and analgesia*. 2008;107(2):507-24.
94. Fulda S, Debatin KM. Extrinsic versus intrinsic apoptosis pathways in anticancer chemotherapy. *Oncogene*. 2006;25(34):4798.
95. Butler M, Jenkins H. Nutritional aspects of the growth of animal cells in culture. *Journal of Biotechnology*. 1989;12(2):97-110.
96. Hall A. The cytoskeleton and cancer. *Cancer and Metastasis Reviews*. 2009;28(1):5-14.
97. Kenny PA, Lee GY, Myers CA, Neve RM, Semeiks JR, Spellman PT, et al. The morphologies of breast cancer cell lines in three-dimensional assays correlate with their profiles of gene expression. *Molecular oncology*. 2007;1(1):84-96.

98. de Almagro MC, Selga E, Thibaut R, Porte C, Noé V, Ciudad CJ. UDP-glucuronosyltransferase 1A6 overexpression in breast cancer cells resistant to methotrexate. *Biochemical Pharmacology*. 2011;81(1):60-70.
99. Street IP, Hung-Kuei L, Laliberte F, Ghomashchi F, Zhaoyin W, Perrier H, et al. Slow- and tight-binding inhibitors of the 85-kDa human phospholipase A2. *Biochemistry*. 1993;32(23):5935.
100. Proskuryakov SYa, Konoplyannikov AG, Gabai VL. Necrosis: a specific form of programmed cell death? *Experimental Cell Research*. 2003;283(1):1-16.
101. Riendeau D, Guay J, Weech PK, Laliberté F, Yergey J, Li C, et al. Arachidonyl trifluoromethyl ketone, a potent inhibitor of 85-kDa phospholipase A2, blocks production of arachidonate and 12-hydroxyeicosatetraenoic acid by calcium ionophore-challenged platelets. *The Journal of biological chemistry*. 1994;269(22):15619.
102. Mete A, Andrews G, Bernstein M, Connolly S, Hartopp P, Jackson CG, et al. Design of novel and potent cPLA 2 α inhibitors containing an α -methyl-2-ketothiazole as a metabolically stable serine trap. *Bioorganic & Medicinal Chemistry Letters*. 2011;21(10):3128-33.
103. Chen M, Huang J, Yang X, Liu B, Zhang W, Huang L, et al. Serum Starvation Induced Cell Cycle Synchronization Facilitates Human Somatic Cells Reprogramming (Synchronization Facilitates Reprogramming). *PLoS ONE*. 2012;7(4):e28203.
104. Fritsch C, Huang A, Chatenay-Rivauday C, Schnell C, Reddy A, Liu M, et al. Characterization of the novel and specific PI3K α inhibitor NVP-BYL719 and development of the patient stratification strategy for clinical trials. *Molecular cancer therapeutics*. 2014;13(5):1117.
105. Yu Z. NVP-BEZ235, a novel dual PI3K-mTOR inhibitor displays anti-glioma activity and reduces chemoresistance to temozolomide in human glioma cells. *Cancer Lett*. 2015;367.
106. Netland IA, Førde HE, Sleire L, Leiss L, Rahman MA, Skeie BS, et al. Dactolisib (NVP-BEZ235) toxicity in murine brain tumour models. *BMC Cancer*. 2016;16(1):1-12.
107. Zheng Y, Yang J, Qian J, Zhang L, Lu Y, Li H, et al. Novel phosphatidylinositol 3-kinase inhibitor NVP-BKM120 induces apoptosis in myeloma cells and shows synergistic anti-myeloma activity with dexamethasone. *Journal of Molecular Medicine*. 2012;90(6):695-706.
108. Basu G, Pathangey L, Tinder T, Gendler S, Mukherjee P. Mechanisms underlying the growth inhibitory effects of the cyclo-oxygenase-2 inhibitor celecoxib in human breast cancer cells. *Breast Cancer Research*. 2005;7(4):R422-R35.
109. Greenhough A, Smartt HJM, Moore AE, Roberts HR, Williams AC, Paraskeva C, et al. The COX-2/PGE 2 pathway: key roles in the hallmarks of cancer and adaptation to the tumour microenvironment. *Carcinogenesis*. 2009;30(3):377-86.
110. Kim SW, Kim S-J, Langley RR, Fidler IJ. Modulation of the cancer cell transcriptome by culture media formulations and cell density. *International Journal of Oncology*. 2015;46(5):2067-75.
111. Lüpertz R, Wätjen W, Kahl R, Chovolou Y. Dose- and time-dependent effects of doxorubicin on cytotoxicity, cell cycle and apoptotic cell death in human colon cancer cells. *Toxicology*. 2010;271(3):115-21.
112. Koul D, Fu J, Shen R, Lafortune TA, Wang S, Tiao N, et al. Antitumor activity of NVP-BKM120--a selective pan class I PI3 kinase inhibitor showed differential forms of cell death based on p53 status of glioma cells. *Clinical cancer research : an official journal of the American Association for Cancer Research*. 2012;18(1):184.

APPENDIX

A. All biological replicas (n=3) for the representative experiment in figure 8:

Table A.1 The data represent the mean \pm SD of etoposide where control was set up to 100 % viability. * indicates results significantly different from the control ($p < 0.05$)

Treatment	72 hours	72 hours
	SF-RPMI	RPMI/10 % FBS
120 μ M etoposide	32.4*	27.5*
\pm SD	2.6	2.65
80 μ M etoposide	32.6*	25.1*
\pm SD	2.4	2.4
40 μ M etoposide	34.9*	28.0*
\pm SD	3.0	2.0
10 μ M Etoposide	51.4*	43.8*
\pm SD	3.1	7.7

Table A.2 The data represent the mean \pm SD of methotrexate where control was set up to 100 % viability. * indicates results significantly different from the control ($p < 0.05$)

Treatment	72 hours	72 hours
	SF-RPMI	RPMI/10 % FBS
100 μ M Methotrexate	39.7*	41.4*
\pm SD	3.6	4.5
80 μ M Methotrexate	42.3*	41.8*
\pm SD	3.2	3.97
40 μ M Methotrexate	40.6*	40.8*
\pm SD	4.3	3.1
10 μ M Methotrexate	43.5*	41.7*
\pm SD	5.3	3.6

Table A.3 The data represent the mean \pm SD of doxorubicin where control was set up to 100 % viability. * indicates results significantly different from the control ($p < 0.05$)

Treatment	72 hours	72 hours
	SF-RPMI	RPMI/10 % FBS
10 μ M Doxorubicin	21.8*	30.5*
\pm SD	2.1	3.7
5 μ M Doxorubicin	32.1*	41.7*
\pm SD	2.9	3.5
1 μ M Doxorubicin	43.8*	54.7*
\pm SD	4.8	4.4
0.5 μ M Doxorubicin	57.9*	61.1*
\pm SD	6.0	4.7

Table A.4 The data represent the mean \pm SD of EGF where control was set up to 100 % viability. * indicates results significantly different from the control ($p < 0.05$)

Treatment	72 hours	72 hours
	SF-RPMI	RPMI/10 % FBS
200 ng/mL EGF	38.0*	79.5*
\pm SD	5.4	9.6
100 ng/mL EGF	39.4*	78.7*
\pm SD	4.5	9.2
50 ng/mL EGF	60.4*	76.6*
\pm SD	10.0	11.2
10 ng/mL EGF	76.4*	84.6*
\pm SD	9.9	10.6

Table A.5 The data represent the mean \pm SD of DMSO where control was set up to 100 % viability.

Treatment	hours
	SF-RPMI
DMSO	100.3
\pm SD	2.9

B. All biological replicas (n=3) for the representative experiment in figure 9:

Table B.1 The data represent the mean \pm SD of AVX235 where control was set up to 100 % viability. * indicates results significantly different from the control ($p < 0.05$)

Treatment	72 hours	72 hours
	SF-RPMI	RPMI/10 % FBS
100 μ M AVX235	19.0*	48.5*
\pm SD	4.7	3.6
50 μ M AVX235	42.2*	68.6*
\pm SD	3.2	9.1
25 μ M AVX235	54.7*	97.2
\pm SD	8.5	5.3
5 μ M AVX235	97.3	102.0
\pm SD	13.7	4.4
1 μ M AVX235	119.9	105.4
\pm SD	13.7	5.5

Table B.2 The data represent the mean \pm SD of AVX420 where control was set up to 100 % viability. * indicates results significantly different from the control ($p < 0.05$)

Treatment	72 hours	72 hours
	SF-RPMI	RPMI/10 % FBS
100 μ M AVX420	9.6*	32.2*
\pm SD	0.43	3.3
50 μ M AVX420	9.9*	87.6*
\pm SD	0.35	7.8
25 μ M AVX420	48.7*	94.7*
\pm SD	6.6	7.8
5 μ M AVX420	88.3*	96.7
\pm SD	12.8	8.0
1 μ M AVX420	111.2	96.5
\pm SD	7.5	6.7

Table B.3 The data represent the mean \pm SD of AVX002 where control was set up to 100 % viability. * indicates results significantly different from the control ($p < 0.05$)

Treatment	72 hours	72 hours
	SF-RPMI	RPMI/10 % FBS
100 μ M AVX002	11.3*	14.9*
\pm SD	0.4	0.6
50 μ M AVX002	10.7*	14.9*
\pm SD	0.48	0.62
25 μ M AVX002	11.7*	16.3*
\pm SD	1.6	6.9
5 μ M AVX002	124.8	92.1*
\pm SD	8.3	8.9
1 μ M AVX002	119.4	112.3
\pm SD	9.5	6.6

Table B.4 The data represent the mean \pm SD of ATK where control was set up to 100 % viability. * indicates results significantly different from the control ($p < 0.05$), which was set to 100 % viability

Treatment	72 hours	72 hours
	SF-RPMI	RPMI/10 % FBS
50 μ M ATK	9.1*	7.87*
\pm SD	2.32	0.39
25 μ M ATK	62.2*	73.86*
\pm SD	8.6	6.8
5 μ M ATK	96.1	98.2
\pm SD	7.5	4.8
1 μ M ATK	100.8	99.3
\pm SD	7.0	5.6

C. All biological replicas (n=3) for the representative experiment in figure 10:

Table C.1 The data represent the mean \pm SD of dactolisib/BEZ235 where control was set up to 100 % viability. * indicates results significantly different from the control ($p < 0.05$)

Treatment	72 hours	72 hours
	SF-RPMI	RPMI/10 % FBS
Dactolisib/BEZ235 100 μ M	11.6*	10.36*
\pm SD	0.84	1.33
Dactolisib/BEZ235 50 μ M	11.34*	15.5*
\pm SD	1.0	3.4
Dactolisib/BEZ235 25 μ M	23.5*	30.1*
\pm SD	2.5	9.0
Dactolisib/BEZ235 5 μ M	61.0*	79.1*
\pm SD	5.8	8.4
Dactolisib/BEZ235 1 μ M	94.7*	107.8
\pm SD	7.5	7.4

Table C.2 The data represent the mean \pm SD of alpelisib/BYL719 where control was set up to 100 % viability. * indicates results significantly different from the control ($p < 0.05$)

Treatment	72 hours	72 hours
	SF-RPMI	RPMI/10 % FBS
Alpelisib/BYL719 100 μ M	31.5*	25.8*
\pm SD	6.0	2.5
Alpelisib /BYL719 50 μ M	34.5*	38.0*
\pm SD	2.7	6.1
Alpelisib /BYL719 10 μ M	73.8*	80.3*
\pm SD	6.9	8.9
Alpelisib /BYL719 1 μ M	97.7	97.4
\pm SD	7.0	9.2

Table C.3 The data represent the mean \pm SD of buparlisib/BKM120 where control was set up to 100 % viability. * indicates results significantly different from the control ($p < 0.05$)

Treatment	72 hours	72 hours
	SF-RPMI	RPMI/10 % FBS
20 μ M Buparlisib/BKM120	34.9*	28.6*
\pm SD	3.4	2.3
10 μ M Buparlisib/BKM120	40.7*	38.6*
\pm SD	7.5	6.0
5 μ M Buparlisib/BKM120	45.3*	42.8*
\pm SD	12.3	3.0
1 μ M Buparlisib/BKM120	84.36*	93.7*
\pm SD	5.6	9.9

D. All biological replicas (n=3) for the representative experiment in figure 11:

Table D.1 The data represent the mean \pm SD of dactolisib/BEZ235 combined with selective cPLA₂ α inhibitors where control was set up to 100 % viability. * indicates results significantly different from the control (p<0.05)

Treatment	hours SF-RPMI
Dactolisib/BEZ235 (5 μ M)	88.7*
\pm SD	4.9
AVX235 (7.5 μ M)	96.6
\pm SD	4.9
AVX420 (7.5 μ M)	98.4
\pm SD	6.2
AVX002 (7.5 μ M)	102.2
\pm SD	4.7
AVX235 (5 μ M) + Dactolisib/BEZ235 (5 μ M)	78.7*
\pm SD	3.4
AVX420 (5 μ M)+ Dactolisib/BEZ235 (5 μ M)	77.8*
\pm SD	6.8
AVX002 (5 μ M) + Dactolisib/BEZ235 (5 μ M)	45.1*
\pm SD)	7.4

Table D.2 The data represent the mean \pm SD of alpelisib/BYL719 combined with selective cPLA₂ α inhibitors where control was set up to 100 % viability. * indicates results significantly different from the control (p<0.05)

Treatment	hours SF-RPMI
Alpelisib/BYL719 (5 μ M)	80.45*
\pm SD	5.3
AVX235 (5 μ M)	100.7
\pm SD	6.9
AVX420 (5 μ M)	99.6
\pm SD	4.6
AVX002 (5 μ M)	87.3*
\pm SD	5.2
AVX235 (5 μ M) + Alpelisib/BYL719 (5 μ M)	82.6*
\pm SD	7.11
AVX420 (5 μ M)+ Alpelisib/BYL719 (5 μ M)	87.8*
\pm SD	8.4
AVX002 (5 μ M) + Alpelisib/BYL719 (5 μ M)	79.4*
\pm SD	6.9
Doxorubicin (5 μ M)	22.3*
\pm SD	1.9

Table D.3 The data represent the mean \pm SD of buparlisib/BKM120 combined with selective cPLA₂ α inhibitors where control was set up to 100 % viability. * indicates results significantly different from the control (p<0.05)

Treatment	24 hours, SF-RPMI	\pm SD
Buparlisib/BKM120 (2 μ M)	69.8*	3.3
DMSO	93.2*	5.0
AVX235 (20 μ M)	97.9	4.5
AVX235 (10 μ M)	99.6	6.0
AVX420 (20 μ M)	96.2	2.6
AVX420 (10 μ M)	95.5	4.3
AVX002 (5 μ M)	44.8*	3.2
ATK (7.5 μ M)	32.6*	4.3
ATK (5 μ M)	68.6*	3.9
AVX235 (20 μ M)+ Buparlisib/BKM120 (2 μ M)	46.6*	5.0
AVX235 (10 μ M)+ Buparlisib/BKM120 (2 μ M)	54.9*	1.8
AVX420 (20 μ M)+ Buparlisib/BKM120 (2 μ M)	65.8*	4.3
AVX420 (10 μ M)+ Buparlisib/BKM120 (2 μ M)	79.5*	6.7
AVX002 (5 μ M)+ Buparlisib/BKM120 (2 μ M)	26.2*	1.7
ATK (5 μ M)+ Buparlisib/BKM120 (2 μ M)	32.8*	2.5
Doxorubicin (1 μ M)	80.2*	3.9

E. All biological replicas (n=3) for the representative experiment in figure 12:

Table E.1 The data represent the mean relative light units (RLU) of the MDA-MB468 cells treated with different inhibitors and \pm SD of caspase assay. * indicate results significantly different from the control ($p < 0.05$),

Treatment	hours SF-RPMI
AVX235 (20 μ M)	94.68*
\pm SD	35.5
AVX235 (20 μ M) + buparlisib/BKM120 (5 μ M)	227.5*
\pm SD	23.8
AVX420 (20 μ M)	98.66*
\pm SD	20.67
AVX420 (20 μ M) + buparlisib/BKM120 (5 μ M)	213.69*
\pm SD	12.99
Buparlisib/BKM (5 μ M)	176.29*
\pm SD	12.45
AVX002 (5 μ M)	106.0*
\pm SD	9.8
AVX002 (5 μ M) + buparlisib/BKM120 (5 μ M)	232.37*
\pm SD	24.87
Doxorubicin (1 μ M)	78.3*
\pm SD	18.46